



UNIVERSITÀ
DEGLI STUDI
DI PADOVA

University of Padua

Department of Cardiac, Thoracic and Vascular Sciences

PhD course in Traslational Specialistic Medicine "G.B. Morgagni"

Curricula: Clinical and Traslational Neurosciences

XXXIV Cycle

"Nano-engineering of the human ear"

Coordinator: Professor Annalisa Angelini

Supervisor: Professor Laura Astolfi

Co-Supervisor: Dr Erica Gentilin

PhD Candidate: Mariarita Candito

“If we can reduce the cost and improve the quality of medical technology through advances in nanotechnology, we can more widely address the medical conditions that are prevalent and reduce the level of human suffering.”

Ralph C. Merkle, nanotechnology researcher (cited by Turney, 2008)

Abstract

Sensorineural hearing loss (SNHL) is the most common permanent ear disorder affecting people worldwide. The treatment of profound SNHL requires the use of a cochlear implant (CI) whose implantation involve some disadvantages related to its construction and to quality of life of implanted patient. In order to decrease side effects, scientists are working on innovative CI to achieve a better hearing sensitivity and quality in deaf population.

Another common ear disorder is the perforation of the tympanic membrane. In case of serious perforation, the surgical treatments currently used are the myringoplasty and the tympanoplasty but, both techniques have suboptimal outcome. For this reason, many studies are focused on the creation of scaffolds, to be used in tympanic membrane regeneration.

The aim of this thesis was to analyse the *in vitro* biocompatibility and efficacy of new nanomaterials and biomaterials to be used in developing innovative ear devices useful to improve the compliance of patients with inner or middle ear diseases.

Firstly, the biocompatibility of piezoelectric nanoparticles barium titanate and lithium niobate was analysed on two different cell lines, an Organ of Corti cell line (OC-k3) and a neuron-like cell line deriving from rat pheochromocytoma (PC12). These piezoelectric nanoparticles are involved in the construction of an innovative “self-powered” CI, which, by exploiting its piezoelectric features, will stimulate the cochlear neurons bypassing the damaged inner ear cells. The biocompatibility effect was assessed by analysing cytotoxic, apoptotic, oxidative and neurotoxic stimuli.

In the second part of the study, the aim was to analyse the biocompatibility of different patches and nanoparticles involved in the construction of biodegradable scaffolds produced using copolymers of poly(ethylene oxide-terephthalate)/poly(butylene terephthalate) (PEOT/PBT), containing chitin nanofibrils (CNs), and covered by different types of nanoparticles loaded with the antibiotic ciprofloxacin. These scaffolds aim to facilitate the healing process of the tympanic membrane by improving the proliferation and migration of

keratinocytes and by reducing the middle ear inflammation and the incidence of infection during the wound healing process. The biocompatibility was assessed on OC-k3 cells by analysing the cytotoxicity and the morphological changes induced by the PEOT/PBT copolymers containing different (w/w %) weight ratio of CNs: polyethylene glycol (PEG) pre-composite; and of the ciprofloxacin-loaded poly (lactic-co-glycolic acid) (PLGA), polycaprolactone (PCL), molecular imprinting (MIP) and non-molecular imprinting (NIP) nanoparticles.

The results showed that barium titanate and lithium niobate did not induce any cytotoxic or apoptotic effects on OC-k3 and PC12 cells, but actually increased cell viability and improved neuritic network. These piezoelectric nanoparticles appear biocompatible for inner ear cells and are good candidates for improving the efficiency of new implantable hearing devices without damaging neurons. Overall, these results confirm that the electric stimulation has neuromodulatory effects on neurons and highlight the importance of developing new scaffolds coated with piezoelectric nanoparticles to be exploited in the treatment of neuronal diseases.

Concerning the second part of this project, the results showed the biocompatibility of all materials involved in the production of the biodegradable scaffolds made of the PEOT/PBT copolymers, containing CNs, and covered by ciprofloxacin loaded nanoparticles, on the inner ear cell line OC-k3. Although further tests are required to clarify the effects of these materials, the construction of scaffolds containing chitin nanofibrils and ciprofloxacin-loaded nanoparticles, could be a great advantage for new implantable biodegradable devices to be used for repair of damaged tympanic membrane, without inducing any toxic effects on the delicate inner ear cells.

Index

1. Introduction.....	1
1.1 Auditory system	1
1.1.1 Cochlea.....	3
1.1.2 Organ of Corti	4
1.1.3 Phisiology of hearing	5
1.1.4 Hearing loss.....	6
1.2 Cochlear implant.....	7
1.2.1 Innovative cochlear implants.....	8
1.2.2 Piezoelectric materials.....	9
1.2.3 Natural piezoelectric materials.....	10
1.2.4 Syntetic piezoelectric materials	10
1.2.4.1 Polymers	10
1.2.4.2 PVDF	11
1.2.4.3 Ceramics	11
1.2.5 Barium titanate.....	13
1.2.6 Lithium niobate.....	14
1.3 Tympanic membrane	16
1.3.1 Common procedures to heal a perforated eardrum	17
1.3.2 Innovative strategies to heal a perforated eardrum	18
1.3.3 PEOT/PBT polymers	19
1.3.4 Chitin.....	19
1.3.5 Drug delivery: Antibiotics.....	20
1.3.6 PLGA and PCL nanoparticles.....	22
1.3.7 MIP and NIP nanoparticles.....	23
1.3.8 Biocompatibility.....	24
2 Aim	26
3 Materials.....	28
3.1 Cell lines.....	28

3.1.1 OC-k3	28
3.1.2 PC12.....	28
3.2 Tested materials.....	29
4 Methods.....	30
4.1 Cell cultures.....	30
4.2 Treatments.....	30
4.3 Cell viability assay.....	32
4.4 Cell viability by direct method	34
4.5 Cell viability by indirect method	34
4.6 Cell morphology.....	35
4.7 Cytochrome c expression	36
4.8 ROS production	36
4.9 Western blot	37
4.10 Neurite outgrowth	38
4.11 Statistical analyses.....	39
5 Results	40
5.1 Effect of piezoelectric nanoparticles on OC-k3 cells	40
5.2 Effect of piezoelectric nanoparticles on PC12 cells.....	47
5.3 Biocompatibility of materials involved in the new eardrum scaffolds	57
5.3.1 Biocompatibilty of chitin nanofibrils	57
5.3.2 Biocompatibility of PEOT/PBT copolymers	58
5.3.3 Biocompatibility of PLGA/PCL nanoparticles	60
5.3.4 Biocompatibility of MIPNP and NIPNP nanoparticles	67
6 Discussion	71
7 Conclusions.....	80
8 Bibliografy.....	83

1. Introduction

Our world is constantly evolving and, with it, knowledge and future perspectives of human beings are increasing. Over time, curiosity and the ceaseless research for innovation have shifted human attention from the macroscopic world to the microscopic one. The advent of nanotechnologies dates back a few decades (Patil et al., 2008) and nanotechnologies are presently used in many research fields, including medicine, engineering, physics, chemistry and biology. The features of nanocompounds are used to obtain nanodevices that could allow previously unimaginable results (Patil et al., 2008; Ray et al., 2009; Jones et al., 2013). Concerning the field of sensorineural pathologies, although hearing and balance problems are very common, their diagnosis and treatment are often problematic due to the anatomy of the temporal bone, the difficult access to the inner ear and the presence of barriers that maintain the homeostasis of fluids. New technologies are therefore under development to overcome these barriers and treat many disorders affecting the human ear (Juhn, 1988; Zou et al., 2016).

1.1 Auditory system

Sound consists of vibrations transmitted by vibrating objects through water, air or solids. A vibrating diapason, for example, transmits the pressure to air molecules that collide and deliver the vibrations to the ear. The sound waves are characterized by a pitch and a width. The pitch describes the frequency of vibration and is measured in hertz (Hz), the width describes the intensity of waves and is measured in decibel (dB).

The human ear is the sensory organ that perceives and transmits sound waves (with pitch from 20 to 20000 Hz and width from 0 to 120 dB) to the brain, and regulates the equilibrium and head coordination (Kenneth, 2019; Sánchez López de Nava et al., 2021). Anatomically it is divided in three parts: external, middle and inner ear (Fig. 1). The external part of the ear consists of the auricle, which protrudes from the side of the head and collects sound waves; and of the external auditory canal, that crosses the temporal bone and receives the

waves from the auricle, transmitting them to the tympanic membrane (Kollmeier, 2008; Hawkins, 2020).

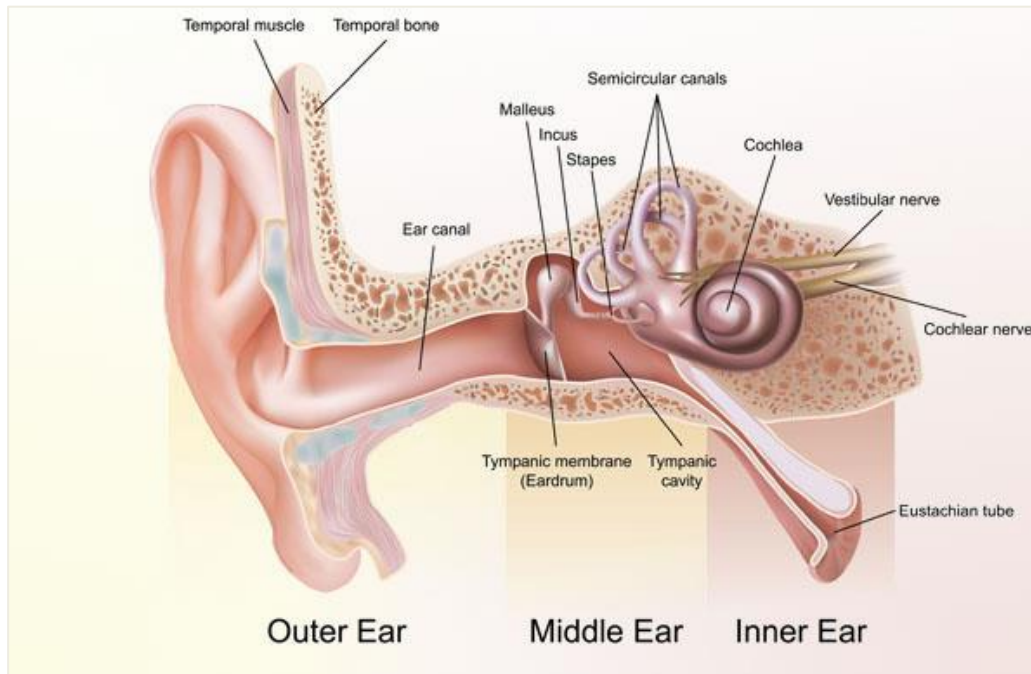


Fig. 1. Anatomy of the human ear. (redrawn from: Ear Audities, an educational blog on ears, <https://earaudities.wordpress.com/basic-anatomy/>)

The middle ear is an air-filled canal, localized in the tympanic cavity, consisting of a tympanic membrane (eardrum) that vibrates in response to incoming waves, and three tiny bones (malleus, incus and stapes) that by their related muscles and ligaments allow sound to pass from the eardrum to the inner ear. The Eustachian tube connects the middle ear with the nasopharynx, and maintains the ear ventilation, drains fluids and equilibrates the air pressure on both sides of eardrum, avoiding its impairment (Staecker et al., 2008; Carreiro, 2009).

The inner ear, deeply inserted into the temporal bone, is localized inside the membranous labyrinth, in turn contained within the bony labyrinth. The membranous labyrinth is filled with endolymph, a fluid similar to the extracellular one, rich of K^+ ions; the space between the two labyrinths is filled with perilymph, similar to cerebrospinal fluid, rich of Na^+ ions.

The inner ear begins with the vestibule, a cavity connected to the middle ear through the oval window, which contains the organs of equilibrium (also called “balance organs” or “vestibular system”), the “semicircular canals”, the “utricle” and the “sacculle”. The vestibular system shares the embryological origin with the cochlea, the spiral tube containing the sensory organ of hearing (Kollmeier, 2008; Kenneth, 2019; Hawkins, 2020).

1.1.1 Cochlea

The human cochlea is a fluid-filled tube, coiled for 2.5 turns around an axis of conical spongy bone called “modiolus”. It has a base of 9 mm in diameter and a height of 5 mm. The inside of cochlea is divided in three chambers: the vestibular duct (*scala vestibuli*), the cochlear duct (*scala media*) and the tympanic duct (*scala tympani*) (Fig. 2). The vestibular duct begins near the oval window and envelops the modiolus up to the cochlear apex, where it meets the scala tympani that, in turn, winds towards the cochlear base ending near the round window.

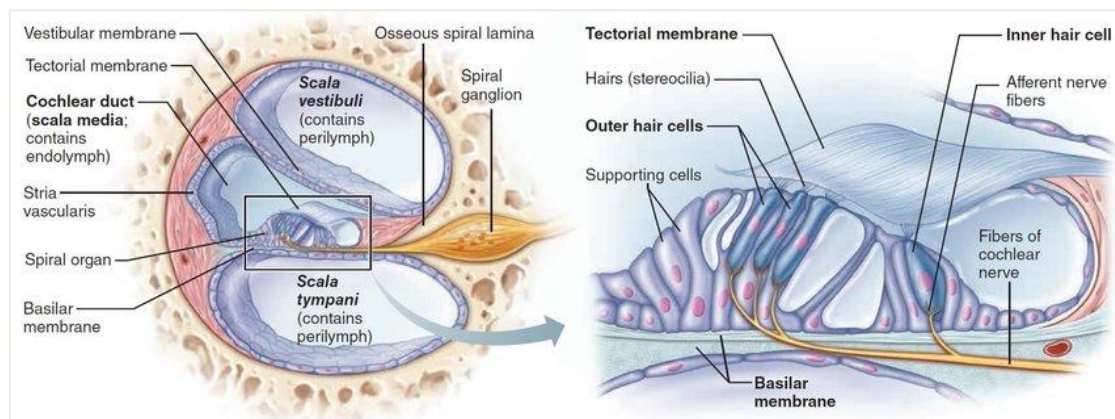


Fig.2. Section of the human cochlea and enlargement of the organ of Corti (Russo et al., 2019).

These two chambers are filled with perilymph and communicate with each other through the “helicotrema”, a small opening at the apex of cochlea that maintains the pressure balance of the perilymph between the two ducts (Javel, 2003; Kollmeier, 2008; Martini et al., 2011).

The *scala media*, the cochlear part of the membranous labyrinth, has a triangular shape and is filled with endolymph. It is separated from the overlying *scala vestibuli* by a thin membrane called “Reissner’s membrane”, and from the underlying *scala tympani* by the “basilar membrane” (Javel, 2003; Kollmeier, 2008). The lateral border of *scala media* is defined by the spiral ligament and by the stria vascularis that maintains the K⁺ concentration of the endolymph (Zhang & Duan, 2009).

1.1.2 Organ of Corti

The auditory organ, the “organ of Corti”, is located inside the cochlear duct, on the basilar membrane. The basilar membrane is a 35mm long membrane with an increasing width, proceeding from the base (0.1 mm) to the cochlear apex (0.65 mm) and associated with a decreasing stiffness (the base is stiffer than the apex). These differences are important for the sound perception, and make the basilar membrane a tonotopic map that vibrates in a specific way according to the frequency of sound stimuli.

The basilar membrane acts as a support for the organ of Corti, made up of sensory neuroepithelium and supporting cells. The pillar supporting cells create the tunnel of Corti, which runs lengthwise along the cochlear duct and separates the sensory inner hair cells (IHC), arranged in a single row near the modiolus, from the outer hair cells (OHC), arranged in three rows far from the modiolus. The hair cells are highly specialized mechanosensitive cells, characterized by long stiff microvilli, the stereocilia, arranged in 3-4 rows on the top of the cells in ascending order, from the lowest to the highest. The stereocilia transform the sound vibrations into neural impulses (Kenneth, 2019; Martini et al., 2011; Hawkins, 2020). On the top of hair cells lies the tectorial membrane, an acellular structure made up of fibrils anchored to OHC stereocilia. The deflection of the stereocilia in response to the movements of the basilar membrane causes the opening of the ionic channels present on the hair cells; this causes the cellular depolarization and the consequent release of a neurotransmitter (glutamate) which stimulates sensitive neurons. The nerve fibres that innervate hair cells

are the peripheral processes of the bipolar neurons of the spiral ganglion, located at the base of the osseous spiral lamina; the axons of bipolar neurons form the cochlear nerve. Afferent and efferent dendritic fibres therefore innervate the cochlea; each IHC is connected directly to 10-20 afferent fibres, while more OHC are connected to the same afferent fibre and possess most of the efferent innervation. This peculiar innervation is related to the different function of hair cells: the IHCs transfer the sound information to the central nervous system, while the OHCs tune each point of the basilar membrane with a specific wave frequency, allowing IHCs to have greater accuracy (Kenneth, 2019; Martini et al., 2011).

1.1.3 *Physiology of hearing*

The acoustic waves are collected by the auricle and directed to the eardrum through the external auditory canal. The vibrations are then transferred to malleus, incus and stapes that, in turn, transmit them to the oval window. There the vibrations are converted in pressure waves that cause the oscillation of the perilymph inside the *scala vestibuli*. These fluid oscillations produce a movement of the basilar membrane that vibrates with a frequency directly proportional to the sound frequency. High frequency waves allow the short fibres of the basilar membrane to resonate in the basal turn of the cochlea; low frequency waves cause the apical turn to resonate. The sound wave travel along the basilar membrane, generating a minimum perturbation until the point of maximum displacement, corresponding to the specific sound frequency, is reached. The movement of the basilar membrane induces a vibration of the hair cell body, triggering the deflection of the stereocilia and the consequent cell depolarization. The release of neurotransmitter by the IHCs then generates the action potential in afferent neurons and the potential will be propagated through the cochlear nerve to the central nervous system (Martini et al., 2011).

1.1.4 Hearing loss

Hearing loss is a partial or total reduction of hear and is the third chronic condition that affects adults (Martini et al., 2011; Mahmoudi et al., 2021; WHO, 2021). The World Health Organization (WHO) estimates that by 2050 over 700 million people will be suffering of hearing loss (WHO, 2021). Hearing loss may be classified on the following bases:

- *date of appearance*, congenital (present at birth) or acquired (appeared after birth);
- *cause of injury*, endogenous (hereditary/genetics) or exogenous (caused by environmental factors);
- *grade*, mild (20-40 dB), moderate (41-70 dB), severe (71-94 dB), profound (≥ 95 dB);
- *site of lesion*, conductive (affection of the external or medium ear); or sensorineural (SNHL) (affection of the inner ear or the neuronal fibres) (Martini et al., 2011).

Conductive hearing loss affects people of all ages, especially young, and is caused by a damage or malformation of the external (pinna or auditory canal) or medium ear (eardrum), resulting in a less efficient reception/transmission of vibrations to the inner ear (Mamo et al., 2018; Wroblewska-Seniuk et al., 2018). This type of hearing loss could be congenital, genetically related or not, and acquired because of a trauma, an ear inflammation (for example an otitis), or also an eardrum perforation caused by noise or incorrect use of cotton swabs (Sooriyamoorthy and De Jesus, 2021). The treatment of conductive hearing loss is usually pharmacological or surgical and the patient is usually able to achieve a good recovery of hearing (Wroblewska-Seniuk et al., 2018).

Sensorineural hearing loss (SNHL), the most common permanent ear disorder affecting people worldwide, is characterised by an unsuccessful transduction of sound vibrations into neural impulses. It may be caused by damaged inner ear hair cells, or by a dysfunctional basilar membrane or cochlear nerve fibres (Wroblewska-Seniuk et al., 2018; Tanna et al., 2021). The SNHL could be congenital, hereditary or not, or acquired following an acoustic trauma (explosions, loud music or sound pollution at work), ototoxicity (induced by antibiotics or chemotherapeutic drugs), stroke, age or infections (cytomegalovirus) (Marlow

et al., 2000; Isaacson and Vora, 2003). The treatment of SNHL involves the use of different types of hearing aids depending on the grade of the disorder. Mild to medium hearing loss are treated with endoauricular or retroauricular external prostheses, but the severe or profound hearing loss require the use of an implantable prosthesis called "cochlear implant" (CI) (Wroblewska-Seniuk et al., 2018).

1.2 Cochlear implant

Over the years there have been major technological innovations in hearing aids production but, as mentioned in a recent study (Haile et al., 2021), over 1,5 billion people currently live with hearing problems and about 80% of them still do not have hearing aids or cochlear implants. The invention of the cochlear implant (CI) (Fig. 3) is credited to Dr. William F. House who implanted the first device between 1960 and 1970, even before obtaining approval from the U.S. Food and Drug Administration (FDA) (Eshraghi et al., 2012).

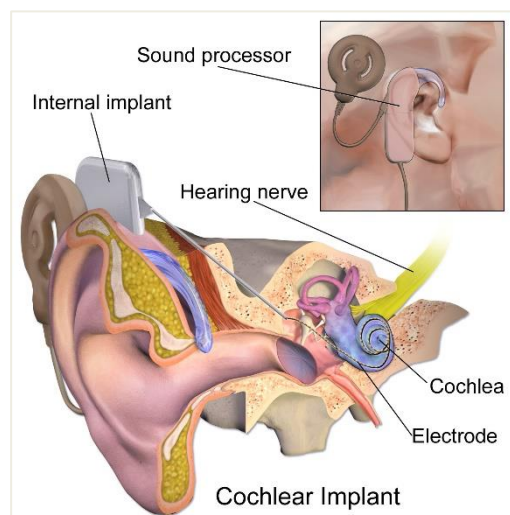


Fig.3 Cochlear Implant. From Blausen.com staff, "Medical gallery of Blausen Medical 2014". WikiJournal of Medicine 1. <https://doi.org/10.15347/wjm/2014.010>. ISSN 2002-4436.

The CI consist of an external part, a "speech processor" with a microphone and a "transmitter" that receives the sound from the environment and transfers it to the internal part of the CI. The internal part consists of a "receiver" that converts the sound into an

electric stimulus, and an “electrode array” implanted inside the cochlea, which stimulates the auditory cochlear nerve (Zeng et al., 2008; NIDCD, 2021).

The CI is therefore an implantable device that stimulates the cochlear nerve, bypassing damaged sensory cells and allowing the brain to receive the auditory stimulus (Astolfi et al., 2014). The advantages of using CI are many, as the patient is able to clearly perceive sounds coming from the external environment, to hear his/her own voice, to use the mobile phone, to hear music and, for young patients, to receive adequate education and language development. Alongside these advantages, however, there are many disadvantages due to actual surgery, among which the possibility of post-operative infections or changes in the sense of equilibrium (Cohen and Hoffman, 1991; Kelsay and Tyler, 1996; Haile et al., 2021). There are also possible disadvantages related to the patient’s quality of life, among which the impossibility to practice water sports without removing the external part of the implant, the necessity of replacing exhausted batteries or undergoing a new surgical operation in case of CI malfunction, and, last but not least, the difficulty in hiding the CI external part (Cohen and Hoffman, 1991; Kelsay and Tyler, 1996; Haile et al., 2021). For these reasons, many researchers are working on innovative cochlear implants around the world.

1.2.1 Innovative cochlear implants

The development of cochlear implants has made possible extraordinary innovations in the rehabilitation of sound perception but, unfortunately, not all implanted patients achieve the same results. The current research aim is to develop a “bionic ear” which, by simulating the physiological process of hearing, would allow a better sensitivity and quality of hearing in the deaf population (Mukherjee et al., 2000; Lenarz, 2018).

The most serious problems that reduce the success of cochlear implants are the positioning of the CI with respect to the modiolus, and the distance between the electrode and the nerve fibres, which causes a dispersion of the electric field produced and consequently a reduced separation of the electric channels. The strategies currently employed to achieve an optimal

positioning of the electrode include the use of devices capable of adapting their shape to the tympanic duct of the patient, or the use of artificial intelligence able to perform the surgery in a more precise way (Lenarz, 2018). To reduce the electrode/nerve distance, it is necessary to obtain the regeneration of auditory nerve fibres, the "dendrites". For this purpose, the releasing of neuronal growth factor (NGF) into the cochlear environment may be employed to stimulate the elongation of dendrites in the direction of the electrode. The production of NGF within the cochlea can be induced by a transplantation of stem cells that, differentiating within the cochlear environment, release NGF spontaneously. The researchers are presently trying to develop bio-hybrid electrodes that could transport stem cells directly inside the tympanic duct, and on nanoengineered CI that could transport molecules inside the cochlea using nanoparticles as carriers (Lenarz, 2018).

The cochlear implant is able to stimulate the cochlear nerve fibres, but the quantity and quality of the detected sound is not comparable to that heard by people with normal hearing, especially in the presence of noise. Sensitivity is therefore a key parameter in the development of new devices, sensitive enough to perceive sounds coming from the external environment and to generate a signal suitable to stimulate nerve fibres. Piezoelectric materials have peculiar properties that make them able to generate an electrical impulse in response to a mechanical stimulation; they are therefore perfectly suitable for use within the cochlea as signal transducers, which, by reducing the electrode/nerve distance and inducing neuron growth, can stimulate the nerve fibres of people with SNHL (Mukherjee et al., 2000).

1.2.2 Piezoelectric materials

The discovery of piezoelectricity dates back to 1880 and is credited to Paul-Jacques and Pierre Curie (Katzir, 2003). By analysing natural crystals, the Curie brothers discovered that some of them (such as quartz) had the ability to transform a mechanical input into electrical output. Piezoelectric materials have therefore the ability to generate an electrical charge

when subjected to mechanical deformation (direct piezoelectric effect) and similarly, to undergo a deformation when subjected to an external electric field (inverse piezoelectric effect). Some piezoelectric compounds have a permanent polarization and form a subclass of compounds called ferroelectrics. A ferroelectric material has the ability to modify its surface charge in wet conditions: this characteristic is very important for the development of implantable devices because, when immersed in a wet physiological environment, their surface charge can be used to modulate adhesion and cellular response (An et al., 2014; Tandon et al., 2018). Piezoelectricity is a widely found natural feature in synthetic and non-synthetic materials, such as polymers and ceramics, and each of these materials has peculiarities that make them useful in different fields of research and medical/biological applications (Azimi et al., 2020).

1.2.3 Natural piezoelectric materials

Quartz (SiO_2) and Rochelle salt ($\text{NaKC}_4\text{H}_4\text{O}_6 \cdot 4\text{H}_2\text{O}$) are the natural piezoelectric compounds that have been most widely used by researchers around the world. The Rochelle salt is used for the production of transducers, but its use is restricted by susceptibility to humidity and high temperature. Quartz, on the other hand, has an internal structure that makes it highly stable to thermal changes and is therefore considered the most reliable piezoelectric material. Quartz is currently used in the production of accelerometers and biosensor transducers, and for pressure measurements (Wilson, 2005; An et al., 2014).

1.2.4 Synthetic piezoelectric materials

1.2.4.1 Polymers

New synthetic piezoelectric materials have been recently developed, among which polymers, ceramics and crystals, improving piezoelectricity and ferroelectricity, and obtaining materials useful in many research fields (Sezer and Koç, 2020). The piezoelectric

polymers, with their unique features such as flexibility and solvent resistance, caught the attention of researchers that preferred them to ceramics and others compounds. Among these polymers, the poly (vinylidene fluoride) (PVDF) and its copolymer poly (vinylidene fluoride-co-trifluoroethylene) (PVDF-TrFE) are the most commonly used (He et al., 2021).

1.2.4.2 PVDF

Poly(vinylidene fluoride) (PVDF) is a semi-crystalline polymer that presents five different conformations (α , β , γ , δ , ϵ). Only three of these are polar and the most used is the β form, which gives the PVDF the highest piezoelectric coefficient (Tandon et al., 2018). The PVDF can be produced in films, membranes, rods and fibres, and is used in different fields due to its properties of transparency, flexibility, biocompatibility and resistance to gamma rays, which make it perfect for use in biomedical devices (Tandon et al. 2018; Azimi et al., 2020; He et al., 2021). The PVDF is one of the few materials already approved by FDA (Azimi et al., 2020). Many studies describe it as an optimal material to induce wound healing processes and tissue regeneration, and to stimulate stem cells differentiation (Tandon et al., 2018; Jeon et al., 2020) as well as migration, adhesion and proliferation of fibroblasts, bone and neuronal cells (Lee et al., 2011; Guo et al., 2012; Pärssinen et al., 2015; Li et al., 2019).

1.2.4.3 Ceramics

The piezoelectric ceramics are synthetic compounds produced by mixing and heating metal and non-metal powdered materials. The resulting piezoelectric powders are mixed in the desired shape resulting in a ceramic material with casually oriented dipoles. Finally, the process called “poling” is performed, in which a strong electric field is applied to ceramic, aligning the dipoles and giving the material a permanent net polarization (An et al. 2014; Sunar, 2018). These compounds are widely used thanks to their characteristics, and among them there are barium titanate (BaTiO_3) and lead titanate (PbTiO_3), whose piezoelectricity is

higher than that of quartz, and lithium niobate (LiNbO_3) and lithium tantalite (LiTaO_3), insoluble and resistant to high temperatures (An et al., 2014). These materials can be used in many applications, among which ceramic filters for electrical wave frequencies, piezoelectric actuators, piezoelectric sensors or surface acoustic wave devices (Sōmiya, 2003; Wilson, 2005; An et al. 2014).

Lead zirconate titanate (PZT) is one of the most used piezoelectric ceramics in material sciences and engineering. Flexible and chemically inert, it is widely used for sensors, capacitors and hydrophones. The major component of PZT is lead (Pb), toxic and volatile at high temperature (Panda, 2009), classified by the European Union as a hazardous substance of restricted use in electrical and electronic equipment (Directive 2011/65/EU; Alikin et al, 2017). For these reasons, new lead-free piezoelectric ceramics have been developed, such as potassium niobate (KNbO_3), BaTiO_3 and LiNbO_3 which, while maintaining the characteristics of lead-based compounds, are non-toxic and can be used in medical devices (Sunar, 2018; Panda, 2009). Researchers are also investigating novel manufacturing methods to develop lead-free and biocompatible piezoelectric compounds of nanoscale size (Azimi et al., 2020). Piezoelectric nanoparticles offer many advantages especially in medical applications, because their nano-size allows for non-invasive procedures and for induction of positive cell responses, such as cell growth, proliferation and tissue regeneration (Kapat et al., 2020). Among the new processes already developed, there is electrospinning, which allows the easy construction of piezoelectric nanostructures with specific and modifiable parameters. This process is used for the production of polymers and ceramics and, when associated with a process called “sol-gel”, allows the production of ceramic nanofibers or electrospun composite fibres, polymeric matrices containing nanoceramics that combine the properties of piezoelectric polymers with those of nanoceramics.

This innovation has made it possible to use piezoelectric nanofibers for the production of self-powered wearable devices, capable of converting biomechanical actions (heartbeat, muscle contractions, etc.) into electrical stimuli; or the production of bioactive scaffolds

("smart scaffold") useful in tissue engineering to promote tissue regeneration (Azimi et al., 2020).

1.2.5 Barium titanate

Barium titanate is an inorganic compound with an excellent dielectric constant and piezoelectricity, useful in bioengineering or electronic applications (Serra-Gómez et al., 2016). It can be prepared as clear powder or solid crystal (Fig. 4), and synthesized by different methods, depending on final desired characteristics and applications. The conventional method to produce BaTiO_3 is the solid-state reaction between titanium dioxide (TiO_2) and barium carbonate (BaCO_3), but the resulting powder has particles of large size and limited electrical properties.



Fig.4. Barium titanate crystals, from Buscaglia M.T. 2019.
(https://commons.wikimedia.org/wiki/File:Oxides_particles.jpg)

Other synthesizing reactions are the sol-gel and the hydrothermal methods, able to preserve all properties of ceramics (Vijatovic et al., 2008).

The *in vitro* biocompatibility of BaTiO_3 nanoparticles on human neuroblastoma SH-SY5Y cell line was analysed for the first time in 2010 (Ciofani et al., 2010a). The same authors

verified that these nanoparticles were cytocompatible and able to enhance the internalization and the cytotoxic activity of doxorubicin (Ciofani et al., 2010a). To date, has been shown that BaTiO₃ is biocompatible for different cell lines (Ball et al., 2014; Ciofani et al., 2013; Mota et al., 2017), and is also able to induce the osteogenic process (Jianqing et al., 1997) and to enhance neurite outgrowth and neural stimulation (Marino et al., 2015). To increase its stability in water solution, this type of ceramic has been used in the development of biocomposites for innovative medical applications (Serra-Gómez et al., 2016), among which biomedicine, cancer therapy (Ciofani et al., 2010a), and nanomedicine for drug delivery or tissue engineering (Genchi et al., 2016; Elsayed and Norredin, 2019). It is also under study for the production of smart piezoelectric membranes able to induce the regeneration of osteoarticular tissues (Vannozzi et al., 2019; Ahmadi et al., 2020).

1.2.6 Lithium niobate

Lithium niobate is a crystalline solid with trigonal structure, insoluble in water and organic compounds (Fig. 5). It is conventionally synthesized by a solid-state reaction between lithium carbonate (Li₂CO₃) and niobium pentoxide (Nb₂O₅), and has properties useful in many applications, such as ferroelectricity, piezoelectricity, pyroelectricity and a high electro-optical and photoelastic coefficient (Weis and Gaylord, 1985; Meinan et al., 2006; Kamali and Fray, 2014).

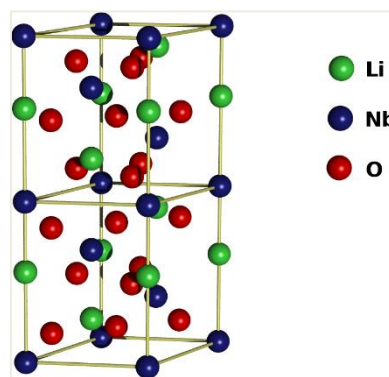


Fig.5. Crystalline structure of Lithium niobate. From Ahellwig, CC BY-SA 2.0 DE (https://commons.wikimedia.org/wiki/File:Linbo3_Unit_Cell).

Due to its properties, LiNbO₃ is widely used in acoustic waves transducers, optical phase modulators and memory elements (Weis and Gaylord, 1985). Only recently, studies have been undertaken on the effects of lithium niobate in a biological environment in order to broaden its fields of use (Marchesano et al., 2015). The bioactivity of this ferroelectric material was analysed for the first time in 2014 (Vilarinho et al., 2014). Later, other groups investigated the biocompatibility and the ability of this crystal to affect cells behaviour. The negatively charged surface of lithium niobate was shown to enhance the proliferation and adhesion of osteoblasts (Carville et al., 2015) and later other authors showed that this crystal regulates the adhesion, proliferation and migration of fibroblasts, depending on the surface polarity (Marchesano et al., 2015; Mandracchia et al., 2018). Considering these results and the fact that the polarization of the crystal is easily modifiable by applying an external electric field, lithium niobate is currently under examination for the development of innovative biomaterials for tissue bioengineering and implantable devices, to improve tissue regeneration and healing (Marchesano et al., 2015; Mandracchia et al., 2018).

1.3 Tympanic membrane

The tympanic membrane, or “eardrum” (Fig. 6) is a thin translucent membrane with a flattened conical shape: it is a rigid but flexible structure with a diameter of 8-10 mm (Hawkins, 2020; Szymanski et al., 2021). The eardrum is composed of three layers. The external layer consists of squamous connective tissue in continuity with the epidermis that lines the external auditory canal. The central layer (“lamina propria”) consists of fibrous connective tissue whose circular and radial fibres provide the typical stiffness and tension to the tympanic membrane. The inner layer consists of mucous tissue in continuity with the mucous epithelium that covers the middle ear cavity (Hawkins, 2020; Szymanski et al., 2021).

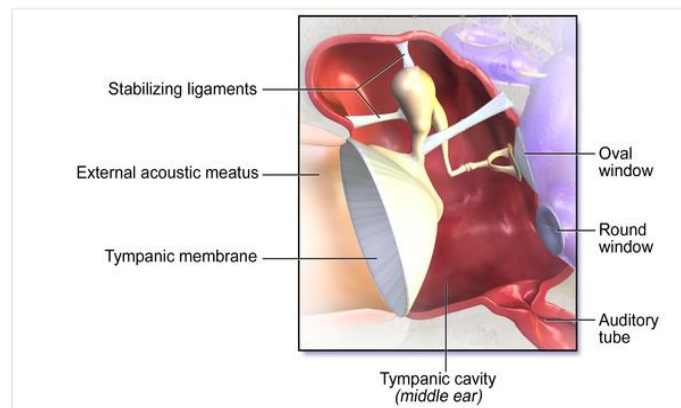


Fig. 6. Middle Ear Anatomy. Modified image from: Bruce Blaus "Medical gallery of Blausen Medical 2014". WikiJournal of Medicine 1. <https://doi.org/10.15347/wjm/2014.010>. ISSN 2002-4436

The tympanic membrane closes the external auditory canal and vibrates in response to incoming sound waves from the external environment, magnifying their pressure by 18 times, and transmitting them to the inner ear (Hawkins, 2020; Sundar et al., 2021)

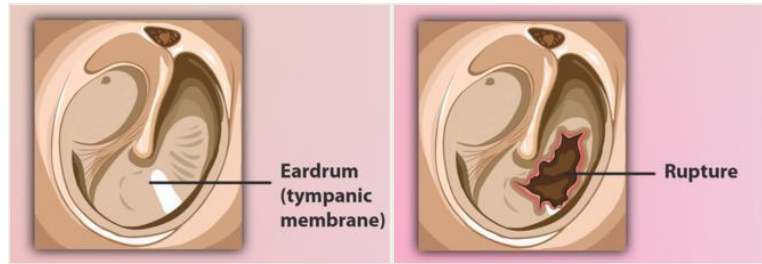


Fig. 7. Raptured Eardrum. Modified from myUpchar 2019. <https://www.myupchar.com/en/disease/ruptured-eardrum>.

Along life, this thin membrane can be damaged or perforated for various events, including trauma, barotrauma or exposure to a loud noise (Fig. 7). Damages to the eardrum can also be caused by acute or chronic middle ear diseases or by invasive medical procedures such as the trans-tympanic electrical stimulation of the cochlea (Bevis et al., 2021; Dolhi and Weimer, 2021).

1.3.1 Common procedures to heal a perforated eardrum

A perforated eardrum usually auto-regenerates itself within 6-12 weeks, but in case of serious perforation a surgical intervention may be necessary (Sagiv et al., 2020). The current surgical treatments are the myringoplasty and the tympanoplasty (Sagiv et al., 2020; Niazi et al., 2021). The myringoplasty is used to heal small central perforations using rice paper patches, gel foam or fat. The rice paper patch, the most commonly used material, serves as a scaffold to guide the epithelial cells, which should close the perforation by proliferating and migrating from the edges to the centre.

The myringoplasty has a low success rate because the materials used are not flexible or transparent, and do not have any anti-infective properties. When myringoplasty is unsuccessful or the eardrum perforation is too large, the treatment of choice is tympanoplasty (Hong et al., 2013). This intervention requires general anaesthesia and the perforated membrane is repaired using an autologous graft (“autograft”) implantation, namely scaffold grafting with autologous tissue (Xu et al., 2021). Although with a higher

success rate than myringoplasty, the outcome of this medical procedure is nevertheless suboptimal. Numerous studies are therefore underway to improve therapies to heal eardrum perforation, exploiting tissue engineering and innovative strategies to enhance the proliferation and migration rate of keratinocytes (Hong et al., 2013; Sagiv et al., 2020; Danti et al., 2021).

1.3.2 Innovative strategies to heal a perforated eardrum

Many researchers are currently evaluating the use of new implantable biomaterials for developing innovative patches or scaffolds, including synthetic polymers produced by electrospinning or 3D printing techniques for use as tympanic membrane transplants. These materials should be able to reproduce the mechanical properties of the tympanic membrane and face problems related to durability and the possible appearance of infections (Sagiv et al., 2020; Danti et al., 2021).

Electrospinning is one of the most common method to produce electrospun scaffolds from biocompatible polymers. This technique allows the control and regulation of many parameters, among which the flow rate or the electric field applied during the process, the size of fibres, the temperature, or viscosity of the solutions, in order to obtain an electrospun fibrous scaffold that mimics the native tissue. To date, several types of electrospun fibre scaffolds have been obtained for use in regenerative medicine, able to reproduce the structure of many native tissues including bone, cartilage, skin, or tympanic membrane (Danti et al., 2015; Jun et al., 2018). Using biocompatible polymers, the electrospun scaffolds not only are non-toxic for the biological environment, but also have been shown to enhance proliferation and migration of keratinocytes and mesenchymal stem cells, facilitating the tissue healing process (Danti et al., 2015; Chen et al., 2017).

1.3.3 PEOT/PBT polymers

Tissue engineering has recently engaged in research into new biomaterials for use in medicine, focusing on poly(ether ester)s copolymers based on poly(ethylene glycol) (PEG) and poly(butylene terephthalate) (PBT). The PBT is an aromatic polyester with excellent mechanical features but relatively stable in physiological conditions: its use is therefore limited in recent medical applications that require biodegradability (Deschamps et al., 2004). To overcome these limits, copolymers of poly (ethylene oxide-terephthalate) (PEOT/PBT) have been developed not only with biodegradability, but also able to reproduce the mechanical characteristics of skin, being composed of soft (PEO) and hard (PBT) parts (Xiao et al., 1991; Deschamps et al., 2004).

The copolymers PEOT/PBT have proven to be excellent candidates for use as scaffolds in tympanic membrane transplantation, and tissue regeneration and repair. They possess a good biodegradability in physiological environments, a good *in vitro* biocompatibility for fibroblasts and keratinocytes (Xiao et al., 1991; Deschamps et al., 2004), a good re-epithelization by keratinocytes deriving from human tympanic membrane, and a good colonization by human mesenchymal stem cells (Danti et al., 2015; 2021).

1.3.4 Chitin

Unfortunately, the PEOT/PBT biodegradable polymers do not have any anti-inflammatory or anti-infective properties: therefore, in case of tympanic membrane transplantation, it is necessary to combine them with some other compound able to counteract these clinical conditions (Danti et al, 2021). To meet this need, researchers focused their attention on chitin.

Chitin (N-acetylglucosamine), the second most abundant polysaccharide after cellulose, is a natural glucose derivative found in exoskeletons of arthropods and in fungi, and is easily extractable from food industry waste (Naghdi et al., 2020). Chitin and its deacetylated

derivate chitosan are widely used in biomedical applications due to their biocompatibility, biodegradability and antimicrobial properties (Elieh-Ali-Komi and Hamblin, 2016). These biopolymers are currently used as supports for drug delivery (Prabaharan, 2008), nanoparticles, nanocomposites (Jayakumar et al., 2010; Danti et al., 2021) and scaffolds for tissue engineering (Maeda et al., 2008).

From chitin, it is also possible to prepare nanofibers with submicrometric dimensions, which lose their allergenic action and acquire anti-inflammatory effects (Morganti et al., 2017; Danti et al., 2021). The construction of polymers and scaffolds containing chitin nanofibrils (CNs) could be very useful to develop new implantable biodegradable devices for reparation of damaged tympanic membrane (Danti et al., 2021).

1.3.5 Drug delivery: Antibiotics

Until now, the advantages in using biomaterials for construction of new electrospun scaffolds and implantable devices for tissue reparation and regeneration were discussed. Although these new polymers have a greater biocompatibility and are able to control the inflammatory state after the implantation, it is necessary to use molecules that provide antibacterial activity. Ear infections are the most common disorders affecting head and neck (Yang et al., 2021) and among them the otitis media is one of the common inflammatory disease that can causes the tympanic membrane perforation (Massa et al., 2021). The pathogens that usually causes ear infections are Gram-positive and Gram-negative bacteria, among which the most frequent ones are *Pseudomonas sp.* Migula 1894 (Pseudomonadales: Pseudomonadaceae) and *Staphylococcus sp.* Rosenbach 1884 (Bacillales: Staphylococcaceae)(Wall et al., 2009; Yang et al., 2021).

Researchers are therefore working to add antibiotics to these scaffolds to achieve a better implant outcome by releasing the molecules *in situ*, with reduction of side effects caused by systemic administration of antibiotics (Khorshidi and Karkhaneh, 2018; Günday et al., 2020).

Electrospun biodegradable scaffolds containing antibiotics are widely used in wound healing processes where they not only achieve excellent results with a significant reduction in the onset of infections, but also reduce the need for medications, increasing patient satisfaction and compliance (Hashemikia et al., 2021). Antibiotic agents can be incorporated into the electrospun scaffolds during the electrospinning process using different methods, for example coaxial electrospinning or emulsion electrospinning, resulting in a scaffold embedded with antibiotics. This scaffold releases the antibiotic during the degradation process, in a concentration depending on the degradation time of the implant (Günday et al., 2020).

These antibiotic incorporation methods cannot be used in the production of scaffolds for the regeneration of tympanic membrane, or cartilage and bone, because in this case a stable implant is required for a few months. A new producing method, co-electrospinning/electrospraying, was recently reported to meet this need. The method adds antibiotic-loaded nanoparticles directly to the surface of polymeric scaffolds, using Poly (lactic-co-glycolic acid) (PLGA), and Polycaprolactone (PCL) nanoparticles, produced with two different methods and loaded with ciprofloxacin. The electrospun scaffolds obtained by this innovative method allow a gradual and prolonged dispersion of antibiotic after implantation, enhancing the process of tissue healing with a reduction of side effects (Günday et al., 2020).

Several types of antibiotics are currently used in electrospun scaffolds and the most common is ciprofloxacin. This drug is a third-generation fluorinated quinolone with wide-spectrum antibiotic activity against the most common Gram-positive and Gram-negative bacterial genera, among which *Staphylococcus*, *Pseudomonas*, and *Streptococcus* sp. Rosenbach 1884 (Coccacea: Streptococcaceae). Electrospun scaffolds containing ciprofloxacin-loaded nanoparticles are an important research tool to obtain quick tissue regeneration avoiding infections and other side effects (Campoli-Richards et al., 1988; Hashemikia et al., 2021; Xue et al., 2021).

1.3.6 PLGA and PCL nanoparticles

In recent years, progresses have been made in the production of new materials to be used as carriers of macromolecules to specific target sites in the human organism. Nanoparticles, spherical nanostructures with adjustable features, appear excellent candidates as carriers. The main characteristic that nanoparticles must possess in order to be used in drug delivery are biocompatibility, biodegradability, and drug-compatibility, because after the administration the nanocarriers must release the transported macromolecules to the target site, without causing toxicity.

The ability of polymer nanoparticles to release macromolecules in a controlled way was demonstrated for the first time in 1976 (Langer and Folkman, 1976), and these nanostructures are currently used in many fields of research, such as cancer therapy, tissue engineering and biomedical sciences, to carry antibodies, genes, drugs and vaccines (Tabatabaei Mirakabad et al., 2014).

The PLGA nanoparticles are currently the most widely used material in drug delivery, along with PCL. Both are biocompatible and biodegradable polymers, already approved in human clinical trials by the FDA and the European Medicines Agency (EMA). Besides drug delivery, they are currently used in biomedicine and anticancer therapy to transport chemotherapeutics (paclitaxel, cisplatin), insulin, antibiotics (doxorubicin), and antifungals (amphotericin) (Kumari et al., 2010; Witt et al., 2019; Günday et al., 2020).

There are several methods for the production of polymeric nanoparticles. The most common are the nanoprecipitation, one-step process often used for the encapsulation of hydrophobic drugs; the single-emulsion-solvent evaporation method, involving the oil-in water emulsion (o/w) and preferred for encapsulation of insoluble drugs; and the double-emulsion-solvent evaporation, involving a water-oil-in water emulsion (w/o/w) and used for encapsulation of soluble drugs (Tabatabaei Mirakabad et al., 2014).

The PLGA and PCL nanoparticles loaded with ciprofloxacin were tested on human immortalized keratinocyte (HaCat) and human mesenchymal stem cells, showing that these

nanoparticles were biocompatible and enhanced the antibiotic effect of ciprofloxacin. These polymeric nanoparticles can therefore be used not only for general drug delivery but, when inserted into electrospun scaffolds, they could also reduce oral drug delivery, releasing drugs directly *in situ* (Günday et al., 2020).

1.3.7 MIP and NIP nanoparticles

Another new strategy currently investigated by researchers in drug delivery is the use of molecular imprinting polymers nanoparticles (MIPNP). Molecular imprinting polymers (MIPs) are compounds that can efficiently recognize and bind a specific target. During the polymerization phase, the chosen molecule or a fragment of it (template) is added to the polymer and incorporated into it. Subsequently, the template is removed from the MIP, using a specific solvent, leaving a complementary imprint on the polymer. In this way, the MIP will be able to specifically bind the molecular target, mimicking the “lock and key” process that normally occurs in physiological reactions.

The MIPs possess many features of synthetic polymers such as resistance to changes in temperature, pH and pressure, and have greater selectivity and efficiency than analogous polymers prepared without the use of molecular imprinting, the molecularly non-imprinted polymers (NIP) (Fresco-Cala et al, 2020). These ligand-selective polymers are usually produced as monoliths that are subsequently ground, resulting in small irregular fragments. The MIPs prepared with this method are widely used in chromatography or micro-extractions, but their irregular shape and size and the long manufacturing process limit their range of use (Moczko et al., 2013). For these reasons, new production methods have been developed to obtain imprinted polymers with nanoscale dimensions (Poma et al., 2010). The MIP nanoparticles (MIPNPs) have a higher surface to volume ratio, can be stored for long time at room temperature, labelled with fluorescent or magnetic molecules, and are homogeneous in size and shape. The MIPNPs have therefore attracted interest in *in vitro* tests as substitutes of enzymes or antibodies (very expensive) for use in diagnostic and

therapeutic applications, and in drug delivery (Canfarotta et al., 2018; Refaat et al., 2019; Fresco-Cala et al., 2020).

Some studies described the use of MIPNPs as carrier of insulin or chemotherapy drugs (Refaat et al., 2019), and the antitoxin effects of MIPNPs in living mouse with blood concentration of melittin, a component of the bee venom (Hoshino et al., 2010). The MIPNPs have therefore great potential as multifunctional tool in life science and *in vivo* applications. As research progresses, their use is expected to increase in a wide range of fields (Canfarotta et al., 2018; Refaat et al., 2019).

1.3.8 Biocompatibility

The evaluation of the biocompatibility of materials is fundamental in the pharmacological and biomedical fields to verify their cytotoxicity, pathogenic risk and inflammatory response. This issue is therefore important even more if the tested materials need to be used for the construction of implantable prostheses. The *in vitro* and *in vivo* biocompatibility of materials could be confirmed using different assays described in the International Standard ISO 10993 (Kejlová et al., 2005; Muller, 2008). The *in vitro* assays are useful to characterize and screening the materials that could be safely used in the biological environment, before testing them *in vivo* (Kuete et al., 2017; Hanks et al., 1996).

One of the most important aspect in the *in vitro* biocompatibility is the evaluation of the impact of compounds on cell viability. In this regard, the most widely used assay is the MTS; a colorimetric method that allows the quantification of proliferative and metabolically active cells. The 3-(4,5-dimethylthiazol-2-yl)-5-(3-carboxymethoxyphenyl)-2-(4-sulfophenyl)-2H-tetrazolium (MTS), in the presence of phenazine methosulfate (PMS), is reduced by living cells to the coloured product formazan, which has a maximum absorbance at 490-500 nm. The amount of coloured formazan is proportional to the number of living cells (Cory et al., 1991; Kuete et al., 2017).

Other important aspects to test in vitro biocompatibility are the analyses of apoptotic and oxidative stimuli induced by the materials using qualitative and quantitative methods. Living cells produce ROS during physiological enzymatic reactions, but an excessive amount of them may lead to cell death by apoptosis or necrosis, binding and damaging proteins, lipids and nucleic acids (Phaniendra et al., 2015).

The in vitro biocompatibility assays allow to measure the toxicity of substances with the advantages of testing a wide range of concentrations and measuring the effects of prolonged exposure over time (Keong and Halim, 2009).

2. Aim

The interest in the study of cellular interactions with synthetic materials arises from the need to understand which compounds can be used for the construction of implantable devices or engineered tissues. The implanted materials that should be exposed to biological environments such as blood, proteins and extracellular matrix, may modify and affect cellular behaviour (Marchesano et al., 2015; Mandracchia et al., 2018). The evaluation of biocompatibility of each compound used in medical applications is therefore very important in pharmacology and biomedicine. It is necessary to verify whether the compound may be harmful to the organism, release toxic substances or be recognized as external agents, thus inducing an inflammatory or immune response (Vilarinho et al., 2014; Pandey et al., 2016).

The aim of this thesis was to analyse the *in vitro* biocompatibility and efficacy of new nanomaterials and biomaterials for use in the inner and middle ear for functional recovery or replacement of damaged tissues and cells. The study first analysed the biocompatibility of two types of piezoelectric nanoparticles, lithium niobate and barium titanate, on two different cell lines, the OC-k3, inner ear cells deriving from the organ of Corti of Immortomouse® (Kalinec et al., 1999), and the PC12, neuron-like cell line deriving from rat pheochromocytoma (Greene and Tischler, 1976). These piezoelectric nanoparticles will be involved in the development of innovative “self-powered” cochlear implants that will be implanted on the basilar membrane and, due to their piezoelectric characteristics, will stimulate the cochlear neurons, bypassing the damaged IHCs. The biocompatibility was assessed by analysing the cytotoxic, apoptotic, oxidative and neurotoxic stimuli. Later, the study analysed the biocompatibility of all materials involved in the production of innovative biodegradable scaffolds useful in the tympanic membrane healing process, produced using the PEOT/PBT copolymers, containing chitin nanofibrils (CNs), covered by different types of ciprofloxacin-loaded nanoparticles. These innovative devices will be produced using the PEOT/PBT copolymers as base, and alternating rigid and soft segments to obtain the mechanical features of the tympanic membrane. The chitin nanofibrils will be used as filler and surface coating of the scaffold, using the electrospinning and the

electrospray techniques to allow a gradual *in situ* dispersion of chitin over time that will regulate the inflammatory state and the antibacterial action after the implantation. Finally, the tympanic patch will be covered by ciprofloxacin loaded nanoparticles that, by releasing the antibiotic directly *in situ*, will enhance the antibacterial action and reduce the side effects related to the systemic administration of ciprofloxacin. This innovative biocompatible device aims to facilitate healing process of the tympanic membrane, enhancing the proliferation and migration of keratinocytes and reducing the middle ear inflammatory state and the incidence infection rates during the wound healing process. The samples tested were the poly(ethylene oxide) terephthalate and poly(butylene terephthalate) PEOT/PBT copolymers containing different weight ratios of chitin nanofibrils (CNs): Polyethylene glycol (PEG) pre-composites; and various type of ciprofloxacin loaded nanoparticles, among which the poly (lactic-co-glycolic acid) (PLGA), the polycaprolactone (PCL), and the molecularly imprinted (MIPNP) and molecularly non-imprinted (NIPNP) polymeric nanoparticles. The *in vitro* biocompatibility was assessed on the OC-k3 cells, analysing the cytotoxicity and the morphological changes induced by all nanomaterials tested.

The results presented in this thesis will contribute to increase the knowledge on the effects of piezoelectric nanoparticles and antibiotic-containing biodegradable polymers, on inner ear cells, with the hope of increasing the number of safe compounds useful for developing innovative smart devices that could be employed for treatment of disorders affecting the human ear.

3. Materials

3.1 Cell Lines

3.1.1 OC-k3

The OC-k3 are an inner ear cell line derived from the organ of Corti of Immortomouse®. This cell line shows the characteristics of epithelial cells and expresses molecular markers typical of auditory sensorial cells and supporting cells. For these reasons the OC-k3 are a perfect model to study the *in vitro* effects of compounds and materials on the organ of Corti, and they are widely used for ototoxicity tests (Kalinec et al., 1999; Astolfi et al., 2015).

3.1.2 PC12

This cell line, obtained from Interlab Cell Line Collection (ICLC ATL98004, Genoa, Italy), consists in chromaffin cells derived from rat pheochromocytoma that can differentiate into neuron-like cells when stimulated with NGF.

The PC12 cells are widely used as neuronal cell model in neuroscience, thanks to their ability to acquire morphological and functional features of sympathetic neurons after NGF stimulation (Hu et al., 2018). However, differentiated PC12 cells acquire neuronal features and therefore react to drugs or molecules in different way in comparison with undifferentiated cells. Differentiated PC12 cells have been reported as more sensitive to reactive oxygen species (Sasaki et al., 2001), cyanide (Mills et al., 1996) and zinc (Sánchez-Martín et al., 2010), but less sensitive to chemotherapeutic drugs (Sakagami et al., 2018).

There are several methods to obtain differentiated cells, and recently it has been shown that the Opti-MEM™ I Reduced Serum Medium could improve and optimize the neuronal differentiation of PC12 cells (Hu et al., 2018).

Once differentiated, these cells stop proliferation, extend neurites and axons, and acquire the morphological characteristics of sympathetic neurons. For this reason, they are widely used in studies of neurotoxicity, neuroprotection and neuroinflammation (Radio and Mundy, 2008; Wiatrak et al., 2020).

3.2 Tested materials

- Barium titanate (BaTiO_3 , pm 233.192 g/mol, CAS Number 12047-27-7) nanopowder and lithium niobate (LiNbO_3 , pm 147.846 g/mol, CAS Number 12031-63-9) powder were purchased from Sigma-Aldrich (Milan, Italy). Before use, the nanoparticles were suspended in sterile filtered 1% gelatine/double distilled water solution, and sonicated for 24h in an Elma Transsonic Ultrasonic Bath T 460 (35 kHz) (Elma Schmidbauer GmbH, Singen, Germany), to obtain well-dispersed nanoparticle suspensions.
- Chitin nanofibrils (CNs) (2% solution in water) were obtained by the Department of Civil and Industrial Engineering, University of Pisa (Italy).
- The poly(ethylene oxide terephthalate)/poly(butylene terephthalate) (PEOT/PBT) copolymers loaded with CNs/polyethylene glycol (PEG) pre-composite at different (w/w %) weight ratios (50/50; 65/35; 70/30; 75/25), were prepared by the 4NanoEARDRM research group.
- The poly (lactic-co-glycolic acid) (PLGA) or polycaprolactone (PCL) nanoparticles loaded with ciprofloxacin were obtained from MJR PharmJet GmbH, (Uberherrn, Germany).
- The ciprofloxacin-loaded molecularly imprinted polymer nanoparticles (MIPNP) and ciprofloxacin-loaded molecularly non-imprinted polymer nanoparticles (NIPNP) nanoparticles were obtained from the Department of Biomedical Engineering Bioinspired Functional Polymers and Nanomaterials Laboratory, AREL University (Istanbul, Turkey). All nanoparticles were resuspended in sterile phosphate-buffered saline (PBS, Sigma Aldrich) 1X.

4. Methods

4.1 Cell cultures

The OC-k3 cells were grown in presence of 10% CO₂ at 33°C in complete medium: Dulbecco's Modified Eagle Medium (DMEM) High Glucose (Euroclone, Pero, Milan, Italy) supplemented with fetal bovine serum (FBS) 10%(Euroclone), L-Glutamine 2mM (Biowest, Nuaille, France), penicillin/streptomycin (Pen/Strep) 1% (Sigma-Aldrich) and interferon- γ 50 U/ml (IFN, Genzyme, Cambridge, Massachusetts, U.S.A.).

The PC12 cells were grown in the presence of 5% CO₂ at 37°C in complete medium: Roswell Park Memorial Institute (RPMI) medium (Euroclone) supplemented with horse serum (HS) 10% (Carlo Erba, Milan, Italy), FBS 5%, L-glutamine 2mM, Pen/Strep 1%. Before treatment, in order to obtain the neuron-like cell line, the PC12 cells were plated and cultured for 6 days in differentiating medium: Opti-MEM™ I Reduced Serum Medium (ThermoFisher Scientific, Waltham, Massachusetts, U.S.A.), supplemented with FBS 0.5%, Pen/Strep 1% and NGF (Sigma-Aldrich)50 ng/ml. The differentiation medium was replaced with fresh one every 2 days.

4.2 Treatments

- Piezoelectric nanoparticles

Before treatments, the BaTiO₃ and LiNbO₃ nanoparticles suspensions were sonicated for 90 min in Elma Transsonic Ultrasonic Bath T 460 (35 kHz) and resuspended in fresh medium. The concentrations initially tested were from 0.1 to 1000 nM, and then three concentrations of the range were chosen (5.8, 100 and 500 nM).

The OC-k3 cells were treated with BaTiO₃ and LiNbO₃ nanoparticles resuspended in complete medium, 24h after seeding. The PC12 cells, instead, were treated with BaTiO₃ and LiNbO₃ nanoparticles resuspended in differentiation medium on the first day after differentiation.

For both cell lines, the tests were performed 24, 48 and 72 h after treatments. Samples of untreated cells were used as negative control (NT). The anticancer drug cis-diamminedichloroplatinum (II) (cisplatin) was used as positive control. For OC-K3 cells, only one concentration of cisplatin was used (13 μ M), while for PC12 cells two concentrations (13 and 25 μ M) were used.

- *Chitin nanofibrils*

The OC-k3 cells were treated with three different concentrations of chitin nanofibrils solution 2% in water (5, 10 and 20 μ g/ml) diluted in complete medium. The results were evaluated 24 and 48h after treatment.

- *PEOT/PBT*

Before treatment, the copolymers of poly(ethylene oxide terephthalate)/poly(butylene terephthalate) (PEOT/PBT) loaded with CNs/PEG pre-composite at different (w/w %) weight ratios (50/50; 65/35; 70/30; 75/25) were sterilized with absolute ethanol (EtOH) (Carlo Erba), washed with PBS 1X and incubated with FBS for 30 minutes.

- *PLGA/PCL nanoparticles*

The tested nanoparticles (stock solutions stored at room temperature) were the following:

- PLGA nanoparticles loaded with 200 μ g/ml ciprofloxacin, prepared by the nanoprecipitation method (PLGA-Cipro);
- PLGA nanoparticles without ciprofloxacin, prepared by nanoprecipitation method (Blank PLGA);
- PCL nanoparticles loaded with 200 μ g/ml ciprofloxacin (PCL-Cipro);
- PCL nanoparticles without ciprofloxacin (Blank PCL);
- PLGA nanoparticles loaded with 200 μ g/ml ciprofloxacin, prepared by the water-oil-in water emulsion (w/o/w) method (PLGA-Cipro w/o/w);

- PLGA nanoparticles without ciprofloxacin, prepared by the w/o/w method (Blank PLGA w/o/w).

The OC-k3 cells were treated with the above samples at different dilutions, obtained from 200 µg/ml stock solutions. The dilutions were 1:5, 1:10, 1:40, 1:100, 1:1000, and 1:10000, respectively resulting in concentrations 40, 20, 5, 2, 0.2 and 0.02 µg/ml. The tests were performed at 24 and 48h after treatment.

- *MIP and NIP nanoparticles*

The tested nanoparticles (stock solutions stored at room temperature) were the following:

- MIPNP_Cipro (molecularly imprinted polymer nanoparticles loaded with ciprofloxacin);
- NIPNP_Cipro (molecularly non-imprinted polymer nanoparticles loaded with ciprofloxacin);
- Blank MIPNP (molecularly imprinted polymer nanoparticles);
- Blank NIPNP (molecularly non-imprinted polymer nanoparticles);
- Ciprofloxacin powder.

Before treatment, the samples were resuspended in sterile PBS 1X at concentration of 200 µg/ml. The OC-k3 cells were treated with the above samples diluted in culture medium up to 40, 20 and 2 µg/ml for 24 and 48h.

4.3 Cell viability assay

Cell viability was measured by CellTiter 96® Aqueous MTS Reagent Powder (Promega, Milan, Italy) according to the manufacturer's suggestions. The reagents used in this method were the tetrazolium compound (3-(4,5-dimethylthiazol-2-yl)-5-(3-carboxymethoxyphenyl)-2-(4-sulfophenyl)-2H-tetrazolium (MTS) and phenazine

metasulphate (PMS). The OC-k3 cells were seeded 7000 cells/well in 96-well plates with 100 μ l of complete medium; the next day the cells were treated with BaTiO₃ and LiNbO₃ nanoparticles or chitin nanofibers, and PLGA, PCL, MIPNP and NIPNP nanoparticles, as previously described.

The PC12 cells were seeded 5000 cells/well in 6-well plates with 2 ml of complete medium and then induced to differentiate. Once differentiated, the cells were treated with BaTiO₃ and LiNbO₃ nanoparticles as previously described.

At the end of each time interval, a mixture of MTS and PMS 20:1 was added to each well, containing fresh medium. The plates were incubated for 3 h at 37 °C. Absorbance was measured at 490 nm with Mithras LB 940 Multimode Microplate Reader (Berthold Technologies GmbH, Bad Wildbad, Germany).

4.4 Cell viability by direct method

In the direct cell viability test (Fig. 8), the PEOT/PBT copolymers loaded with CNs/PEG at different (w/w %) ratios, after sterilization and preparation as previously described, were positioned at the bottom of the 96-well plates and 10^5 OC-k3 cells were seeded directly on the surface of samples. The plates were left in incubator for 24 and 48h. At the end of each time interval, a mixture of MTS and PMS at 20:1 ratio was added to each well, containing fresh medium. The plates were incubated for 3 h at 37 °C. Absorbance was measured at 490 nm with the Mithras LB 940 Multimode Microplate Reader (Berthold Technologies GmbH).

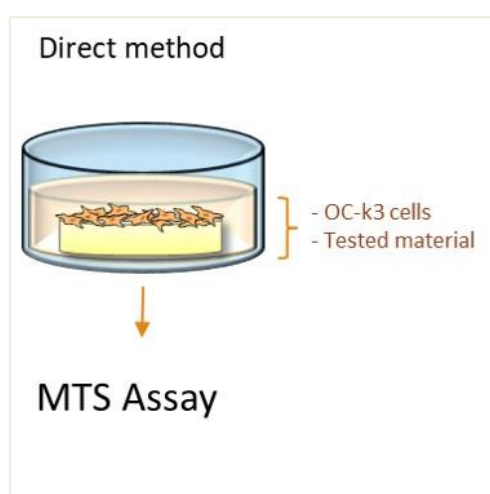


Fig. 8. Scheme of the cell viability test performed by the direct method in a well of a 96 well plate.

4.5 Cell viability by indirect method

In the indirect cell viability test (Fig. 9), the PEOT/PBT copolymers loaded with CNs/PEG at different (w/w %) ratio, after sterilization and preparation as previously described, were positioned at the bottom of the 24 well plates and immersed in culture medium for 24h. The following day, the media where the material was immersed (conditioned media) were used to treat 10^5 OC-k3 cells seeded in 24 well plates for 24 and 48h. At the end of each time interval, a mixture of MTS and PMS at 20:1 ratio was added to each well, containing fresh medium. The plates were incubated for 3 h at 37 °C. Absorbance was measured at 490 nm with Mithras LB 940 Multimode Microplate Reader.

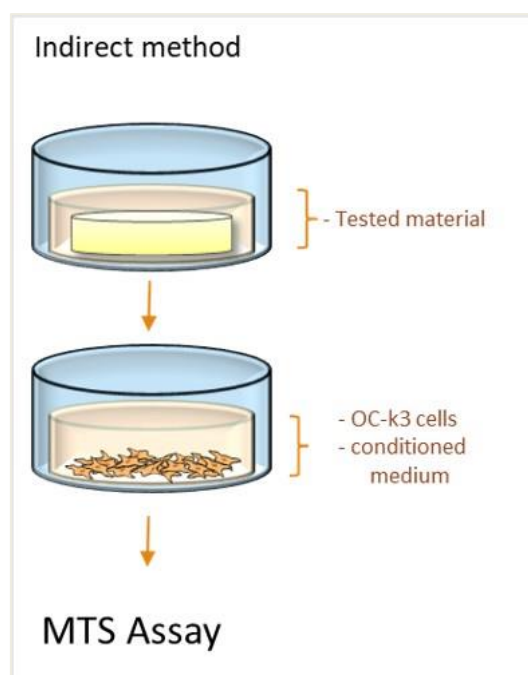


Fig. 9. Scheme of the cell viability test performed by the indirect method in a well of a 96 well plate.

4.6 Cell morphology

The morphological features of cell cytoskeleton and nuclei were evaluated using phalloidin – tetramethylrhodamine (TRITC) /4', 6-diamidino-2-phenylindole (DAPI) staining. The OC-k3 and the PC12 cells were seeded on glass slides, and cultured and treated as previously described with BaTiO₃, LiNbO₃, PLGA, PCL, MIPNP and NIPNP nanoparticles as previously described. At the end of each treatment, the cells grown on slides were fixed with Shandon™ Glyo-Fixx™ (ThermoFisher Scientific) for 30 minutes, washed 3 times in Phosphate Buffered Saline (PBS) (Sigma-Aldrich) 1X and stained for 2 h in the dark with phalloidin – TRITC 1 µg/ml (Sigma-Aldrich). After two washes in PBS 1X, the cells were stained with DAPI 1 µM (Sigma-Aldrich) for 5 min in the dark. Finally, after two washes with PBS 1X, the slides were mounted with 20% glycerol (Carlo Erba) and observed under the optical fluorescence microscope Nikon Eclipse TE2000-U (Nikon, Milan, Italy). The images were acquired using 40X magnification with the NIS element software (Nikon).

4.7 Cytochrome c expression

The OC-k3 and PC12 cells were seeded on glass slides, and cultured and treated with BaTiO₃ and LiNbO₃ nanoparticles, as previously described. At the end of each time interval the cells were fixed in Shandon™ Glyo-Fixx™ (ThermoFisher Scientific) for 30 minutes, washed 3 times in PBS 1X, incubated 30 min at 37°C with rabbit serum (Sigma-Aldrich) in PBS 1X and incubated overnight at 4°C with anti-cytochrome c primary antibody sc13560 (Santa Cruz Biotechnology, Dallas, Texas, U.S.A.). The following day the samples were washed twice with PBS 1X and incubated 1h in the dark with a TRITC-conjugated secondary antibody (Sigma Aldrich). After washing with PBS 1X, the cell nuclei were stained in blue by DAPI and the slides were mounted as previously described. The images were acquired using 40X magnification with the NIS element software (Nikon).

4.8 ROS production

Cellular levels of reactive oxygen species (ROS) were measured using the H₂DCFDA assay (Sigma- Aldrich). The 2',7'-dichlorodihydrofluorescein diacetate (H₂DCFDA) is deacetylated in living cells to 2', 7'- dichlorodihydrofluorescein (H₂DCF) whose oxidation by ROS produces the fluorescent 2', 7'-dichlorofluorescein (DCF). The fluorescence generated is proportional to the amount of H₂DCF oxidized to DCF (Jakubowski and Bartosz, 2000). The OC-k3 and PC12 cells were seeded in 96-well plates, and cultured and treated with BaTiO₃ and LiNbO₃ nanoparticles, as previously described. At the end of each time interval, the cells were treated with H₂DCFDA 10 μM for 30 min at 37°C in the dark. After washing with PBS 1X, the fluorescence produced was measured at 485 nm excitation and 540 nm emission with Mithras LB 940 Multimode Microplate Reader (Berthold Technologies GmbH).

4.9 Western blot

The Western blot technique was used to evaluate the expression of apoptotic proteins in OC-k3 and PC12 cells treated with BaTiO₃ and LiNbO₃ nanoparticles. The cells were seeded on 25-cm² flask, and cultured and treated as previously described. At the end of each time interval, the cells were harvested and the pellet was collected in a plastic tube. Total proteins were extracted from cells using radioimmunoprecipitation assay RIPA buffer (NaCl 150 mM, NP40 1%, sodium deoxycholate 0.5 %, sodium dodecyl sulfate SDS 0.1%, Tris/HCL, pH 8 50mM and protease inhibitors) and quantified with the Pierce™ BCA Protein Assay Kit (ThermoFisher Scientific). The total proteins were then separated on 12% polyacrylamide gel and transferred on 0.2 μM polyvinylidene difluoride (PVDF) transfer membrane (ThermoFisher Scientific) using Semi-dry Transfer (Euroclone).

The primary antibodies were diluted with 5% (w/v) milk in TBST buffer (Tris base 200mM, NaCl 1.5 M, pH 7.6, Tween-20 0.1 % (v/v)) or with 5 % (w/v) bovine serum albumin (BSA) in PBST buffer (PBS 1X, Tween-20 0.1% (v/v)). The membranes were incubated overnight at 4°C with primary antibodies, according to manufacturer's instructions (Table 1). The membranes were then incubated with the recommended dilution of horseradish peroxidase (HRP)-conjugated secondary antibody (Table 2) diluted in 5% (w/v) milk in TBST at room temperature for 1 h.

Table 1. Primary antibodies used for Western blot.

Antibody	Host species	Molecular weight	Catalogue number	Company
Caspase 3	Rabbit	32 – 17 kDa	GTX110543	Genetex (Irvine, California, USA)
Poly (ADP-ribose) polymerase (PARP)	Rabbit	116 – 89 kDa	GTX100573	Genetex

Gliceraldeide-3-phosphate dehydrogenase (GAPDH)	Mouse	37 kDa	sc32233	Santa Cruz Biotechnology (Dallas, Texas, USA)
--	-------	--------	---------	---

Table 2. Secondary antibodies used for Western blot.

Antibody	Host species	Dilution	Catalogue number	Company
Anti-mouse peroxidase	goat	1:5000	A4416	Sigma Aldrich
Anti-rabbit peroxidase	goat	1:2000	A6154	Sigma Aldrich

4.10 Neurite outgrowth

The PC12 cells were seeded at 5000 cells/well in 6-well plates, differentiated and treated with BaTiO₃ and LiNbO₃ nanoparticles as previously described. At the end of each time interval fifteen different fields of view for treatment were acquired at 10X magnification, with Nikon Eclipse (TE2000-U, Nikon). The images were analysed using the ImageJ software (<https://imagej.nih.gov/ij/>). The parameters measured (Fig. 10) were the following:

- the differentiation grade, obtained by the ratio between number of cells with neurites and the total cell number;
- the number of neurites per cell;
- the average length of neurites, obtained by the ratio between the total neurite length and the number of cells with neurites;

- the number of branch points, obtained by the ratio between the number of branch points and the number of neurites per cell.

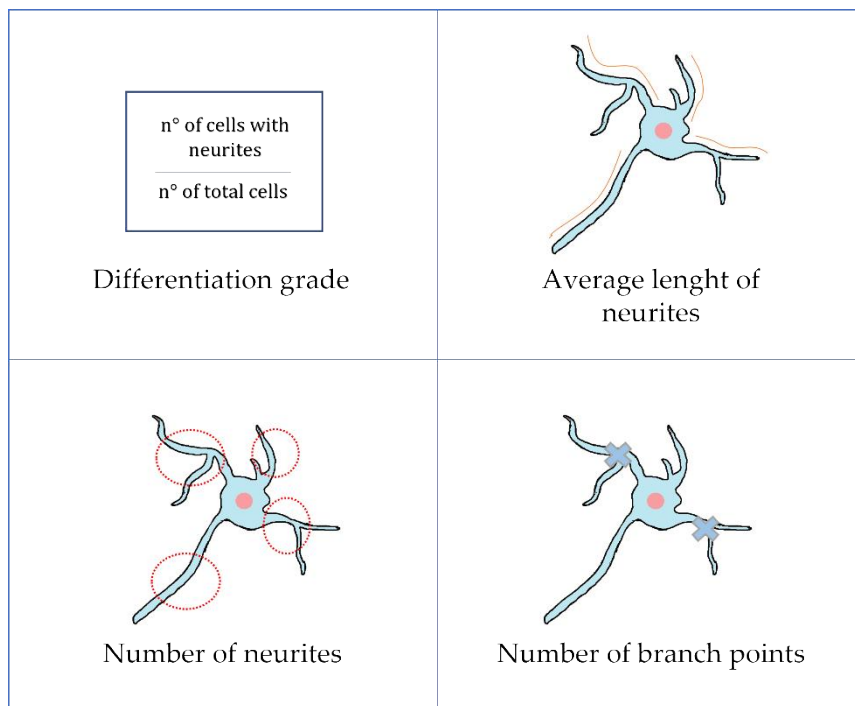


Fig. 10. Schematic representation of the parameters measured on the PC12 cell line to analyse the neuronal outgrowth.

4.11 Statistical analyses

Each test was performed at least three times in triplicate. One-way analysis of variance (ANOVA) or Kruskal-Wallis were used to assess the differences between multiple groups, followed by Student's t test or Mann-Whitney test. The P-value (p) <0.05 was considered statistically significant. All analyses were performed using the software GraphPad Prism 8.0.1. (<https://www.graphpad.com/>).

5. Results

5.1 Effect of piezoelectric nanoparticles on OC-k3 cells

To verify the biocompatibility of barium titanate (BaTiO_3) and lithium niobate (LiNbO_3) nanoparticles, the viability of treated inner ear cells deriving from the organ of Corti of Immortomouse® (OC-k3 cells) was analysed with the MTS assay.

The OC-k3 cells were treated with BaTiO_3 and LiNbO_3 nanoparticles at different concentrations, from 0.1 to 1000 nM. The results showed that the treatment with BaTiO_3 significantly reduced cell viability at concentrations 1 and 500 nM after 24h and at 1000 nM after 24 and 48h. The treatment at concentration 1 nM significantly increased cell viability at 48h post treatment. The cell viability was not affected by the treatment with BaTiO_3 at all other concentrations tested. These results suggest that, although BaTiO_3 initially altered cellular activity, the OC-k3 cells were able to recover their physiological activity after 72h (Fig. 11).

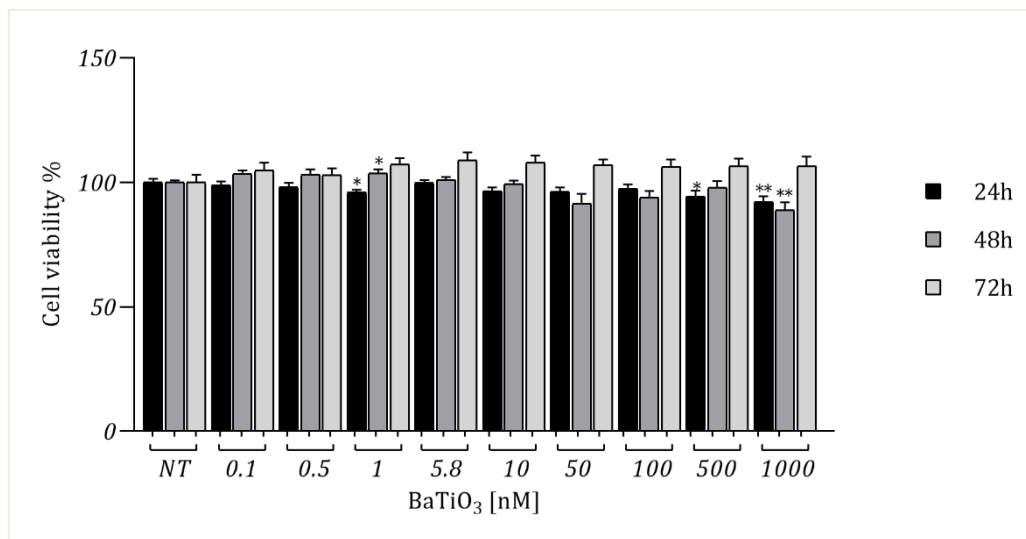


Fig. 11. MTS assay on OC-k3 cells treated for 24, 48 and 72h with BaTiO_3 nanoparticles. Cell viability was expressed as mean value percent \pm standard error of mean (SEM) *vs.* untreated cells (NT). Asterisks indicate significant differences in comparison to NT, with * = $p < 0.05$; ** = $p < 0.01$.

On the other hand, the treatment with LiNbO₃ did not affect OC-k3 cell viability at all concentrations and times tested (Fig. 12).

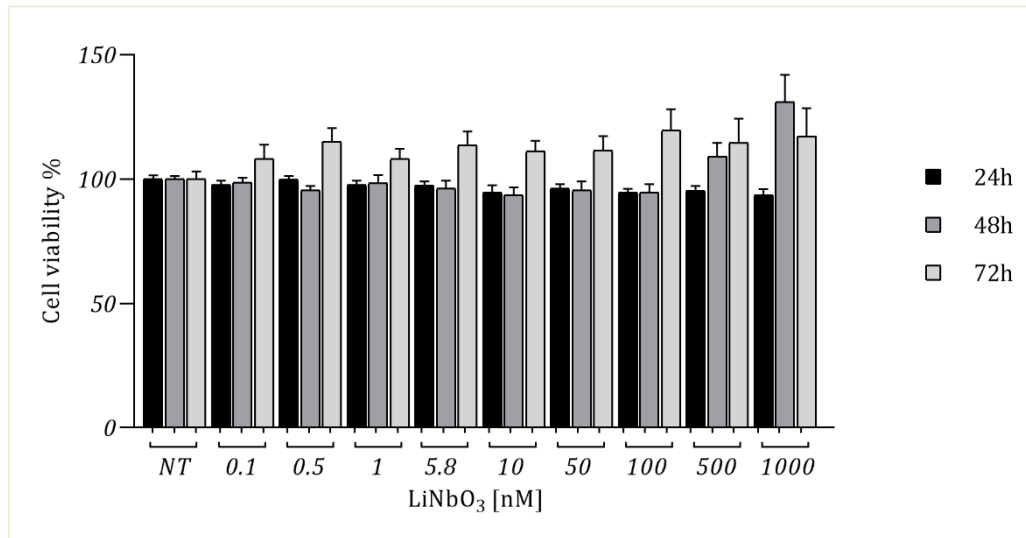


Fig. 12. MTS assay on OC-k3 cells treated for 24, 48 and 72h with LiNbO₃ nanoparticles. Cell viability was expressed as mean value percent \pm SEM vs. untreated cells (NT).

To evaluate the effect of piezoelectric nanoparticles on the morphology of cytoskeleton and nuclei of OC-k3 cells, a morphological analysis was performed using the phalloidin-DAPI staining.

The OC-k3 cells were treated with BaTiO₃ and LiNbO₃ nanoparticles at concentrations 5.8, 100 and 500 nM (Fig. 13, a-u). The results showed that the treatment with BaTiO₃ (Fig.13, d-l) and LiNbO₃ (Fig. 13, m-u), did not induce any morphological changes in OC-k3 cells at all concentrations and times tested.

The actin filaments of the cytoskeleton appeared well extended, and the nuclei were round without signs of piknosis.

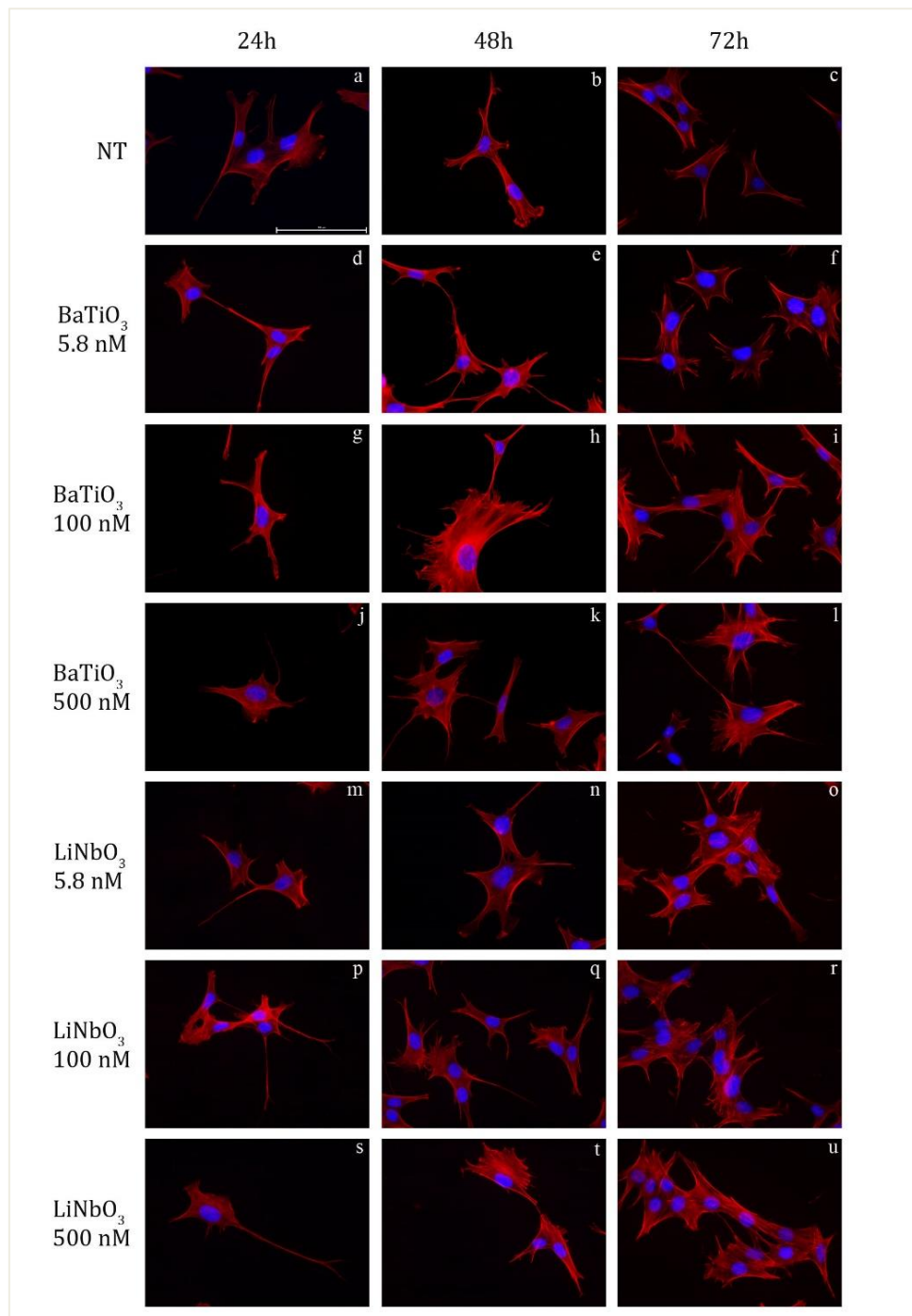


Fig. 13 Immunocytochemical analysis of OC-k3 cells (a-x) treated with BaTiO₃ (d-l) and LiNbO₃ (m-u) for 24, 48 and 72h at concentrations 5.8, 100 and 500 nM. Cells treated with Cisplatin 13μM (v-x) were used as positive control of apoptosis. Cytochrome c primary antibody was stained in red by (TRITC)-conjugated secondary antibody. The cell nuclei were stained in blue by DAPI. Arrows indicate apoptotic cells. Merged images captured at 40X magnification, scale bar 100 μm.

The distribution of cytochrome c within the cells was then evaluated using the immunocytochemical analysis (Fig. 14, a-x). Cells treated with cisplatin 13 μM were used as positive control (Fig. 14, v-x). The results showed that the treatment with BaTiO_3 (Fig. 14, d-l) and LiNbO_3 (Fig. 14, m-u) did not affect the distribution of cytochrome c within the cells.

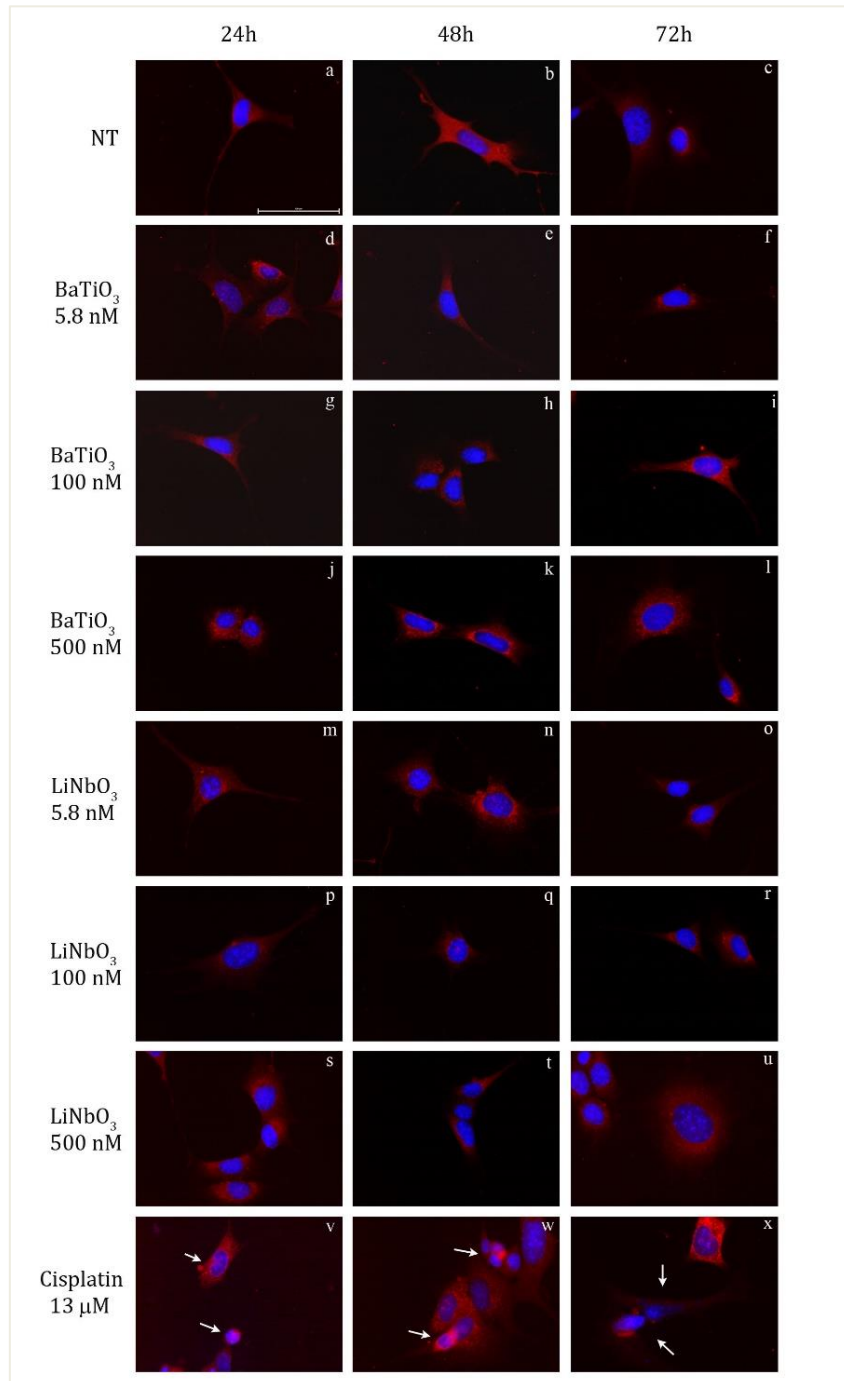


Fig. 14. Morphological analysis of OC-k3 cells (a-u) treated with BaTiO_3 (d-l) and LiNbO_3 (m-u) for 24, 48 and 72h at concentrations of 5.8, 100 and 500 nM. Phalloidin-TRITC (red) stains the actin filaments of the cytoskeleton; DAPI (blue) stains the A-T rich regions of nuclear DNA. NT, untreated control. Merged images captured at 40X magnification, scale bar 100 μm .

The cisplatin treated samples (positive control) showed a widespread distribution of cytochrome c staining, a reduction of cell volume and nuclear alterations (Fig. 14, v-x). Therefore, BaTiO₃ and LiNbO₃ did not induce apoptotic stimuli in OC-k3 cells at all times and doses tested.

Subsequently, the amount of reactive oxygen species (ROS) produced in OC-k3 cells treated with the piezoelectric nanoparticles was analysed. The 2'-7'-dichlorodihydrofluorescein diacetate (DCFDA) assay was performed to evaluate ROS production by measuring the fluorescence of oxidized 2', 7'- dichlorodihydrofluorescein (DCF) proportional to the amount of ROS produced by cells.

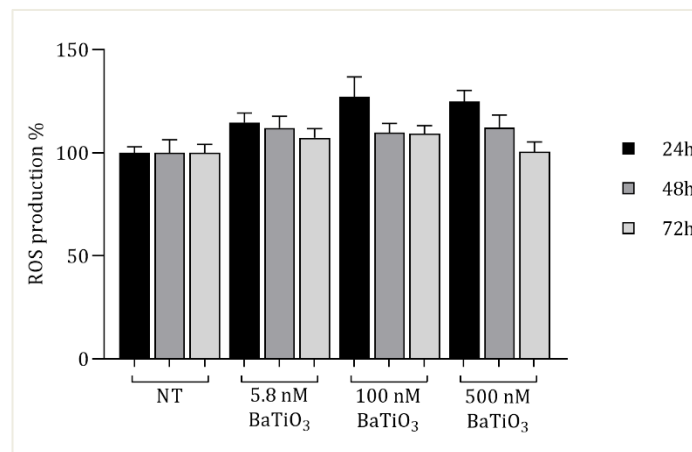


Fig. 15. DCFDA assay on OC-k3 cells treated with BaTiO₃ for 24, 48 and 72h at concentrations 5.8, 100 and 500 nM. The ROS production was expressed as mean value percent \pm SEM vs untreated cells (NT).

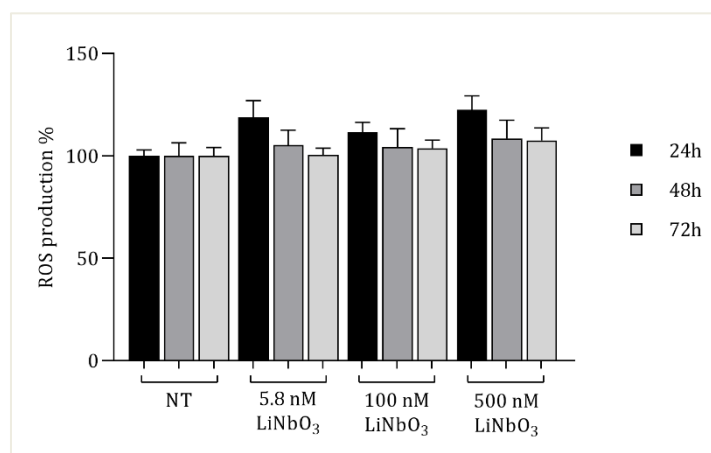


Fig. 16. DCFDA assay on OC-k3 cells treated with LiNbO₃ for 24, 48 and 72h at concentrations 5.8, 100 and 500 nM. The ROS production was expressed as mean value percent \pm SEM vs untreated cells (NT).

The results showed that the treatment with BaTiO₃ (Fig. 15) and LiNbO₃ (Fig. 16) nanoparticles did not induce any significant changes in ROS production at all treatment conditions in comparison with untreated cells.

After that, the variations of the early apoptosis markers caspase 3 and Poly (ADP-ribose) polymerase (PARP) were analysed in OC-k3 cells by Western blot to verify whether the treatment with BaTiO₃ and LiNbO₃ nanoparticles could induce apoptotic stimuli. Cells treated with cisplatin 25 µM for 24h were used as positive control.

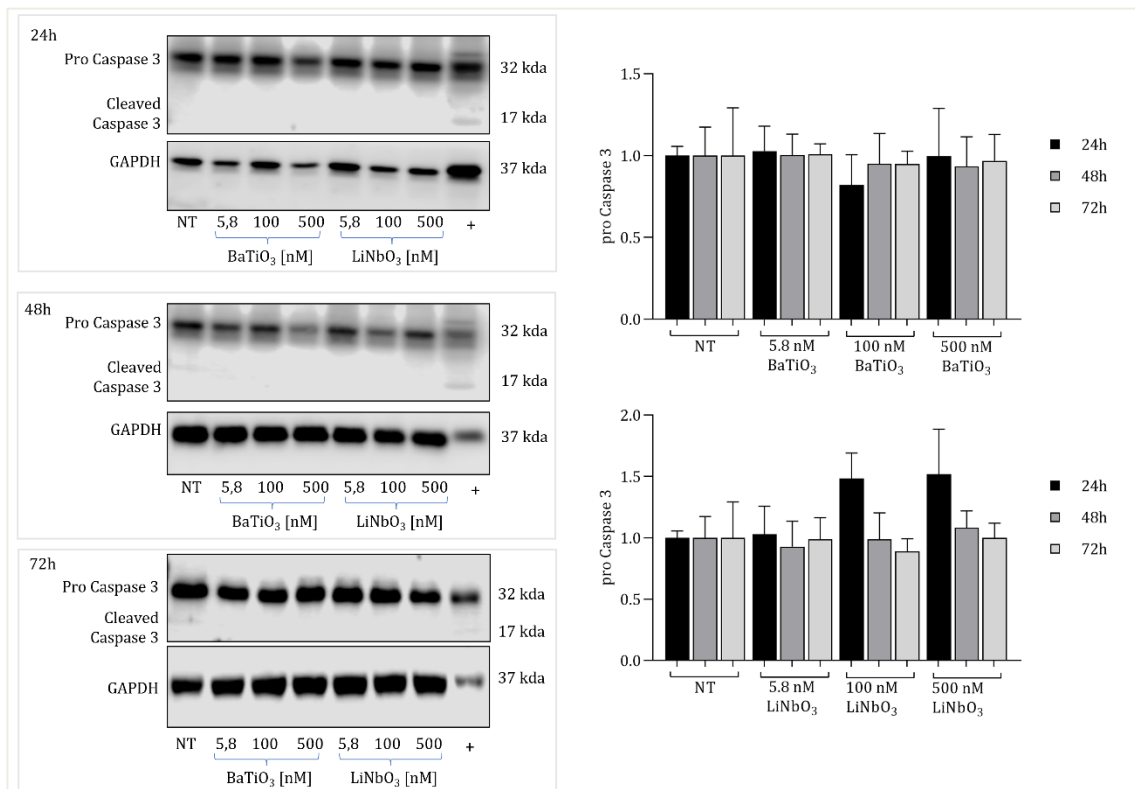


Fig. 17. Western blot and densitometric quantification of the apoptotic protein caspase 3 expressed on OC-k3 cells treated with BaTiO₃ and LiNbO₃ nanoparticles for 24, 48 and 72h at concentrations 5.8, 100 and 500 nM. Glycerolaldehyde-3-phosphate dehydrogenase (GAPDH) was used as housekeeping protein. Cisplatin 25 µM was used as positive control (+). All primary antibodies were diluted 1:1000. The densitometric analysis was performed with ImageJ and the results were expressed as mean value percent ± SEM *vs.* untreated cells (NT).

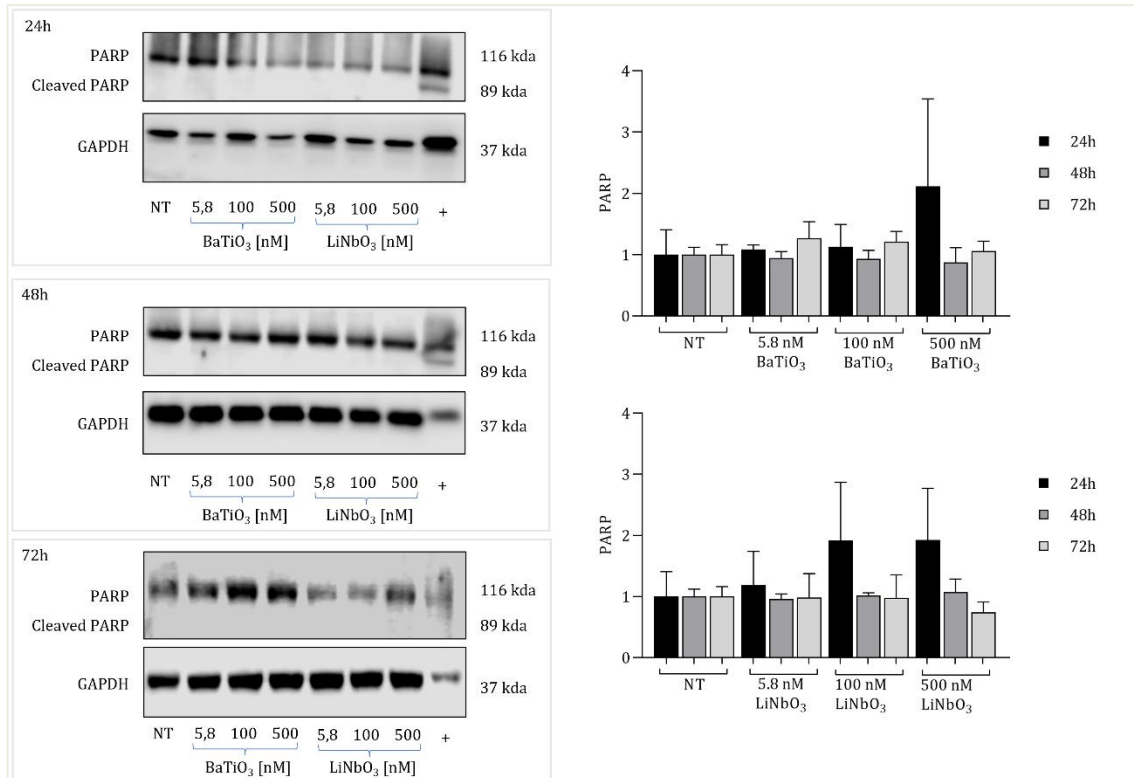


Fig. 18. Western blot and densitometric quantification of the apoptotic protein poly(ADP-ribose) polymerase (PARP) expressed on OC-k3 cells treated with BaTiO₃ and LiNbO₃ nanoparticles for 24, 48 and 72h at concentrations 5.8, 100 and 500 nM. Gliceraldeide-3-phosphate dehydrogenase (GAPDH) was used as housekeeping protein. Cisplatin 25 μ M was used as positive control (+). All primary antibodies were diluted 1:1000. The densitometric analysis was performed with ImageJ and the results were expressed as mean value percent \pm SEM *vs.* untreated cells (NT).

The results showed that the treatment with both piezoelectric nanoparticles did not induce significant changes on the expression of caspase 3 (Fig. 17) and PARP (Fig. 18) in OC-k3 cells compared with untreated cells. In addition, the cleaved forms of caspase 3 and PARP were not found in any of the samples tested, except in the positive control. These results show that BaTiO₃ and LiNbO₃ nanoparticles do not induce apoptotic stimuli on OC-k3 cells.

5.2 Effect of piezoelectric nanoparticles on PC12 cells

The same analyses performed on OC-k3 cells to verify the biocompatibility of BaTiO₃ and LiNbO₃ nanoparticles were repeated on differentiated PC12 cells, a neuron-like cell line deriving from rat pheochromocytoma, in order to analyse the effect of these piezoelectric nanoparticles on neuronal cells.

The effects of BaTiO₃ and LiNbO₃ on the viability of PC12 cells were therefore investigated using the MTS assay. Before the treatment, the PC12 cells were differentiated using the Opti-MEM™ differentiating medium, as described in Materials and Methods. The effects of piezoelectric nanoparticles on PC12 cells were also compared with those of exposure to cisplatin, chemotherapeutic drug known to induce ototoxicity and neurotoxicity (Santos et al., 2020). The results showed that the treatment with BaTiO₃ significantly increased cell viability at concentrations of 5.8 nM after 24h, 500 nM after 24 and 72h, and 100 nM at all times tested (Fig. 19).

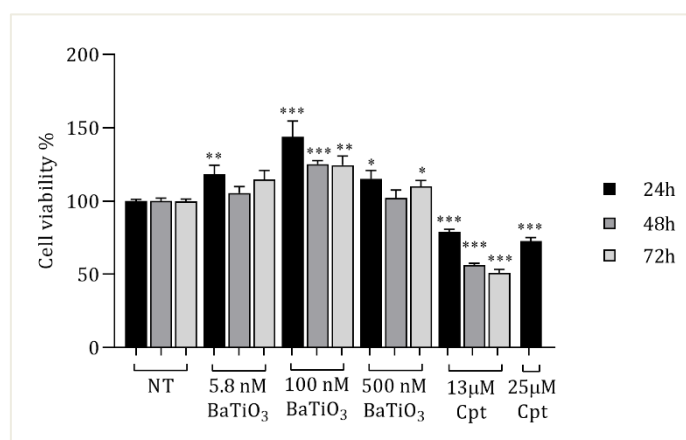


Fig. 19. MTS assay on Opti-MEM differentiated PC12 cells, treated for 24, 48 and 72h with BaTiO₃ nanoparticles at concentrations 5.8, 100 and 500 nM. Cells treated with cisplatin (Cpt) 13 μM for 24, 48 and 72h and 25 μM for 24h were used as positive control. Cell viability was expressed as mean value percent ± SEM *vs.* untreated cells (NT). Asterisks indicate significant differences in comparison to NT. * = p<0.05; ** = p<0.01; *** = p<0.001.

Similarly, the treatment with LiNbO₃ significantly increased cell viability after 24h at all concentrations tested (Fig. 20). The same effects were observed after 48 and 72h at the highest concentrations tested. On the contrary, the treatment with cisplatin at concentration 13 μM and 25 μM significantly decreased PC12 cell viability at all times tested.

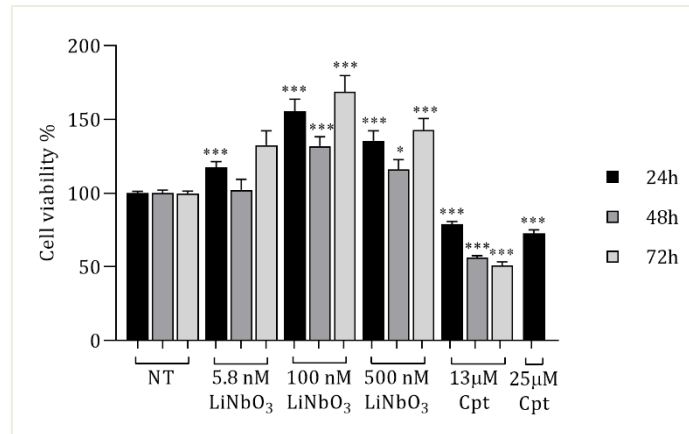


Fig. 20. MTS assay on Opti-MEM differentiated PC12 cells, treated for 24, 48 and 72h with LiNbO₃ nanoparticles at concentrations 5.8, 100 and 500 nM. Cells treated with cisplatin (Cpt) 13 μM for 24, 48 and 72h and 25 μM for 24h were used as positive control. Cell viability was expressed as mean value percent ± SEM *vs.* untreated cells (NT). Asterisks indicate significant differences in comparison to NT. * = p<0.05; *** = p<0.001.

The morphological changes induced by BaTiO₃ and LiNbO₃ on differentiated PC12 cells were subsequently investigated using the phalloidin-DAPI staining. Cells treated with cisplatin 13 μM were used as positive control (Fig. 21, a-u). The results showed that the treatment with BaTiO₃ (Fig. 21, d-l) and LiNbO₃ (Fig. 21, m-u) nanoparticles did not induce any morphological changes in PC12 cells at all concentrations and times tested.

The actin filaments of the cytoskeleton appeared well extended, and the nuclei were round without signs of piknosis. On the contrary, the treatment with cisplatin induced neurotoxic effects on PC12 cells, namely a reduction of the average size of cytoskeletal elements, cell shrinkage, multinucleated cells and fragmentation of nuclei (Fig. 21, v-x)

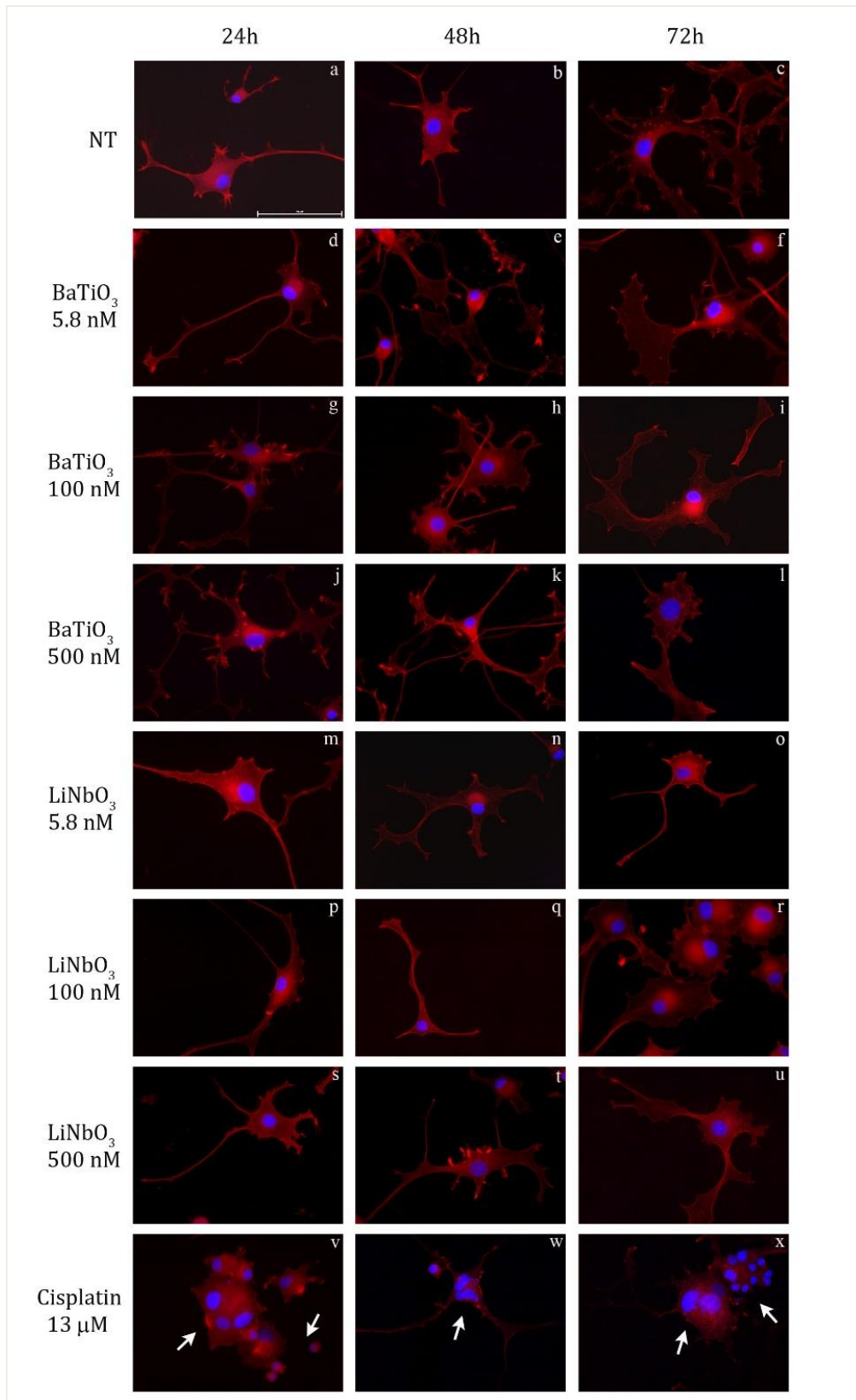


Fig. 21. Morphological analysis of Opti-MEM differentiated PC12 cells (a-x) treated with BaTiO₃ (d-l) and LiNbO₃ (m-u) for 24, 48 and 72h at concentrations 5.8, 100 and 500 nM. Cells treated with cisplatin 13μM (v-x) were used as positive control of neurotoxicity. Phalloidin-TRITC (red) stains the actin filaments of the cytoskeleton; DAPI (blue) stains the A-T rich regions of nuclear DNA. Merged images captured at 40X magnification, scale bar 100 μm.

Subsequently, the distribution of cytochrome c in treated PC12 cells was evaluated using the immunocytochemical analysis. The cells were differentiated and treated with BaTiO₃ and LiNbO₃ as described in Materials and Methods. Cisplatin 13 μM was used as positive control of apoptosis (Fig. 22, a-x). The results showed that the treatment with BaTiO₃ (Fig. 22, d-l) and LiNbO₃ (Fig. 22, m-u) did not induce any change in cytochrome c distribution within the cells. On the contrary, the cisplatin treated cells showed signs of apoptosis (Fig. 22, v-x), namely diffuse cytochrome staining, cell volume reduction and nuclear malformations.

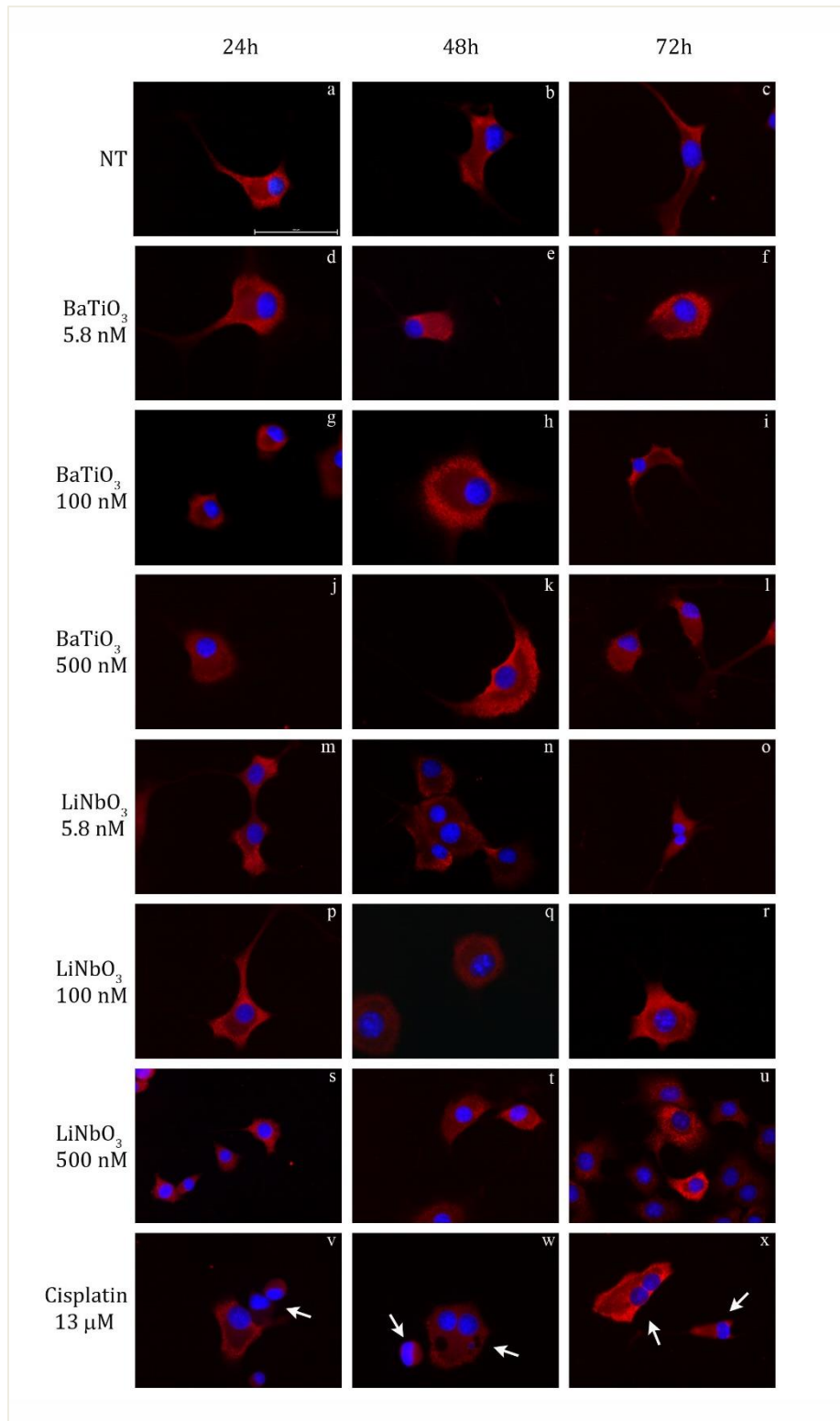


Fig. 22. Immunocytochemical analysis of differentiated PC12 cells (a-x) treated with BaTiO₃ (d-l) and LiNbO₃ (m-u) for 24, 48 and 72h at concentrations 5.8, 100 and 500 nM.

Cells treated with cisplatin 13μM (v-x) were used as positive control of apoptosis. Cytochrome c primary antibody was stained in red by (TRITC)-conjugated secondary antibody. The cell nuclei were stained in blue by DAPI. Arrows indicate apoptotic cells.

Merged images captured at 40X magnification, scale bar 100 μm.

The quantity of ROS produced in differentiated PC12 cells treated with the piezoelectric nanoparticles was analysed by the DCFDA assay measuring the fluorescence of oxidized DCF, which is proportional to the amount of ROS produced by cells. The PC12 cells were differentiated and treated with nanoparticles as described in Materials and Methods. Cells treated with cisplatin 25 μ M for 24h were used as positive control.

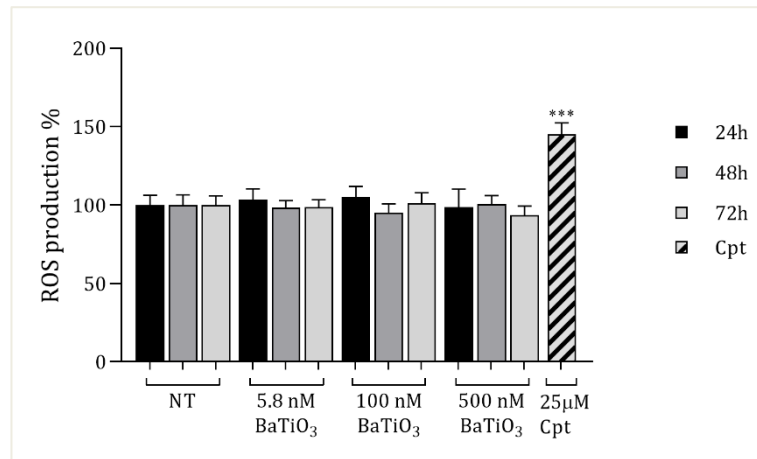


Fig. 23. DCFDA assay on differentiated PC12 cells treated with BaTiO₃ for 24, 48 and 72h at concentrations 5.8, 100 and 500 nM. Cells treated with cisplatin 25 μ M for 24h were used as positive control. The ROS production was expressed as mean value percent \pm SEM vs untreated cells (NT). Asterisks indicate significant differences in comparison to NT, with *** = $p < 0.001$.

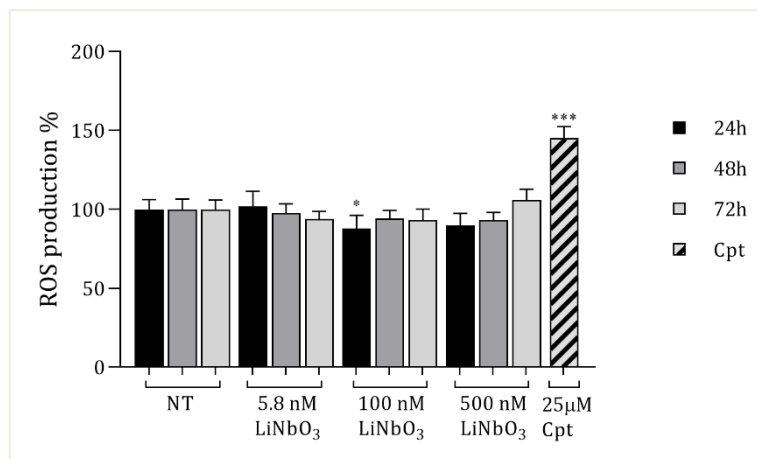


Fig. 24. DCFDA assay on differentiated PC12 cells treated with LiNbO₃ for 24, 48 and 72h at concentrations 5.8, 100 and 500 nM. Cells treated with cisplatin 25 μ M for 24h were used as positive control. The ROS production was expressed as mean value percent \pm SEM vs untreated cells (NT). Asterisks indicate significant differences in comparison to NT, with * = $p < 0.05$; *** = $p < 0.001$.

The results showed that the treatment with BaTiO₃ (Fig. 23) and LiNbO₃ (Fig. 24) did not induce any change in the amount of ROS produced by PC12 in comparison with untreated cells. On the contrary, the treatment with cisplatin significantly increased the amount of ROS produced by PC12 cells.

The variations on the expression of caspase 3 and PARP in differentiated PC12 cells were analysed by Western blot, to verify whether the treatment with BaTiO₃ and LiNbO₃ nanoparticles could induce apoptotic stimuli. Cells treated with cisplatin 25 µM for 24h were used as positive control.

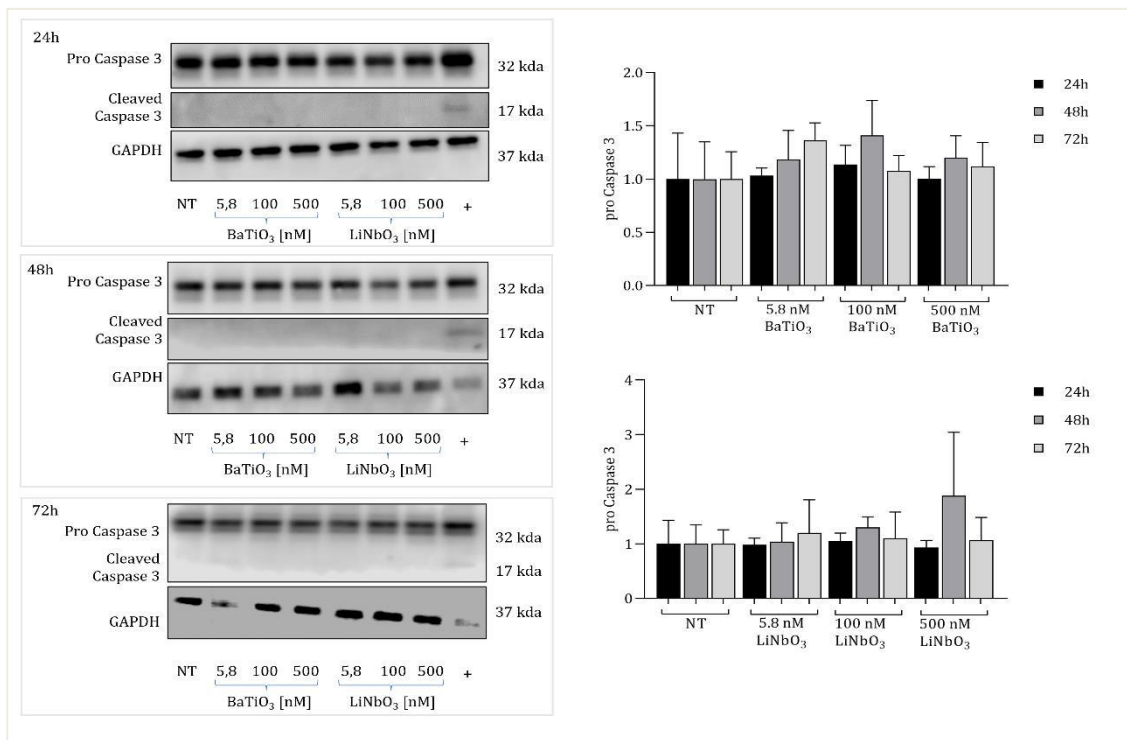


Fig. 25. Western blot and densitometric quantification of the apoptotic protein caspase 3, expressed on PC12 cells treated with BaTiO₃ and LiNbO₃ nanoparticles for 24, 48 and 72h at concentrations 5.8, 100 and 500 nM. Gliceraldeide-3-phosphate dehydrogenase (GAPDH) was used as housekeeping protein. Cisplatin 25 µM was used as positive control of apoptosis (+). All primary antibodies were diluted 1:1000. The densitometric analysis was performed with ImageJ and the results were expressed as mean value percent ± SEM *vs.* untreated cells (NT).

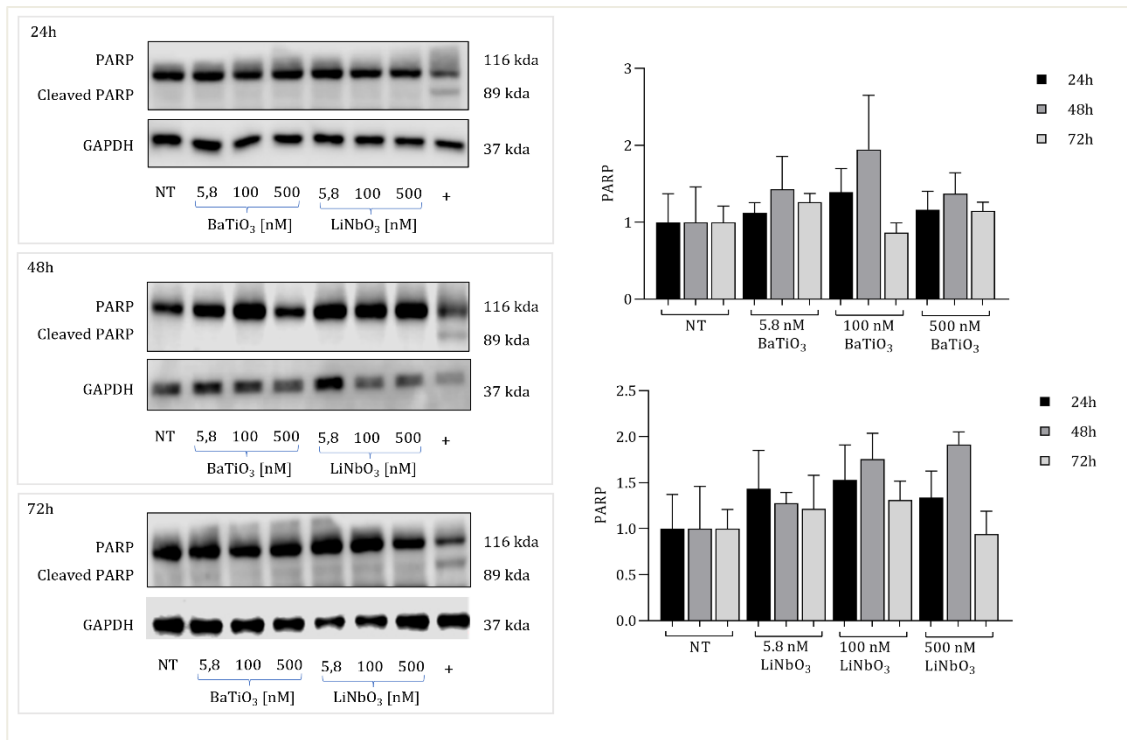


Fig. 26. Western blot and densitometric quantification of the apoptotic protein poly(ADP-ribose) polymerase (PARP), expressed on PC12 cells treated with BaTiO₃ and LiNbO₃ nanoparticles for 24, 48 and 72h at concentrations 5.8, 100 and 500 nM. Gliceraldeide-3-phosphate dehydrogenase (GAPDH) was used as housekeeping protein. Cisplatin 25 μ M was used as positive control of apoptosis (+). All primary antibodies were diluted 1:1000. The densitometric analysis was performed with ImageJ and the results were expressed as mean value percent \pm SEM *vs.* untreated cells (NT).

The results showed that the treatment with BaTiO₃ and LiNbO₃ did not induce significant changes on the expression of caspase 3 (Fig. 25) and PARP (Fig. 26) in differentiated PC12 cells in comparison with control cells. In addition, the cleaved forms of caspase 3 and PARP were absent in all samples tested except in the positive control. These results suggested that BaTiO₃ and LiNbO₃ nanoparticles did not induce apoptotic stimuli on neuronal cells.

Finally, to evaluate the neuromodulatory effect of BaTiO₃ and LiNbO₃ nanoparticles, the neurite outgrowth produced by PC12 cells was analysed, measuring the differentiation grade, the number of neurites per cell, the average length of neurites and the number of branch points. After differentiation, the PC12 cells were treated with the piezoelectric nanoparticles and, after the incubation times, thirty fields per treatment were acquired and analysed using the ImageJ software. Cells treated with cisplatin 13 μ M for 24, 48 and 72h were used as positive control of neurotoxicity (Fig. 27).

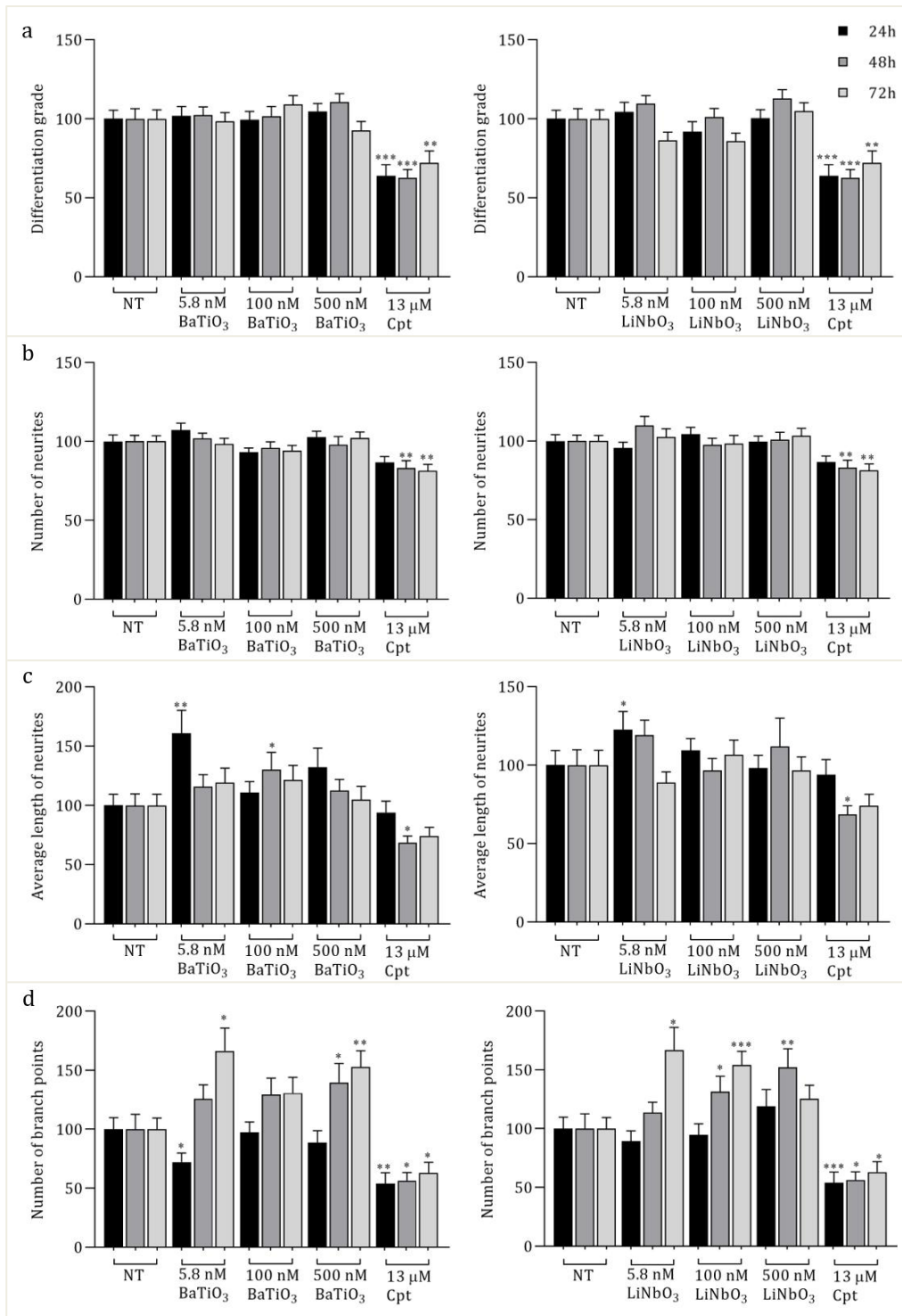


Fig.27. Analysis of neuronal outgrowth produced by differentiated PC12 cells treated with BaTiO₃ or LiNbO₃ for 24, 48, and 72h at concentrations 5.8, 100 and 500 nM. Cells treated with cisplatin were used as positive control (Cpt). After incubation, thirty fields per treatment were acquired at magnification 10X and analysed measuring the differentiation grade (a), the number of neurites per cells (b), the average length of neurites (c) and the number of branch points (d). The data were expressed as mean value percent \pm SEM vs. untreated cells (NT). Asterisks indicate significant differences in comparison to NT, with* = $p < 0.05$, ** = $p < 0.01$, *** = $p < 0.001$.

The summary of the results was the following:

- Differentiation grade (Fig. 27a): the treatment with BaTiO₃ and LiNbO₃ did not induce significant changes on the differentiation grade of PC12 cells at all time and doses tested. On the contrary, the treatment with cisplatin (positive control), significantly reduced the percentage of differentiated cells starting from 24h post treatment.
- Number of neurites per cell (Fig.27b): the treatment with BaTiO₃ and LiNbO₃ did not alter the number of neurites per cell at all time and doses tested. However, the treatment with cisplatin significantly reduced this number starting from 48h post treatment.
- Average length of neurites (Fig.27c): the treatment with BaTiO₃ at concentrations 5.8 nM after 24h and 100 nM after 48h significantly increased the average length of neurites. The treatment with LiNbO₃ did not affect this parameter but rather significantly increased it at concentration 5.8 nM after 24h. The treatment with cisplatin significantly reduced the average length of neurites after 48h.
- Number of branch points (Fig.27d): the treatment with BaTiO₃ nanoparticles significantly increased the number of branch points at concentration 500 nM starting from 48h post treatment. The treatment with BaTiO₃ at concentration 5.8 nM first significantly reduced the number of branches and then significantly increased this parameter at 72h.

The treatment with LiNbO₃ significantly increased the number of branch points at the highest concentrations tested (100 and 500 nM) after 48h and at concentrations 5.8 and 100 nM after 72h. On the contrary, the treatment with cisplatin significantly reduced the number of branch points produced by PC12 cells at all times tested.

These results showed that BaTiO₃ and LiNbO₃ nanoparticles did not induce apoptotic stimuli on the PC12 neuronal cell line.

5.3 Biocompatibility of materials involved in the new eardrum scaffolds

5.3.1 Biocompatibility of chitin nanofibrils

After the biocompatibility tests on piezoelectric nanoparticles, this project analysed the *in vitro* biocompatibility of all materials involved in the production of the innovative scaffolds to be used in the regeneration of the perforated eardrum (Fig. 28).

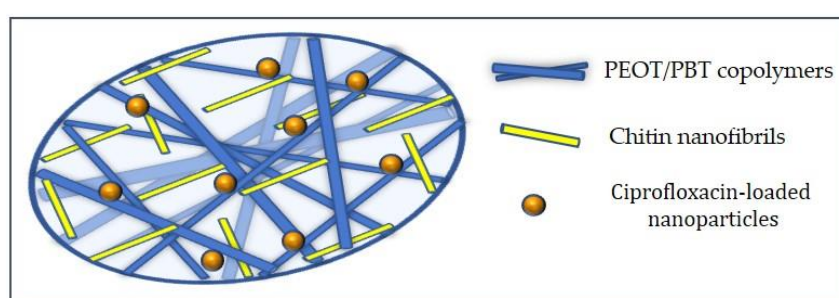


Fig. 28. Schematic representation of the biodegradable scaffold made of PEOT/PBT copolymers (blue fibres) containing chitin nanofibrils (yellow fibrils) and covered by ciprofloxacin loaded nanoparticles (orange spheres).

First, the cytotoxicity of a chitin nanofibril solution 2% in water was measured by CellTiter 96® AQueous MTS Reagent Powder (Promega, Milan, Italy), according to the manufacturer's suggestions. The cells were treated with chitin nanofibrils solution 2% in water at three different concentrations (5, 10 and 20µg/ml), as described in Materials and Methods.

The results showed that the treatment with chitin nanofibrils, at all time and doses tested, did not affect the OC-k3 cell viability in comparison with untreated cells (Fig. 29).

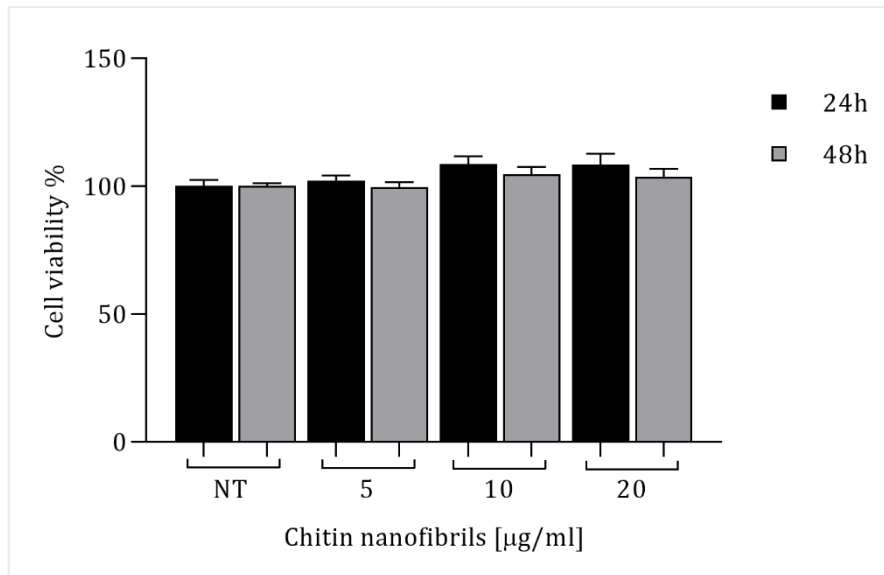


Fig. 29. Cell viability measured by direct method. The OC-k3 cells were seeded on PEOT/PBT copolymers loaded with CNs/PEG pre-composite at (50/50; 65/35; 70/30; 75/25) (w/w %) weight ratios. Cell viability was expressed as mean value percent \pm SEM *vs.* untreated cells (NT). Asterisks indicate significant differences in comparison to NT with * = $p < 0.05$, ** = $p < 0.01$, *** = $p < 0.001$.

5.3.2 Biocompatibility of PEOT/PBT copolymers

- Direct biocompatibility

To verify whether the substances released by nanocomposites could be toxic to inner ear cells, the biocompatibility of copolymers of poly (ethylene oxide terephthalate)/poly (butylene terephthalate) (PEOT/PBT) loaded with different (w/w %) weight ratios of CNs/PEG pre-composite (50/50; 65/35; 70/30; 75/25), was initially analysed using the MTS assay in the direct method, as described in Materials and Methods (Fig. 8).

The results showed that the viability of OC-k3 cells seeded in direct contact with the PEOT/PBT copolymers was reduced by about 30% in all samples tested after 24h. However, the viability was almost entirely recovered at 48h after the treatment (Fig. 30).

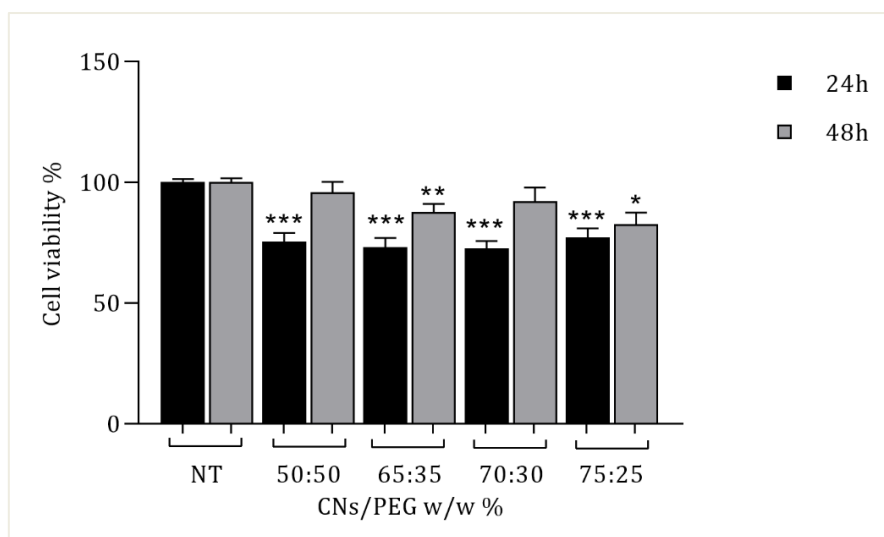


Fig. 30. MTS assay on OC-k3 cells treated for 24 and 48h with chitin nanofibrils solution 2% in water. Cell viability was expressed as mean value percent \pm SEM *vs.* untreated cells (NT).

- *Indirect biocompatibility*

Subsequently, the cytotoxicity of PEOT/PBT copolymers was assessed also by the indirect method, as described in Materials and Methods (Fig. 9), to evaluate the effect of released leachable substances on the viability of cochlear cells.

The OC-k3 cells were treated with conditioned media (media added with PEOT/PBT copolymers) for 24 and 48h. The results showed that the conditioned media of all samples tested did not affect the OC-k3 viability in comparison to control cells (Fig. 31).

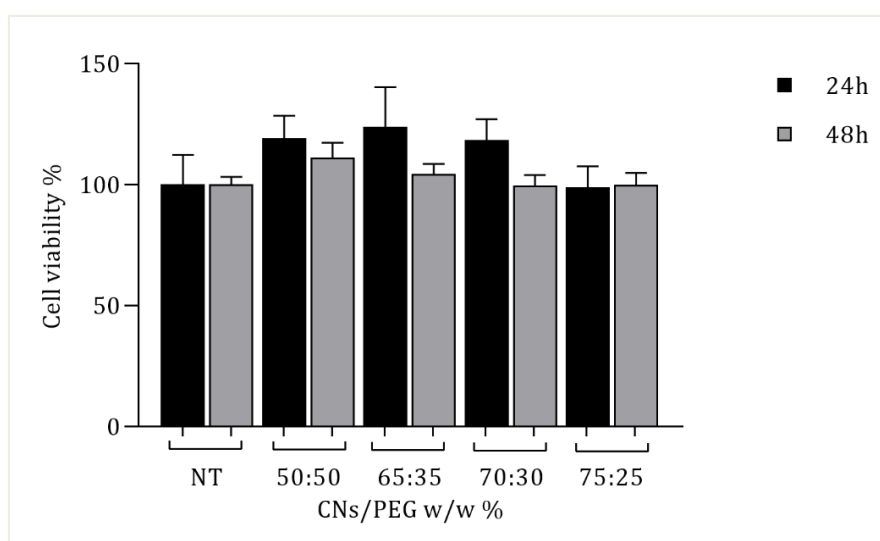


Fig. 31. Cell viability measured by indirect method. The OC-k3 cells were treated with conditioned media of PEOT/PBT copolymers loaded with CNs/PEG pre-composite at (50/50; 65/35; 70/30; 75/25) (w/w%) weight ratios. Cell viability was expressed as mean value percent \pm SEM *vs.* untreated cells (NT).

These results suggest that the PEOT/PBT / (CNs/PEG) nanocomposites are biocompatible for the OC-k3 cells. Nanocomposites could therefore be excellent candidates for use as patches in tympanic membrane transplantation because, even if the materials release leachable substances after implantation, these residues would not be toxic for inner ear cells.

5.3.3 *Biocompatibility of PLGA/PCL nanoparticles*

The effects of exposure to PLGA/PCL nanoparticles containing or not ciprofloxacin on the viability of OC-k3 cells was analysed by the MTS assay. The samples tested were:

- PLGA nanoparticles loaded with 200 µg/ml ciprofloxacin, prepared by the nanoprecipitation method (PLGA-Cipro);
- PLGA nanoparticles without ciprofloxacin, prepared by nanoprecipitation method (Blank PLGA);
- PCL nanoparticles loaded with 200 µg/ml ciprofloxacin (PCL-Cipro);
- PCL nanoparticles without ciprofloxacin (Blank PCL);
- PLGA nanoparticles loaded with 200 µg/ml ciprofloxacin, prepared by the water-oil-in water emulsion (w/o/w) method (PLGA-Cipro w/o/w);
- PLGA nanoparticles without ciprofloxacin, prepared by the w/o/w method (Blank PLGA w/o/w).

The OC-k3 cells were treated with ciprofloxacin-loaded nanoparticles and blank nanoparticles diluted in culture medium at concentrations 2, 20 and 40 µg/ml, for 24 and 48h.

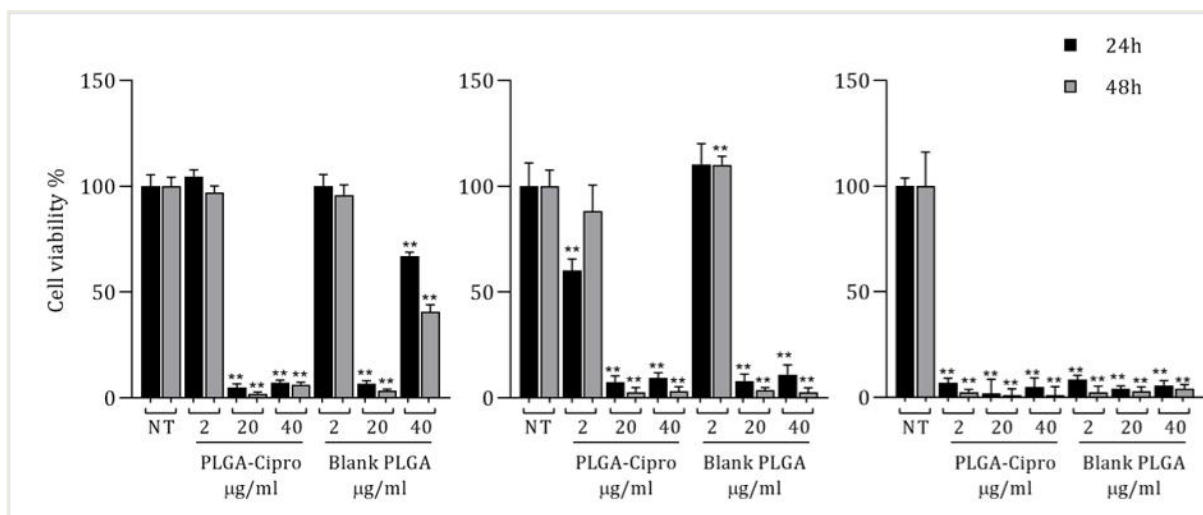


Fig. 32 MTS assay of OC-k3 cells treated with PLGA-Cipro, PCL-Cipro and PLGA-Cipro w/o/w, loaded with ciprofloxacin and blank nanoparticles (Blank PLGA, Blank PCL and Blank PLGA w/o/w) at 2, 20 and 40 µg/ml for 24 and 48 h. Cell viability was expressed as mean value percent ± standard error of mean (SEM) vs. untreated cells (NT). Asterisks indicate significant differences in comparison to NT, with ** = p<0.01.

The results showed that the treatment with the PLGA-Cipro and Blank PLGA prepared by the nanoprecipitation method significantly reduced cell viability starting from 20 µg/ml. The treatment with PCL-Cipro significantly reduced cell viability at all concentrations tested after 24h and at concentrations of 20 and 40 µg/ml after 48h. On the other hand, the treatment with Blank PCL significantly reduced cell viability at 20 and 40 µg/ml ciprofloxacin equivalent concentrations at both times tested. The lowest concentration, 2 µg/ml, did not affect cell viability after 24h and increased it after 48h. The treatment with PLGA-Cipro and Blank PLGA prepared by w/o/w method significantly reduced cell viability at all times and doses tested (Fig. 32).

The MTS assay was then repeated using lower concentrations of nanoparticles, from 20 to 0.02 µg/ml (Fig. 33). The results showed that the treatment with the PLGA-Cipro and Blank PLGA prepared by nanoprecipitation method, as well as with PCL-Cipro and Blank PCL, did not affect cell viability at both times tested in the concentration range 0.02 - 2 µg/ml. The PLGA-Cipro and Blank PLGA prepared by w/o/w method were non-toxic at 0.02µg/ml after 24 and 48h (Fig. 33).

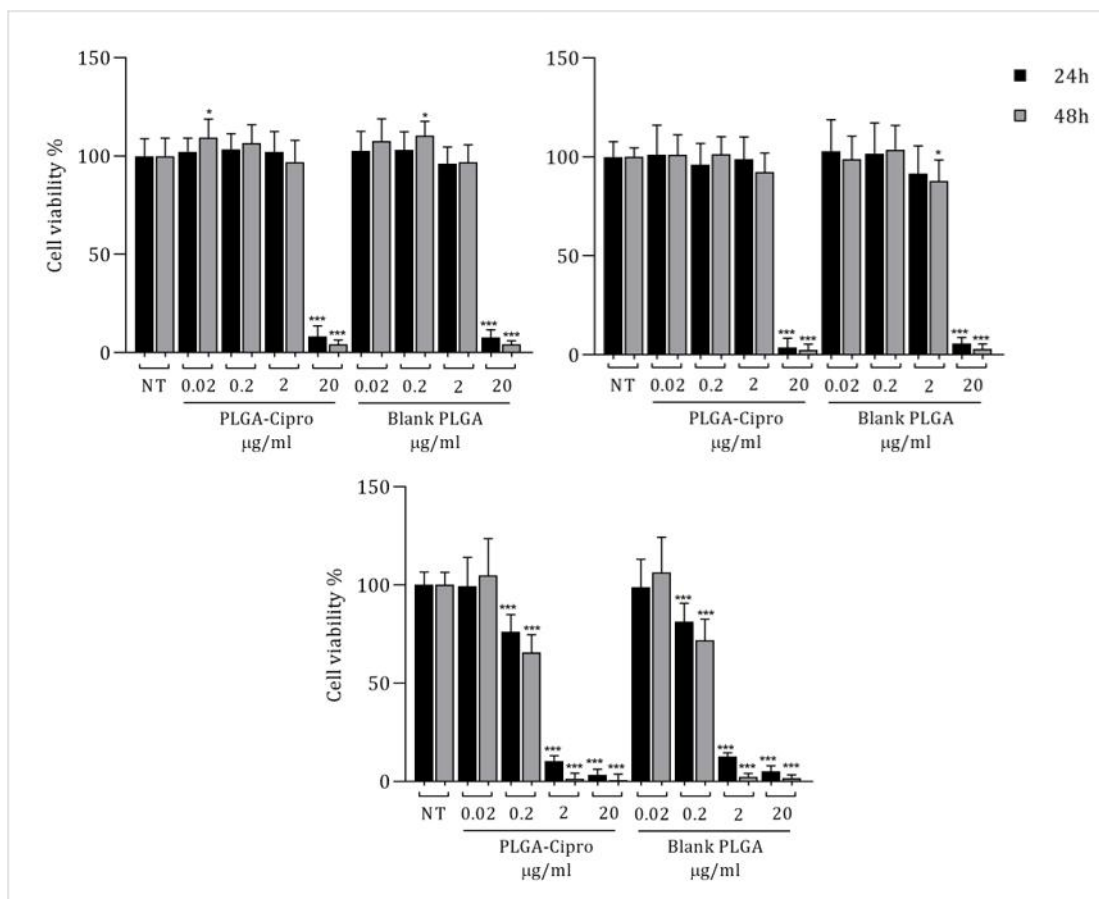


Fig. 33. MTS assay of OC-k3 cells treated with PLGA-Cipro, PCL-Cipro and PLGA-Cipro w/o/w, loaded with ciprofloxacin and blank nanoparticles (Blank PLGA, Blank PCL and Blank PLGA w/o/w) at 2, 20 and 40 µg/ml. Cell viability was expressed as mean value percent ± SEM vs. untreated cells (NT). Asterisks indicate significant differences in comparison to NT, with * = p< 0.05, *** = p<0.001.

After that, to verify whether these nanoparticles could induce any morphological changes on the OC-k3 cells, the phalloidin-DAPI staining was performed as described in Materials and Methods. The OC-k3 cells were treated for 24 and 48h with PLGA-Cipro and Blank PLGA prepared by nanoprecipitation (Fig. 34) and with PCL-Cipro and Blank PCL (Fig. 35) at concentrations 2 and 5 µg/ml. The OC-k3 cells were also treated with PLGA-Cipro and Blank PLGA prepared by w/o/w method for 24 and 48h, and the concentrations tested in these experiments were 0.2 and 2 µg/ml (Fig. 36).

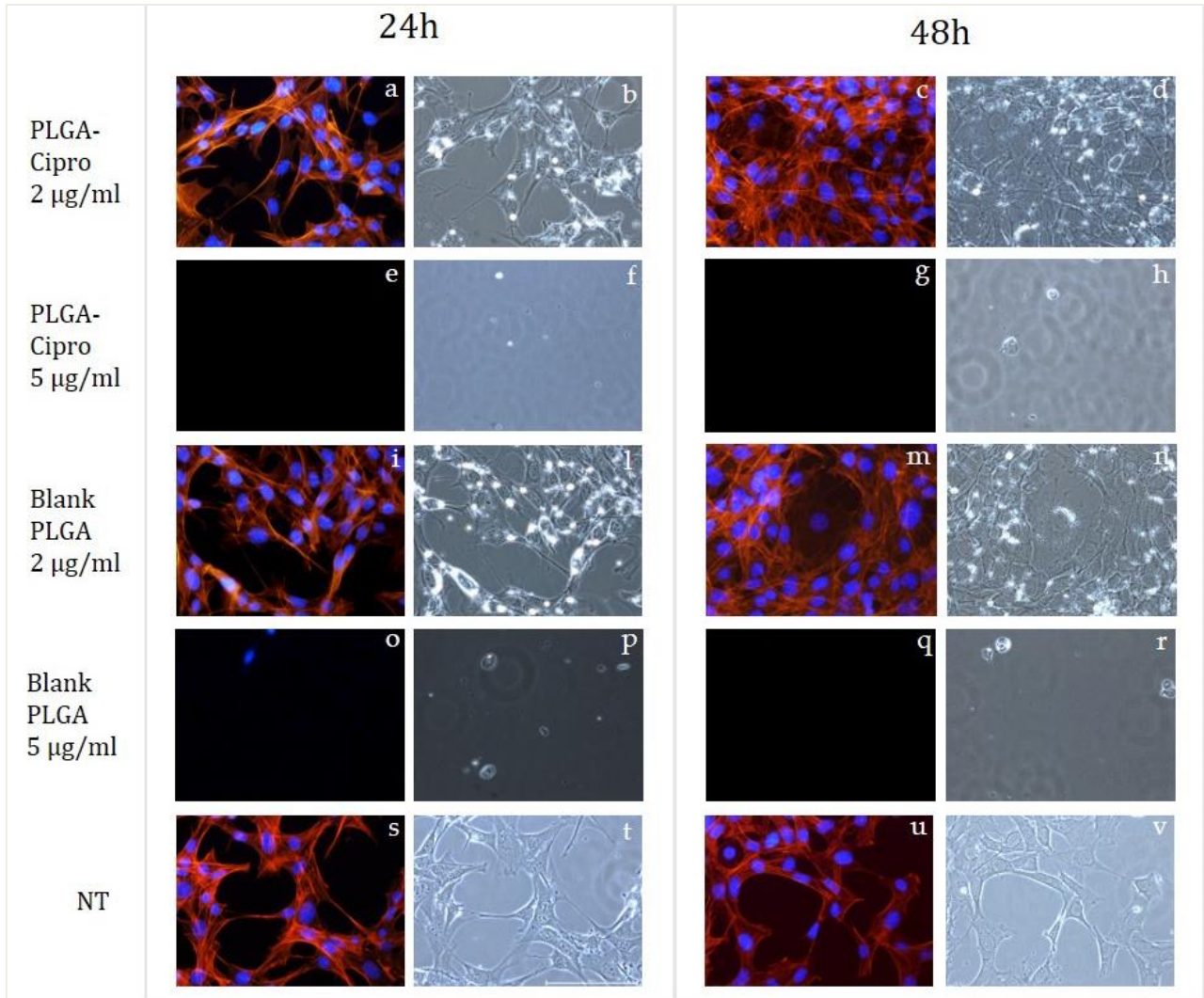


Fig. 34. Morphological analysis of OC-k3 cells treated for 24 and 48h with PLGA-Cipro and Blank PLGA nanoparticles prepared by nanoprecipitation method. The concentrations tested were 2 and 5 µg/ml. Phalloidin-TRITC (red) stains the actin filaments of the cytoskeleton; DAPI (blue) stains the A-T rich regions of nuclear DNA. Merged images (a, c, e, g, i, m, o, q, s, u) and bright field images (b, d, f, h, l, n, p, r, t, v) captured at 40X magnification, scale bar 100 µm.

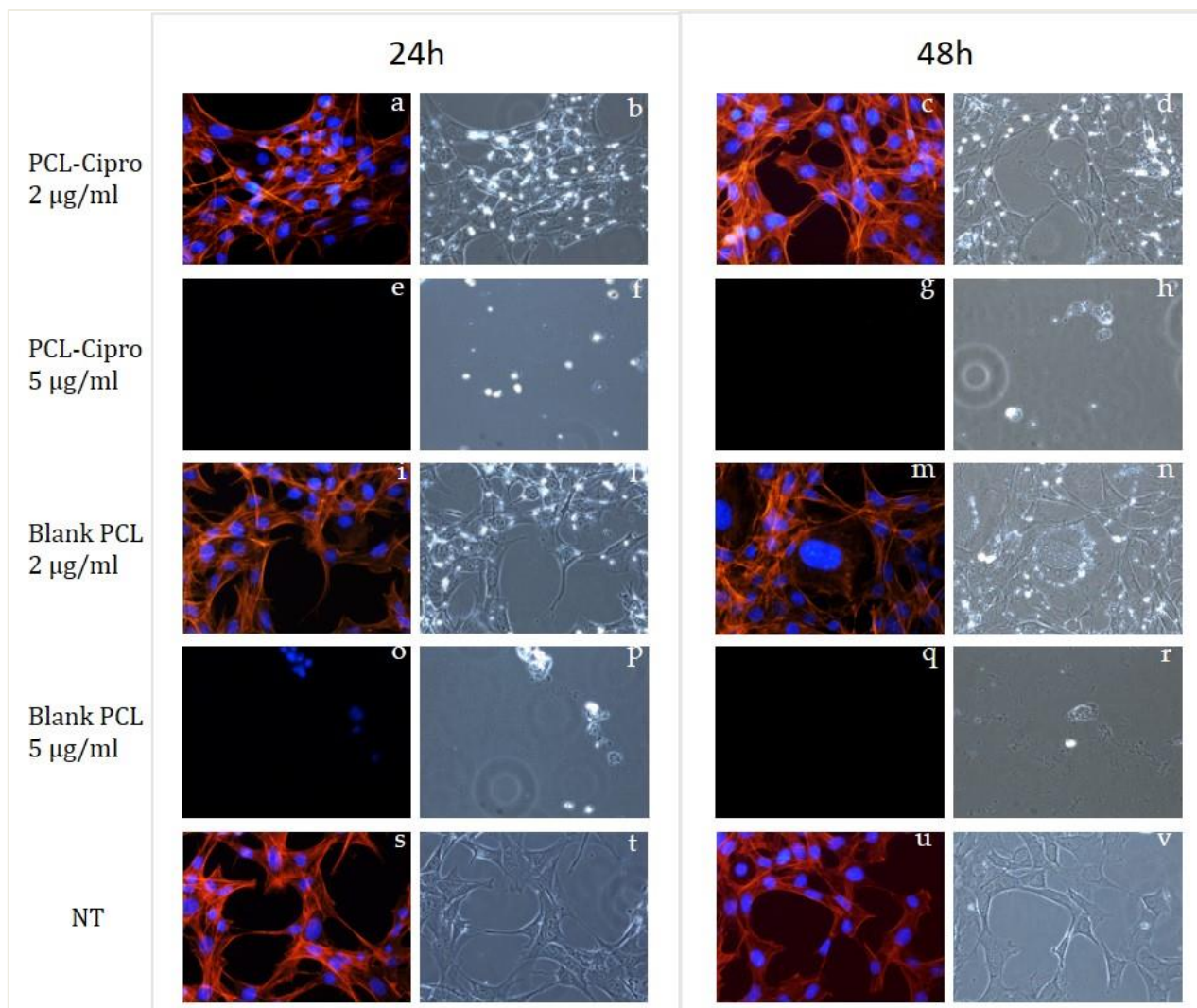


Fig. 35. Morphological analysis of OC-k3 cells treated for 24 and 48h with PCL-Cipro and Blank PCL nanoparticles. The concentrations tested were 2 and 5 $\mu\text{g/ml}$. Phalloidin-TRITC (red) stains the actin filaments of the cytoskeleton; DAPI (blue) stains the A-T rich regions of nuclear DNA. Merged images (a, c, e, g, i, m, o, q, s, u) and bright field images (b, d, f, h, l, n, p, r, t, v) captured at 40X magnification, scale bar 100 μm .

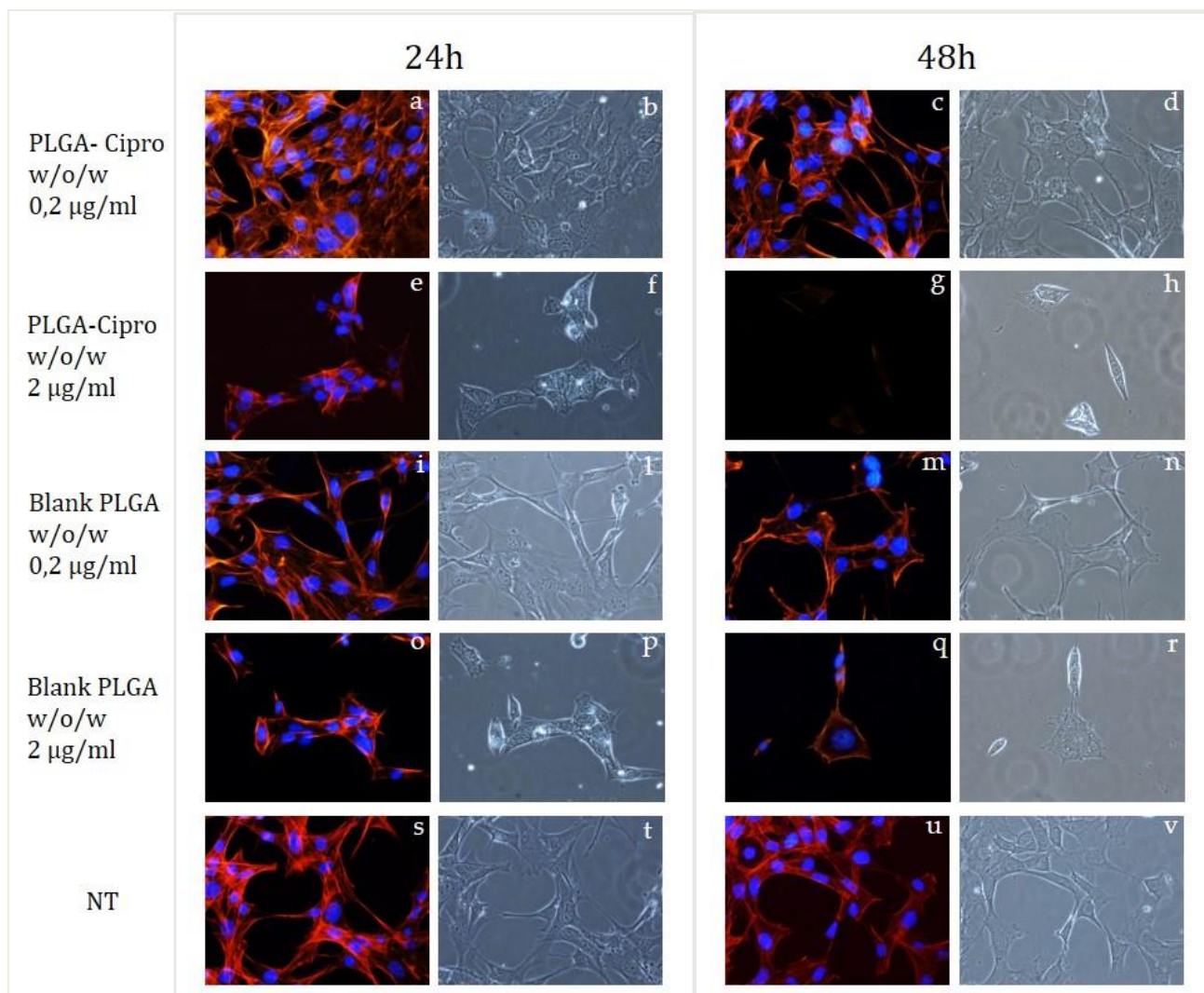


Fig. 36. Morphological analysis of OC-k3 cells treated for 24 and 48h with PLGA-Cipro and Blank PLGA prepared by w/o/w method. The concentrations tested were 0.2 and 2 µg/ml. Phalloidin-TRITC (red) stains the actin filaments of the cytoskeleton; DAPI (blue) stains the A-T rich regions of nuclear DNA. Merged images (a, c, e, g, i, m, o, q, s, u) and bright field images (b, d, f, h, l, n, p, r, t, v) captured at 40X magnification, scale bar 100 µm.

The results showed that the OC-k3 cells treated with PLGA-Cipro and Blank PLGA prepared by nanoprecipitation method (Fig. 34) and with PCL-Cipro and Blank PCL (Fig. 35) at concentration of 5 µg/ml, mostly died after 24h of exposure. However, the cells treated with the same nanoparticles at concentration 2 µg/ml did not show any signs of apoptosis at all times tested.

The OC-k3 cells treated with the PLGA-Cipro NP and Blank PLGA NP prepared by w/o/w method (Fig. 36) at concentration 2 µg/ml showed signs of apoptosis starting from 24h of

exposure. The treatment at concentration 0.2 µg/ml did not affect the morphological features of the OC-k3 cells.

Further cell viability tests were carried out using a wider range of concentrations, to identify the nanoparticle concentration able to cause a 50% reduction in cell growth (IC50), to verify if the IC50 was higher than the minimum inhibitory concentration of ciprofloxacin accepted against susceptible and resistant strains of *Pseudomonas aeruginosa* (0.25– 0.99 µg/ml), one of the most common bacteria affecting the respiratory tract (Günday et al., 2020).

The calculation of IC50 was performed using the software GraphPad Prism 8.0.1. (<https://www.graphpad.com/>) and the results are shown in Table 3.

Table 3. Values of IC50 (concentration of nanoparticles in µg/ml able to cause a 50% reduction in cell growth) on OC-k3 cells exposed for 24 and 48 h to PLGA/PCL nanoparticles (PLGA-Cipro, Blank PLGA, PCL-Cipro, Blank PCL, PLGA-Cipro w/o/w and Blank PLGA w/o/w), loaded or not with ciprofloxacin.

	PLGA- Cipro	Blank PLGA	PCL- Cipro	Blank PCL	PLGA-Cipro w/o/w	Blank PLGA w/o/w
IC50 24h	3.075	2.475	3.062	2.881	0.844	0.961
IC50 48H	2.825	2.059	2.791	2.599	0.388	0.455

Summarizing, the results showed that the PLGA-Cipro NP prepared by the nanoprecipitation method and the PCL-Cipro NP did not affect OC-k3 cells viability and morphology at ciprofloxacin concentrations between 0.2 and 2 µg/ml. The PLGA-Cipro NP prepared by the w/o/w method did not affect OC-k3 cells at ciprofloxacin concentration of 0.02 µg/ml. Moreover, the blank preparations of all nanoparticles tested did not affect cell viability at the same ciprofloxacin equivalent concentrations in comparison to ciprofloxacin-loaded nanoparticles. Therefore, according with the morphological analyses, the cytotoxic effects of the higher concentrations of nanoparticles are probably related to the different production methods used for each nanoparticle type.

5.3.4 Biocompatibility of MIPNP and NIPNP nanoparticles

The effects of exposure to molecularly imprinted polymer nanoparticles (MIPNP) and non-molecularly imprinted polymer nanoparticles (NIPNP) loaded or not with ciprofloxacin on the viability of OC-k3 cells was also analysed by MTS assay. The OC-k3 cells were treated for 24 and 48h with MIPNP loaded with ciprofloxacin (MIPNP-Cipro), MIPNP without ciprofloxacin (Blank MIPNP); NIPNP loaded with ciprofloxacin (NIPNP-Cipro), NIPNP without ciprofloxacin (Blank NIPNP). The concentrations tested were 2, 20 and 40 $\mu\text{g/ml}$. The viability of OC-k3 cells was also tested by MTS assay after exposure to ciprofloxacin powder at three different concentrations (2, 20 and 40 $\mu\text{g/ml}$) for 24 and 48h.

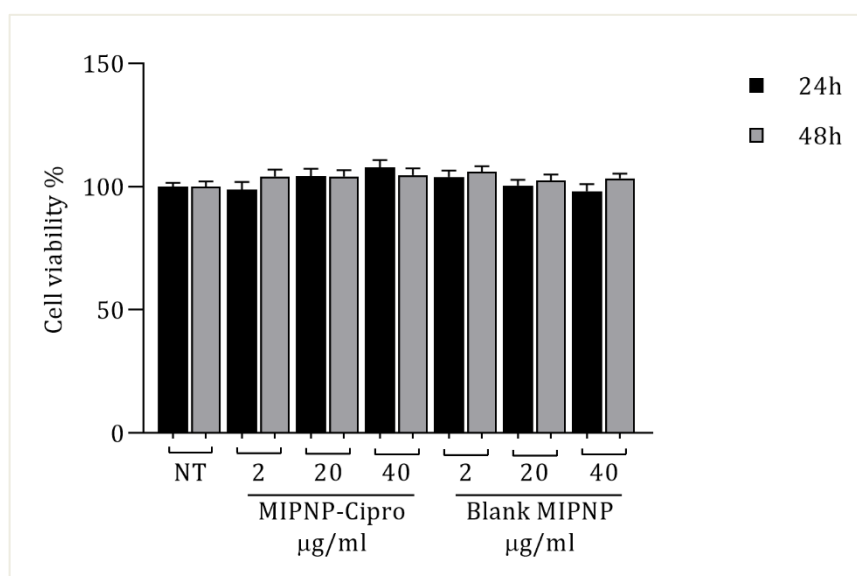


Fig. 37. MTS assay of OC-k3 cells treated with MIPNP-Cipro and Blank MIPNP for 24 and 48h. The concentrations tested were 2, 20 and 40 $\mu\text{g/ml}$. Cell viability was expressed as mean value percent \pm SEM *vs.* untreated cells (NT).

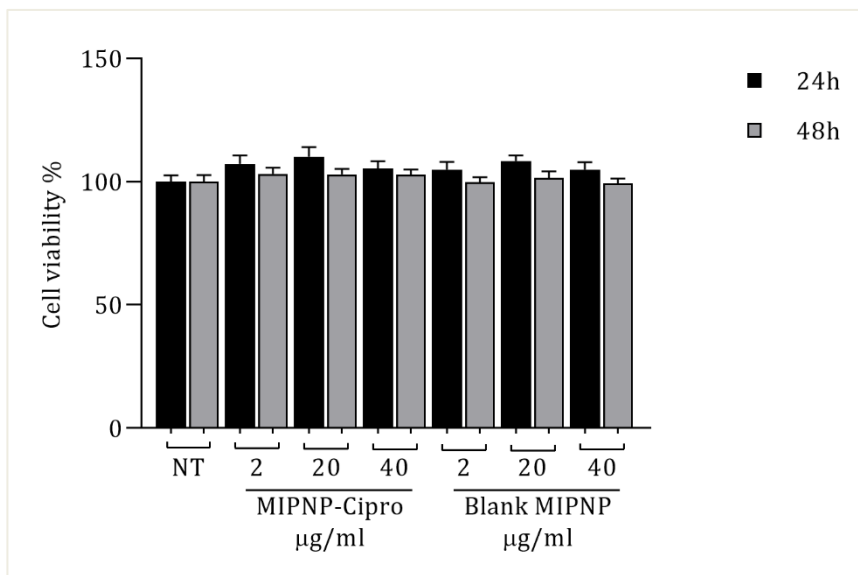


Fig. 38. MTS assay of OC-k3 cells treated with NIPNP-Cipro and Blank NIPNP for 24 and 48h. The concentrations of tested were 2, 20 and 40 µg/ml. Cell viability was expressed as mean value percent \pm SEM *vs.* untreated cells (NT).

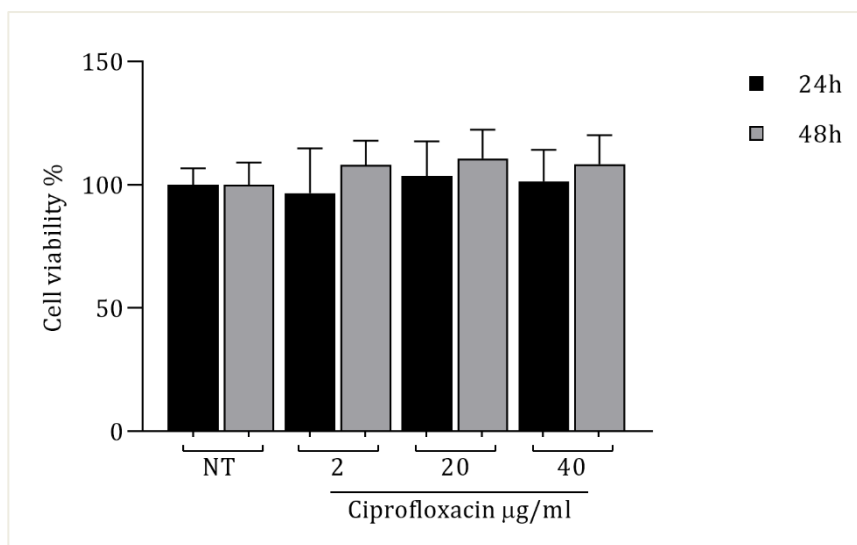


Fig. 39. MTS assay of OC-k3 cells treated with ciprofloxacin powder for 24 and 48h at concentrations 2, 20 and 40 µg/ml. Cell viability was expressed as mean value percent \pm SEM *vs.* untreated cells (NT).

The results showed that the treatment with MIPN- Cipro and Blank MIPNP (Fig. 37), with NIPNP-Cipro and Blank NIPNP (Fig. 38) and ciprofloxacin (Fig. 39), at all times and doses tested, did not induce any change on the OC-k3 viability in comparison with untreated cells.

The phalloidin-DAPI staining was subsequently performed to analyse the effects of these nanoparticles on the morphology of OC-k3 cells. The OC-k3 cells were treated with MIPNP-Cipro and Blank MIPNP, with NIPNP-Cipro and Blank NIPNP, and with ciprofloxacin at the highest concentration tested (40 $\mu\text{g/ml}$) for 24 h and 48h.

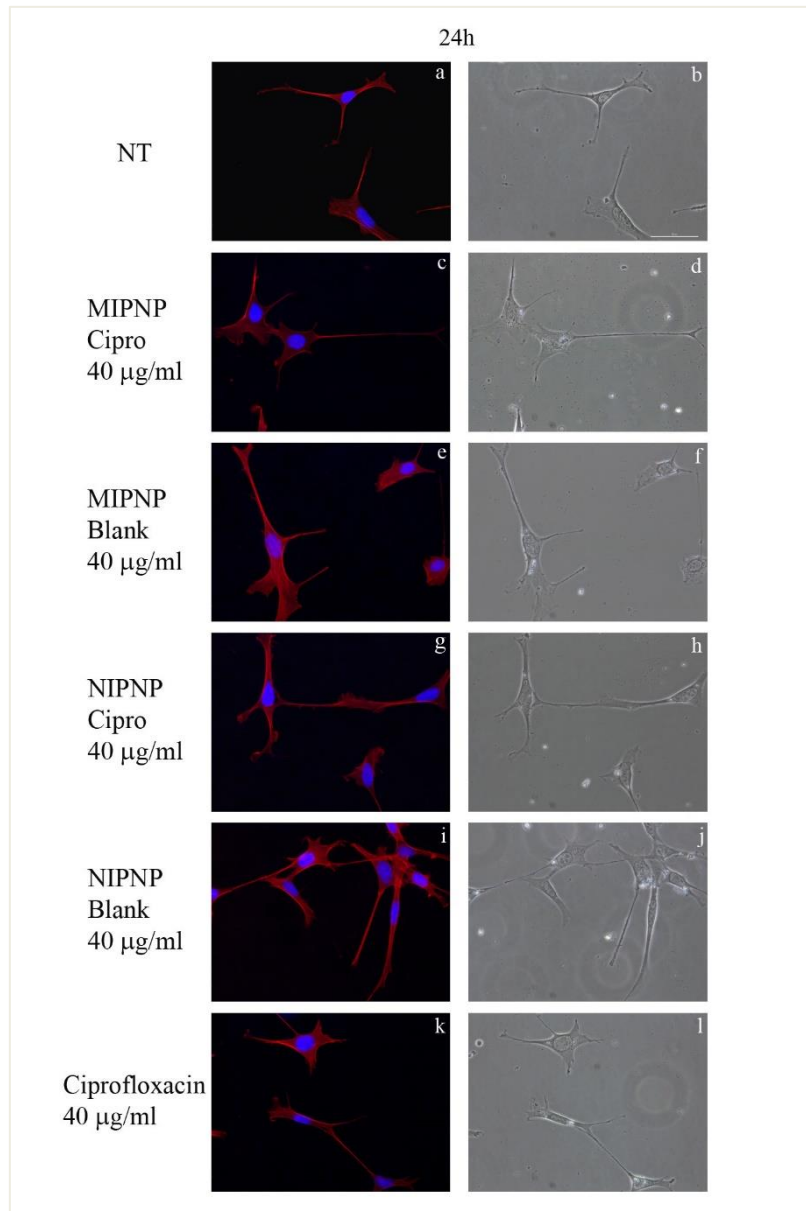


Fig. 40. Morphological analysis of OC-k3 cells treated with MIPNP- Cipro and Blank MIPNP, NIPNP-Cipro and Blank NIPNP, and ciprofloxacin powder (40 $\mu\text{g/ml}$) for 24h. Phalloidin-TRITC (red) stains the actin filaments of the cytoskeleton; DAPI (blue) stains the A-T rich regions of nuclear DNA. Merged images (a, c, e, g, i, k) and bright field images (b, d, f, h, j, l) captured at 40X magnification, scale bar 100 μm .

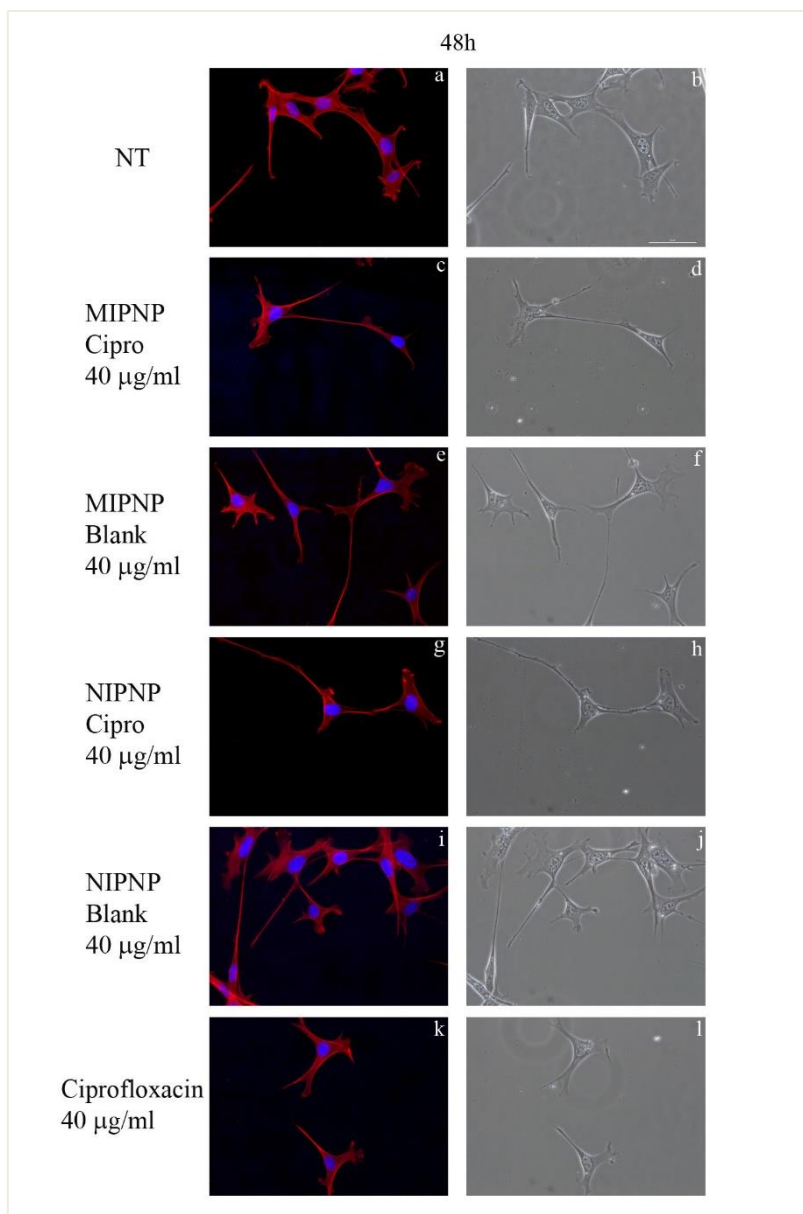


Fig. 41. Morphological analysis of OC-k3 cells treated with MIPN- Cipro and Blank MIPNP, NIPNP-Cipro and Blank NIPNP, and ciprofloxacin powder (40 µg/ml) for 48h. Bright field images (b, d, f, h, j, l). Phalloidin-TRITC (red) stains the actin filaments of the cytoskeleton; DAPI (blue) stains the A-T rich regions of nuclear DNA. Merged images (a, c, e, g, i, k) and bright field images (b, d, f, h, j, l) captured at 40X magnification, scale bar 100 µm.

The results showed that the treatment with MIPN-Cipro and Blank MIPNP, NIPNP-Cipro and Blank NIPNP, and ciprofloxacin powder, at concentration of 40 µg/ml did not affect the morphological features of the OC-k3 cells, after 24 (Fig. 40) and 48h (Fig. 41). The actin filaments of the cytoskeleton appeared well extended and the nuclei were round with no signs of pyknosis.

6. Discussion

Recovery from sensory neural hearing loss (SNHL) requires the implantation of a cochlear implant (CI) that stimulates the cochlear nerve, bypassing damaged sensory cells (Ciorba et al., 2009; Giordano et al., 2014). The CI helps deaf population to rediscover the joy of sound, but the implantation of this device has a lot of disadvantages related to its construction and it is often accompanied by medical side effects that lead to explant (Astolfi et al., 2016; Knipper et al., 2020; Simoni et al., 2020; Van de Heyning et al., 2020).

This study is part of a project involving the production of a new “self-powered” device for cochlear stimulation based on piezoelectric nanomaterials. The device is made of electrospun fibres containing polyvinylidene difluoride (PVDF), a piezoelectric polymer already known to be biocompatible and very flexible (He et al., 2021), to which piezoelectric nanoparticles will be added (Mota et al., 2017; Danti et al., 2020). The piezoelectric materials are already used as scaffolds in many applications due to their biocompatibility and ability to stimulate tissue regeneration (Yu et al., 2016; Mota et al., 2017; Li et al., 2019; Ahmadi et al., 2020; Danti et al., 2020). Furthermore, by producing an electric field, the piezoelectric materials are able to stimulate neuronal extension and proliferation, bone formation and repair, and cellular migration (Rajabi et al., 2015). The present study analysed the *in vitro* biocompatibility of two piezoelectric nanoparticles, barium titanate (BaTiO_3) and lithium niobate (LiNbO_3), on two different cell lines, the OC-k3 and the PC12, to investigate the possible use of these nanoparticles in the construction of the innovative implantable device, without affecting the delicate inner ear cells.

Barium titanate (BaTiO_3) is a piezoelectric ceramic currently used in a wide variety of applications including electronic (Uhl and Andrew, 2020) and electro-optical devices, and transducers (Jiang et al., 2019). The ferroelectric property of this material was discovered in 1945 (Wul, 1946), but its use in biomedical application was investigated only in the last ten years (Ciofani et al., 2010a). To date, BaTiO_3 has been shown to be biocompatible for several cell lines (Genchi et al., 2016), and is currently used in drug delivery systems (Ciofani et al., 2010a) and wireless neuronal stimulation (Marino et al., 2015).

The results presented in this thesis showed that BaTiO₃ nanoparticles did not affect the viability of OC-k3 cells and significantly increased the viability of PC12 cells. These data are in agreement with previous studies that showed increased cell viability and proliferation on human neuroblastoma SH-SYY cell line and rat mesenchymal stem cells treated with glycol-chitosan coated BaTiO₃ nanoparticles (Ciofani et al. 2010a; 2013).

Moreover, the treatment with BaTiO₃ did not affect cell morphology and the amount of ROS produced by both cell lines analysed, confirming that these nanoparticles did not enhance cell oxidative stress, as previously found on mesenchymal stem cells (Ciofani et al., 2013).

The apoptosis is a high-energy requiring program that leads to cell death in physiological and pathological processes and is activated through intrinsic and extrinsic pathways (Smyth et al., 2002; Ward et al., 2008). The apoptotic markers for *in vitro* detection of cell death include an increase in caspase 3 activity, the cleavage of PARP, a decrease in cellular metabolism and the release of cytochrome c from the mitochondria (Smyth et al., 2002). The results obtained in this thesis showed that BaTiO₃ nanoparticles did not induce significant changes on the expression of caspase 3 and PARP proteins in OC-k3 and differentiated PC12 cells. Furthermore, the cleaved forms of both proteins were absent in all samples tested except the positive control. In the same way, the immunocytochemical analysis showed a homogeneous distribution of cytochrome c within the cytoplasm of treated cells. These results showed that BaTiO₃ did not induce apoptotic stimuli on OC-k3 and PC12 cell lines.

The *in vitro* neurotoxicity tests are widely used to pre-screen materials that should not induce *in vivo* side effects. The assessment of neuronal outgrowth is one of the most common methods used to analyse the effects of new materials on neurons because, although neurotoxin is expected to alter many cellular processes including proliferation, differentiation or synapse formation, the neuronal morphology is a key structure for neuronal connectivity (Radio et al., 2008).

The results of this thesis showed that the treatment with BaTiO₃ at all time and doses tested did not affect the differentiation grade and the neurite number in PC12 cells. Furthermore,

the treatment with BaTiO₃, at concentration of 5.8 nM after 24h, and 100 nM after 48h, significantly increased the average length of neurites. These data are in agreement with a previously study showing an increase in the length and number of neurites on differentiated PC12 cells treated with another type of piezoelectric nanostructure, the boron nitride nanotubes (BNNT) (Ciofani et al., 2010b).

Concerning the neurite branching, the treatment with BaTiO₃ at the highest concentration tested (500 nM) significantly increased this parameter starting from 48h post treatment. The treatment with BaTiO₃ at concentration of 5.8 nM first significantly reduced the number of branches and then significantly increased it at 72h. These data suggest that BaTiO₃ nanoparticles increase the complexity of the neuritic network produced by PC12 cells and, combined with the non-toxicity detected by other tests, show the biocompatibility of barium titanate nanoparticles for cochlear and neuronal cells.

Lithium niobate (LiNbO₃) is a ceramic with many properties, among which ferroelectricity, pyroelectricity and piezoelectricity (Meinan et al., 2006; Kamali and Fray, 2014). These properties make this material useful in many applications such as acoustic wave transducers, memory elements and optical phase modulators (Weis and Gaylord, 1985). The use of LiNbO₃ in biomedical applications has been investigated only recently (Vilarinho et al., 2014), and to date there are few studies on its biocompatibility (Carville et al., 2015; Marchesano et al. 2015).

The results presented in this thesis showed that LiNbO₃ did not affect the viability of OC-k3 cells and significantly increased the viability of PC12 cells starting from 24h post treatment. The degree of cell differentiation is known to influence cellular reactions (Ekshyyan and Aw, 2005; Mendonça et al., 2013), for example by exposure to ROS (Sasaki et al., 2001) or chemotherapeutic drugs (Sakagami et al., 2018). The greater biocompatibility of LiNbO₃ nanoparticles obtained in this study could be explained by the different medium used for cell differentiation, which could have modified the response of PC12 to treatment by improving their neuronal characteristics.

Moreover, the treatment with LiNbO₃ nanoparticles did not affect the morphological features and the amount of ROS produced by OC-k3 and PC12 cells. These data are in agreement with previous studies that analysed the cellular response of mouse embryonic fibroblasts (NIH-3t3) (Marchesano et al., 2015), rat bone marrow mesenchymal stem cells (rBMMSCs) (Li J. et al., 2015) and osteoblasts cells (MC3T3) (Carville et al., 2015) seeded on the LiNbO₃ crystal surface. These studies showed that the charged surface of LiNbO₃ enhanced cell proliferation without changing the morphological characteristic of cells.

Concerning the induction of apoptotic stimuli, the results obtained in this thesis showed that LiNbO₃ nanoparticles did not induce significant changes on the expression of caspase 3 and PARP proteins in OC-k3 cells and differentiated PC12 cells. The cleaved forms of both proteins were absent in all samples tested except in the positive control, and the immunocytochemical analysis showed a homogeneous distribution of cytochrome c within the cytoplasm of treated cells. These results showed that LiNbO₃ did not induce apoptotic stimuli on OC-k3 and PC12 cell lines.

The evaluation of neuronal outgrowth in PC12 cells treated with LiNbO₃ nanoparticles showed that the piezoelectric nanomaterials did not affect the degree of differentiation, the number of neurites per cell and the average length of neurites, which was actually increased at concentration 5.8 nM after 24h. Moreover, the number of branch points was significantly increased at the highest concentrations tested (100 and 500 nM) after 48h, and at 5.8 and 100 nM after 72h. These data are consistent with a previous study analysing the neuronal outgrowth of PC12 cells treated with iron oxide nanoparticles. The study detected an increase in neurite length and number, and proved the neuromodulatory effect of metal ions on neurons (Kim et al., 2011).

In conclusion, barium titanate and lithium niobate did not induce any cytotoxic or apoptotic effects on neuronal and cochlear cells, but rather increased cell viability and enhanced the neuritic network. It is known that PC12 cell differentiation may occur by NGF stimulation, which activates the mitogen-activated protein kinases/extracellular signal regulated kinases (MAPK-ERK) pathway, or by the adenylyl cyclase (AC) pathway, which in turn may be

triggered by an increase in extracellular calcium concentration (Hoop et al., 2017). Piezoelectric substances under mechanical stimulation generate electrical charges, which, by increasing the amount of extracellular Ca^{2+} , stimulate the increase of neuronal network through the AC pathway (Brosenitsch and Katz, 2001; Huang et al., 2010). This suggests that the use of piezoelectric nanoparticles on neurons of the cochlear ganglion could induce an increase in the ability of neurons to reach the target inner ear hair cells.

The piezoelectric nanoparticles BaTiO_3 and LiNbO_3 are therefore biocompatible for inner ear cells and are good candidates for improving the efficiency of new implantable hearing devices without damaging the neurons. Overall, these results confirm that the electric stimulation has neuromodulatory effects on neurons (Schlaug et al., 2008; Latchoumane et al., 2018) and highlight the importance of developing new scaffolds coated with piezoelectric nanoparticles, that could be exploited in the treatment of neuronal diseases.

Another common ear disorder that affects many people around the world is the perforation of the tympanic membrane (Hawkins, 2020; Sundar et al., 2021). Along life, this thin membrane can be damaged or perforated (Bevis et al., 2021). In the case of severe perforation, the surgical treatments currently used are the myringoplasty and tympanoplasty, but unfortunately both techniques have suboptimal results (Hong et al., 2013; Sagiv et al., 2020;).

This study is part of a project involving the production of new biodegradable scaffolds for use in tympanic membrane healing processes. These innovative biocompatible devices have the purpose to facilitate healing process of damaged tympanic membrane, by enhancing the proliferation and migration of keratinocytes, and by reducing the middle ear inflammatory state and the incidence of infections during the wound healing process.

These new scaffolds need to be implanted in the middle ear, so it is possible that the materials used will release leachable substances that could reach the inner ear, altering the delicate cochlear balance and causing hearing disorders. Therefore, the second part of this doctoral thesis focused on the *in vitro* analysis of the biocompatibility on OC-k3 cells of

different materials and nanoparticles involved in the construction of these new biodegradable scaffolds.

Chitin is the second most abundant polysaccharide after cellulose and together with its deacetylated derivative chitosan, is widely used in biomedical applications due to its biocompatibility, biodegradability and antimicrobial properties (Elieh-Ali-Komi and Hamblin, 2016). From chitin, nanofibrils can be prepared which are able to lose their allergenic action and acquire anti-inflammatory effects (Danti et al, 2021). The chitin nanofibrils are able to disperse well in biopolymers and are widely used in many applications, for example in food packaging, as anti-microbial agents (de Azeredo, 2013), in the production of anti-age cosmetics (Danti et al., 2019) and in the construction of new medical tools for wound healing (Muzzarelli et al., 2007). The cytotoxicity tests reported in this thesis showed that the treatment with chitin nanofibrils in water solution did not affect OC-k3 cell viability at all times and doses tested in comparison with untreated cells. These data are in agreement with those of previous studies describing the biocompatibility and ability of chitin and chitosan products to stimulate the attachment, proliferation and viability of tissues and stem cells (Muzzarelli et al., 2007; 2009). The chitin nanofibrils may therefore facilitate the eardrum healing process, without inducing toxic effects on OC-k3 cells.

The project involved the incorporation of chitin nanofibrils (CN) through the electrospinning/electrospray technique into a scaffold made of poly (ethylene oxide-terephthalate)/poly (butylene terephthalate) (PEOT/PBT) copolymers. The PEOT/PBT electrospun scaffolds are known to be suitable for eardrum applications and are well tolerated by human mesenchymal stem cells (hMSCs) (Mota et al., 2015; Danti et al., 2021). The combination with chitin nanofibrils aims to develop a biodegradable and biocompatible device, able not only to mimic the mechanical features of eardrum, but also to stimulate the healing process, reducing the inflammatory state and enhancing the antibacterial activity after the implantation (Danti et al., 2021). The viability of OC-k3 cells was analysed by direct and indirect methods to verify the biocompatibility of PEOT/PBT copolymers loaded with

different weigh ratios of CNs/ polyethylene glycol (PEG) pre-composite. The results showed that the viability of OC-k3 cells seeded in direct contact with the PEOT/PBT copolymers was reduced by approximately 30% in all samples tested after 24h but, despite these results, viability was almost entirely recovered at 48h from the treatment. These data are in agreement with those of a previous study analysing the metabolic activity of hMSCs seeded on PEOT/PBT/(CN/PEG 50:50). The results of this study showed a reduction in metabolic activity after 24h, which was then recovered (Danti et al., 2021). Therefore, the reduction on the viability of OC-k3 cells seeded in direct contact with the nanocomposites could be related to the effect of the surface of the materials. On the other hand, the indirect biocompatibility tests showed that the conditioned media of all samples tested did not affect the OC-k3 viability at all times and doses tested, demonstrating that the nanocomposites did not release any toxic compounds. These data showed that the PEOT/PBT/(CNs/PEG) nanocomposites are biocompatible for the OC-k3 cells because, even if the scaffolds were able to release leachable substances after implantation, these residues would not be toxic for inner ear cells.

Ear infections are the most common disorders affecting head and neck (Yang et al., 2021) and among them, otitis media is one of the common inflammatory disease that can cause the perforation of tympanic membrane (Massa et al., 2021). The PEOT/PBT copolymers, in combination with chitin nanofibrils, acquire the ability to reduce the inflammatory state after implantation but, to prevent infections during the healing process and reduce the possible implant rejection, the incorporation of an antibacterial compound may be necessary (Günday et al., 2020). In case of ear infections, the use of antibiotics is required and one of the most commonly used is ciprofloxacin, a third-generation fluorinated quinolone with wide-spectrum antibiotic activity against the most common Gram-positive and Gram-negative bacteria (Wall et al., 2009).

The studies related to this project involved the addition of ciprofloxacin-loaded nanoparticles to the surface of these PEOT/PBT electrospun scaffolds, in order to obtain, by an *in situ* release of ciprofloxacin, an enhanced implantation outcome and a reduction of

side effects caused by systemic antibiotic administration (Khorshidi and Karkhaneh, 2018; Günday et al., 2020).

The poly (lactic-co-glycolic acid) (PLGA) is one of the most widely used materials in drug delivery, along with polycaprolactone (PCL). Both are biocompatible and biodegradable polymers, already approved in human clinical trials by Food and Drug Administration (FDA) and European Medicines Agency (EMA). These polymers are currently used in biomedicine, drug delivery, and cancer therapy to transport several types of drugs, including chemotherapeutics (paclitaxel, cisplatin), diabetes drugs (insulin), antibiotics (doxorubicin), and antifungals (amphotericin) (Kumari et al., 2010; Witt et al., 2019; Günday et al., 2020).

This thesis analysed the biocompatibility of PLGA nanoparticles prepared by the nanoprecipitation or the w/o/w method, and of PCL nanoparticles, loaded or not with ciprofloxacin. The results showed that the PLGA nanoparticles loaded with ciprofloxacin (PLGA-Cipro) prepared by the w/o/w method did not affect OC-k3 cells at ciprofloxacin concentration 0.02 µg/ml. The PLGA-Cipro nanoparticles prepared by the nanoprecipitation method and the PCL-Cipro nanoparticles did not affect OC-k3 cells viability and morphology at ciprofloxacin concentrations between 0.2 and 2 µg/ml. Moreover, the blank preparations of all nanoparticles tested did not affect cell viability at the same equivalent ciprofloxacin concentrations compared to the ciprofloxacin-loaded nanoparticles. Therefore, the cytotoxic effects of the highest concentrations of nanoparticles are probably related to the different production methods used for each type of nanoparticle. These data agree with those reported on a study performed on human immortalized keratinocytes (HaCat), and human mesenchymal stem cells (hMSCs) (Günday et al., 2020). Thus, the PLGA-Cipro prepared by nanoprecipitation method and the PCL-Cipro nanoparticles are biocompatible for OC-k3 cells, with an IC₅₀ value higher than the minimum inhibitory concentration (MIC) of ciprofloxacin accepted against susceptible and resistant strains of *Pseudomonas aeruginosa* (0.25– 0.99 µg/ml), one of the most common bacteria affecting the respiratory tract (Günday et al., 2020). These data therefore suggest that these nanoparticles

could be used for drug delivery in the production of the innovative scaffold for regeneration of the tympanic membrane.

Another strategy for drug delivery under investigation is based on the use of the molecular imprinting polymers (MIP), compounds able to specifically bind the molecular target, mimicking the “lock and key” process that normally occurs in physiological reactions (Fresco-Cala et al, 2020). The MIPs represent an innovation in molecular recognition and are currently used for many applications, among which purification, bioimaging, and immunoassays (Zhang, 2020). The nanosize forms of MIP (nanoparticles), with homogeneous dimensions and shapes, attracted interest for *in vitro* and *in vivo* tests as substitute of enzymes or very expensive antibodies in diagnostic and therapeutic applications, and in drug delivery (Canfarotta et al., 2018; Refaat et al., 2019; Fresco-Cala et al, 2020).

In this thesis, the effects of the MIP and NIP nanoparticles containing or not ciprofloxacin were analysed on viability of cochlear cells, to verify the possible use of these nanoparticles for long-term drug delivery of antibiotic in the construction of the biodegradable device for regeneration of the tympanic membrane. The imprinted polymer nanoparticles, produced with a specific binding site for ciprofloxacin, will slowly release the antibiotic after the implantation, extending the residency and the efficacy of the drug in the middle ear (van Nostrum, 2005). The use of MIP nanoparticles in drug delivery systems was first reported in 1998 (Norell et al., 1998) and to date several studies tested these innovative nanomaterials in different medical fields (Zhang, 2020). A previous study showed that soft lens produced using the molecularly imprinted technique, are promising drug devices, since they were able to enhance the release of timolol in terms of in time and concentration in comparison with non-imprinted contact lenses (Hiratani et al., 2005).

In the same way, a recent study showed by *in vitro* and *in vivo* tests the efficacy of MIP nanoparticles as targeted systems of chemotherapeutic drug delivery in cancer therapy (Asadi et al., 2016).

The MIP and NIP nanoparticles tested in this thesis did not affect the viability and the morphological characteristics of OC-k3 cells at all times and doses tested, suggesting a high biocompatibility of these nanoparticles for cochlear cells. These data are in accordance with previous studies that analysed the cytotoxicity induced by MIP nanoparticles, showing that these nanomaterials did not affect the viability of HaCat, human fibrosarcoma (HT1080), and mouse embryonic fibroblasts (MEF) cells (Canfarotta et al., 2016). These results therefore confirm the biocompatibility of molecularly imprinted polymer nanoparticles and increase the knowledge about their interactions with cells, underlining the importance to develop innovative nanomaterials that will improve the efficacy of current therapeutic approaches.

7. Conclusions

Overall, the results obtained in this project showed the biocompatibility of the piezoelectric nanoparticles barium titanate and lithium niobate on the OC-k3 and the PC-12 cell lines. These nanoparticles actually increased the cell viability and positively influenced the neuritic network produced by the neuron-like cells. These nanoparticles could therefore be used in the construction of an innovative self-powered cochlear implant, without inducing any cytotoxic effect on inner ear cells and neurons. This self-powered CI, exploiting the piezoelectric features of these nanomaterials, could simulate the physiological process of hearing, allowing a better sensitivity and quality of life in deaf population, and reducing the side effects related to the implantation of common cochlear devices.

The effects of barium titanate and lithium niobate on the transmission of action potential are still unclear. A previous study reported that barium titanate nanoparticles were associated to the neurite membrane in human neuroblastoma SY5Y5Y cell line and, in combination with ultrasonic stimulation (US), were able to stimulate the calcium influx and values of voltage compatible with those required for the activation of neural voltage-gated channels (Genchi et al., 2016). Therefore, it would be interesting to investigate in the future

how barium titanate and lithium niobate interact with PC12 cells, and whether these nanoparticles are internalized and remain attached to the cell membrane, or are positioned more internally. Another study showed that PC12 cells differentiated with NGF could develop functional K⁺ and tetrodotoxin (TTX) sensitive Na⁺ channels, fundamental to initiate the action potential (Yang et al., 2011). By using the patch clamp technique, it could be interesting to analyse the amount of Na⁺ and K⁺ channels present on the membrane of differentiated PC12 cells, and analyse the effect of barium titanate and lithium niobate nanoparticles on the cellular polarization. These data would further increase the current knowledge on the biocompatibility of piezoelectric nanoparticles on the neuronal cell line and could open new perspectives for the use of these nanomaterials in the regeneration of damaged neuronal networks.

The perforation of the tympanic membrane is one of the most common ear disorders affecting people worldwide, and the medical procedures currently used have suboptimal outcome. The tissue engineering is currently working on the production of innovative devices that could finally raise medicine to a higher level, increasing the quality of life of patients and reducing the costs and time of medical procedures (Sagiv et al., 2020; Danti et al., 2021). The results collected in this thesis, showed the biocompatibility of all materials involved in the production of the innovative biodegradable scaffold made of PEOT/PBT copolymers, containing chitin nanofibrils (CNs), and covered by ciprofloxacin loaded nanoparticles, on an inner ear cell line. In a previous study was shown that the incorporation of chitin nanofibrils in electrospun scaffolds made of PEOT/PBT reduced the inflammation and enhanced the immune response in HaCat cells, a model of eardrum epithelial cells (Danti et al., 2021). Therefore, this device could finally modify the current approaches used to heal a perforated eardrum, combining different materials that enhance the healing process, preventing the side effects related to the current medical procedures.

The production of this biodegradable scaffold involves the chitin, that is easily extractable from food industry waste (Naghdi et al., 2020), and the ciprofloxacin that is delivered directly into the middle ear, using two different types of nanoparticles that are innovative

and cost effective. The molecular imprinted polymeric nanoparticles represent a promising technology in diagnostic and therapeutic applications. In addition, these nanoparticles are cheaper and more effective than the currently used antibodies (Canfarotta et al., 2018; Refaat et al., 2019; Fresco-Cala et al, 2020). Therefore, this innovative tympanic membrane scaffold will reduce drug administration and medical costs while improving the efficacy of the healing process and the quality of life of patients. Although further tests are needed to fully elucidate the effects of these materials, the construction of these biodegradable scaffolds could therefore be a great advantage in repairing a damaged tympanic membrane, without inducing any toxic effects on the delicate inner ear cells, and definitely changing the medical approach and patients' recovery.

8. Bibliografy

- Ahmadi N., Kharaziha M., Labbaf S., 2020. Core-shell fibrous membranes of PVDF-Ba_{0.9}Ca_{0.1}TiO₃/PVA with osteogenic and piezoelectric properties for bone regeneration. *Biomed. Mater.* 15: 015007. <https://doi.org/10.1088/1748-605X/ab5509>.
- Alikin D., Turygin A., Kholkin A., Shur V., 2017. Ferroelectric domain structure and local piezoelectric properties of lead-free (K_{0.5}Na_{0.5})NbO₃ and BiFeO₃-based piezoelectric Ceramics. *Materials (Basel, Switzerland)*. 10: 47. <https://doi.org/10.3390/ma10010047>.
- An Y.K., Kim M.K., Sohn H., 2014. Piezoelectric transducers for assessing and monitoring civil infrastructures. In: *Woodhead Publishing Series in Electronic and Optical Materials, Sensor Technologies for Civil Infrastructures*, Woodhead Publishing. 55: 86-120. <https://doi.org/10.1533/9780857099136.86>.
- Asadi E., Abdouss M., Leblanc R.M., Ezzati N., Wilson J.N., Azodi-Deilami, S., 2016. In vitro/in vivo study of novel anti-cancer, biodegradable cross-linked tannic acid for fabrication of 5-fluorouracil-targeting drug delivery nano-device based on a molecular imprinted polymer. *RSC Adv.* 6: 37308-37318. <https://doi.org/10.1039/C6RA03704F>.
- Astolfi L., Guaran V., Marchetti N., Olivetto E., Simoni E., Cavazzini A., Jolly C., Martini A., 2014. Cochlear implants and drug delivery: In vitro evaluation of dexamethasone release. *J. Biomed. Mater. Res. Part B.* 102B: 267-273. <https://doi.org/10.1002/jbm.b.33004>.
- Astolfi L., Simoni E., Giarbini N., Giordano P., Pannella M., Hatzopoulos S., Martini A., 2016. Cochlear implant and inflammation reaction: Safety study of a new steroid-eluting electrode. *Hear Res.* 336: 44-52. <https://doi.org/10.1016/j.heares.2016.04.005>.

- Astolfi L., Simoni E., Martini A., 2015. OC-k3 cells, an in vitro model for cochlear implant biocompatibility. *Hear. Balance Commun.* 13: 166-174, <https://doi.org/10.3109/21695717.2015.1063232>.
- Azimi B., Milazzo M., Lazzeri A., Berrettini S., Uddin M.J., Qin Z., Buehler M.J., Danti S., 2020. Electrospinning piezoelectric fibers for biocompatible devices. *Adv. Healthc. Mater.* 9: 1901287. <https://doi.org/10.1002/adhm.201901287>.
- Ball J.P., Mound B.A., Nino J.C., Allen J.B., 2014. Biocompatible evaluation of barium titanate foamed ceramic structures for orthopedic applications. *J. Biomed. Mater. Res. Part A.* 102: 2089-2095. <https://doi.org/10.1002/jbm.a.34879>.
- Bevis N., Sackmann B., Effertz T., Lauxmann M., Beutner D., 2021. The impact of tympanic membrane perforations on middle ear transfer function. *Eur. Arch. Otorhinolaryngol.* <https://doi.org/10.1007/s00405-021-07078-9>.
- Brosenitsch T.A., and Katz D.M., 2001. Physiological patterns of electrical stimulation can induce neuronal gene expression by activating N-type calcium channels. *J. Neurosci.* 21: 2571-2579. <https://doi.org/10.1523/JNEUROSCI.21-08-02571.2001>.
- Campoli-Richards D.M., Monk J.P., Price A., Benfield P., Todd P.A., Ward A., 1988. Ciprofloxacin. A review of its antibacterial activity, pharmacokinetic properties and therapeutic use. *Drugs* 35: 373-447. <https://doi.org/10.2165/00003495-198835040-00003>.
- Canfarotta F., Cecchini A., Piletsky S., 2018. Nano-sized molecularly imprinted polymers as artificial antibodies. (chapter 1). In: *Molecularly Imprinted Polymers for Analytical Chemistry Applications*. pp. 1-27. <https://doi.org/10.1039/9781788010474-00001>.
- Canfarotta F., Waters A., Sadler R., McGill P., Guerreiro A., Papkovsky D., Haupt K., Piletsky S., 2016. Biocompatibility and internalization of molecularly imprinted nanoparticles. *Nano Res.* 9: 3463–3477. <https://doi.org/10.1007/s12274-016-1222-7>.

- Carreiro J.E., 2009. Otolaryngology. (Chapter 11). In: *An Osteopathic Approach to Children* (second edition). Churchill Livingstone, pp. 185–196. <https://doi.org/10.1016/B978-0-443-06738-9.00011-3>.
- Carville N.C., Collins L., Manzo M., Gallo K., Lukasz B.I., McKayed K.K., Simpson J.C., Rodriguez B.J., 2015. Biocompatibility of ferroelectric lithium niobate and the influence of polarization charge on osteoblast proliferation and function. *J. Biomed. Mater. Res. Part A*. 103A: 2540-2548. <https://doi.org/10.1002/jbm.a.35390>.
- Chen S., Liu B., Carlson M.A., Gombart A.F., Reilly D.A., Xie J., 2017. Recent advances in electrospun nanofibers for wound healing. *Nanomedicine* 12: 1335-1352. <https://doi.org/10.2217/nnm-2017-0017>.
- Ciofani G., Danti S., D'Alessandro D., Moscato S., Petrini M., Menciassi A., 2010a. Barium titanate nanoparticles: highly cytocompatible dispersions in glycol-chitosan and doxorubicin complexes for cancer therapy. *Nanoscale Res. Lett.* 5: 1093-1101. <https://doi.org/10.1007/s11671-010-9607-0>.
- Ciofani G., Danti S., D'Alessandro D., Ricotti L., Moscato S., Bertoni G., Falqui A., Berrettini S., Petrini M., Mattoli V., Menciassi A., 2010b. Enhancement of neurite outgrowth in neuronal-like cells following boron nitride nanotube-mediated stimulation. *ACS Nano*. 4: 6267-77. <https://doi.org/10.1021/nn101985a>.
- Ciofani G., Ricotti L., Canale C., D'Alessandro D., Berrettini S., Mazzolai B., Mattoli V., 2013. Effects of barium titanate nanoparticles on proliferation and differentiation of rat mesenchymal stem cells. *Colloids Surf. B. Biointerfaces*. 102: 312-320. <https://doi.org/10.1016/j.colsurfb.2012.08.001>.
- Ciorba A., Astolfi L., Jolly, C., Martini, A., 2009. Cochlear implants and inner ear based therapy. *Eur. J. Nanomed.* 2: 25-28. <https://doi.org/10.1515/EJNM.2009.2.2.25>.

- Cohen N.L. and Hoffman R.A., 1991. Complications of cochlear implant surgery in adults and children. *Ann. Otol. Rhinol. Laryngol.* 100: 708-711. <https://doi.org/10.1177/000348949110000903>.
- Cory A.H., Owen T.C., Barltrop J.A., Cory J.G., 1991. Use of an aqueous soluble tetrazolium/formazan assay for cell growth assays in culture. *Cancer Commun.* 3: 207-212. <https://doi.org/10.3727/095535491820873191>.
- Danti S., Anand S., Azimi B., Milazzo M., Fusco A., Ricci C., Zavagna L., Linari S., Donnarumma G., Lazzeri A., Moroni L., Mota C., Berrettini S., 2021. Chitin nanofibril application in tympanic membrane scaffolds to modulate inflammatory and immune response. *Pharmaceutics.* 13: 1440. <https://doi.org/10.3390/pharmaceutics13091440>.
- Danti S., Azimi B., Candito M., Fusco A., Sorayani Bafqi M.S., Ricci C., Milazzo M., Cristallini C., Latifi M., Donnarumma G., Bruschini L., Lazzeri A., Astolfi L., Berrettini S., 2020. Lithium niobate nanoparticles as biofunctional interface material for inner ear devices. *Biointerphases.* 15: 031004. <https://doi.org/10.1116/6.0000067>.
- Danti S., Mota C., D'alessandro D., Trombi L., Ricci C., Redmond S.L., De Vito A., Pini R., Dilley R.J., Moroni L., Berrettini S., 2015. Tissue engineering of the tympanic membrane using electrospun PEOT/PBT copolymer scaffolds: A morphological in vitro study. *Hear. Balance Commun.* 13: 133-147. <https://doi.org/10.3109/21695717.2015.1092372>.
- Danti S., Trombi L., Fusco A., Azimi B., Lazzeri A., Morganti P., Coltelli M.B., Donnarumma G., 2019. Chitin nanofibrils and nanolignin as functional agents in skin regeneration. *Int. J. Mol. Sci.* 20: 2669. <https://doi.org/10.3390/ijms20112669>.
- de Azeredo H.M.C., 2013. Antimicrobial nanostructures in food packaging. *Trends Food Sci. Technol.* 30: 56–69. <https://doi.org/10.1016/j.tifs.2012.11.006>.
- Deschamps A.A., van Apeldoorn A.A., Hayen H., de Bruijn J.D., Karst U., Grijpma D.W., Feijen J., 2004. In vivo and in vitro degradation of poly(ether ester) block copolymers

based on poly(ethylene glycol) and poly(butylene terephthalate). *Biomaterials*. 25: 247-258. [https://doi.org/10.1016/s0142-9612\(03\)00495-2](https://doi.org/10.1016/s0142-9612(03)00495-2).

Dolhi N. and Weimer A.D., 2021. Tympanic Membrane Perforations. [Updated 2021 Aug 11] In: StatPearls [Internet]. Treasure Island (FL): StatPearls Publishing; 2021 Jan-. <https://www.ncbi.nlm.nih.gov/books/NBK557887/>.

Ekshyyan O. and Aw T., 2005. Decreased susceptibility of differentiated PC12 cells to oxidative challenge: relationship to cellular redox and expression of apoptotic protease activator factor-1. *Cell Death Differ*. 12: 1066-1077. <https://doi.org/10.1038/sj.cdd.4401650>.

Elieh-Ali-Komi D. and Hamblin M.R., 2016. Chitin and chitosan: production and application of versatile biomedical nanomaterials. *Int. J. Adv. Res. (Indore)*. 4: 411-427. PMID: 27819009; PMCID: PMC5094803.

Elsayed M.A. and Norredin A., 2019. The potential contribution of nanoparticles in the treatment of inflammatory diseases. In: *Translational Studies on Inflammation*, IntechOpen. <https://doi.org/10.5772/intechopen.84776>.

Eshraghi A.A., Nazarian R., Telischi F.F., Rajguru S.M., Truy E., Gupta C., 2012. The cochlear implant: historical aspects and future prospects. *Anat. Rec. (Hoboken)*. 295: 1967-1980. <https://doi.org/10.1002/ar.22580>.

EU Directive. 2011. Directive 2011/65/EU of the European Parliament and of the Council of 8 June 2011 on the restriction of the use of certain hazardous substances in electrical and electronic equipment (recast). 02011L0065 -EN- 01.04.2021- 014.001. <http://data.europa.eu/eli/dir/2011/65/2021-04-01>.

Fresco-Cala B., Batista AD., Cárdenas S., 2020. Molecularly imprinted polymer micro- and nano-particles. A review. *Molecules*. 25: 4740. <https://doi.org/10.3390/molecules25204740>.

- Genchi G.G., Marino A., Rocca A., Mattoli V., Ciofani G., 2016. Barium titanate nanoparticles: promising multitasking vectors in nanomedicine. *Nanotechnology*. 27: 232001. <https://doi.org/10.1088/0957-4484/27/23/232001>.
- Giordano P., Hatzopoulos S., Giarbini N., Prosser S., Petruccioli J., Simoni E., Faccioli C., Astolfi L., Martini A., 2014. A soft-surgery approach to minimize hearing damage caused by the insertion of a cochlear implant electrode: a Guinea pig animal model. *Otol. Neurotol*. 35: 1440-1445. <http://dx.doi.org/10.1097/MAO.0000000000000440>.
- Greene L.A., Tischler A.S., 1976. Establishment of a noradrenergic clonal line of rat adrenal pheochromocytoma cells which respond to nerve growth factor. *Proc. Natl. Acad. Sci. USA*. 73: 2424-8. <https://doi.org/10.1073/pnas.73.7.2424>.
- Günday C., Anand S., Gencer HB., Munafò S., Moroni L., Fusco A., Donnarumma G., Ricci C., Hatir PC., Türeli NG., Türeli AE., Mota C., Danti S., 2020. Ciprofloxacin-loaded polymeric nanoparticles incorporated electrospun fibers for drug delivery in tissue engineering applications. *Drug Deliv. Transl. Res.* 10: 706-720. <https://doi.org/10.1007/s13346-020-00736-1>.
- Guo H.F., Li Z.S., Dong S.W., Chen W.J., Deng L., Wang Y.F., Ying D.J., 2012. Piezoelectric PU/PVDF electrospun scaffolds for wound healing applications. *Colloids Surf. B. Biointerfaces*. 96: 29-36. <https://doi.org/10.1016/j.colsurfb.2012.03.014>.
- Haile L.M., Kamenov K., Briant P.S., Orji A.U., Steinmetz J.D., Abdoli A., Abdollahi M., Abu-Gharbieh E., Afshin A., Ahmed H., ... Vos T., Chadha S., 2021. Hearing loss prevalence and years lived with disability, 1990–2019: findings from the Global Burden of Disease Study 2019. *The Lancet*. 397: 996–1009. [https://doi.org/10.1016/S0140-6736\(21\)00516-X](https://doi.org/10.1016/S0140-6736(21)00516-X).
- Hanks C.T., Wataha J.C., Sun Z., 1996. In vitro models of biocompatibility: a review. *Dent Mater*. 12: 186-93. [https://doi.org/10.1016/s0109-5641\(96\)80020-0](https://doi.org/10.1016/s0109-5641(96)80020-0).

- Hashemikia S., Farhangpazhouh F., Parsa M., Hasan M., Hassanzadeh A., Hamidi M., 2021. Fabrication of ciprofloxacin-loaded chitosan/polyethylene oxide/silica nanofibers for wound dressing application: in vitro and in vivo evaluations. *Int. J. Pharm.* 597: 120313. <https://doi.org/10.1016/j.ijpharm.2021.120313>.
- Hawkins J.E., 2020. "Human ear". *Encyclopedia Britannica*. <https://www.britannica.com/science/ear>. Accessed: March, 2021.
- He Z., Rault F., Lewandowski M., Mohsenzadeh E., Salaün F., 2021. Electrospun PVDF nanofibers for piezoelectric applications: a review of the influence of electrospinning parameters on the β phase and crystallinity enhancement. *Polymers*. 13: 174. <https://doi.org/10.3390/polym13020174>.
- Hiratani H., Fujiwara A., Tamiya Y., Mizutani Y., Alvarez-Lorenzo C., 2005. Ocular release of timolol from molecularly imprinted soft contact lenses. *Biomaterials* 26: 1293-1298. <https://doi.org/10.1016/j.biomaterials.2004.04.030>.
- Hong P., Bance M., Gratzner P.F., 2013. Repair of tympanic membrane perforation using novel adjuvant therapies: a contemporary review of experimental and tissue engineering studies. *Int. J. Pediatr. Otorhinolaryngol.* 77: 3-12. <https://doi.org/10.1016/j.ijporl.2012.09.022>.
- Hoop M., Chen XZ., Ferrari A., Mushtaq F., Ghazaryan G., Tervoort T., Poulidakos D., Nelson B., Pané S., 2017. Ultrasound-mediated piezoelectric differentiation of neuron-like PC12 cells on PVDF membranes. *Sci. Rep.* 7: 4028. <https://doi.org/10.1038/s41598-017-03992-3>.
- Hoshino Y., Koide H., Urakami T., Kanazawa H., Kodama T., Oku N., Shea K.J., 2010. Recognition, neutralization, and clearance of target peptides in the bloodstream of living mice by molecularly imprinted polymer nanoparticles: a plastic antibody. *J. Am. Chem. Soc.* 132: 6644-6645. <https://doi.org/10.1021/ja102148f>.

- Hu R., Cao Q., Sun Z., Chen J., Zheng Q., Xiao, F., 2018. A novel method of neural differentiation of PC12 cells by using Opti-MEM as a basic induction medium. *Int. J. Mol. Med.* 41: 195-201. <https://doi.org/10.3892/ijmm.2017.3195>.
- Huang J., Ye Z., Hu X., Lu L., Luo Z., 2010. Electrical stimulation induces calcium-dependent release of NGF from cultured Schwann cells. *Glia.* 58: 622-631. <https://doi.org/10.1002/glia.20951>.
- Isaacson J.E. and Vora N.M., 2003. Differential diagnosis and treatment of hearing loss. *Am. Fam. Physician.* 68: 1125-1132. PMID: 14524400.
- Jakubowski W. and Bartosz G., 2000. 2,7-dichlorofluorescein oxidation and reactive oxygen species: what does it measure? *Cell Biol. Int.* 24: 757-760. <https://doi.org/10.1006/cbir.2000.0556>.
- Javel E., 2003. Auditory System, Peripheral. *Encyclopedia of the Neurological Sciences*, Academic Press. pp. 305-311. <https://doi.org/10.1016/B0-12-226870-9/00529-3>.
- Jayakumar R., Menon D., Manzoor K., Nair S.V., Tamura H., 2010. Biomedical applications of chitin and chitosan based nanomaterials - a short review. *Carbohydr. Polym.* 82: 227-232. <https://doi.org/10.1016/j.carbpol.2010.04.074>.
- Jeon B.M., Yeon G.B., Goo H.G., Lee K.E., Kim D.S., 2020. PVDF nanofiber scaffold coated with a vitronectin peptide facilitates the neural differentiation of human embryonic stem cells. *Dev. Reprod.* 24: 135-147. <https://doi.org/10.12717/DR.2020.24.2.135>. [published correction appears in *Dev. Reprod.* 2021. 25: 73-74. <https://doi.org/10.12717/DR.2021.25.1.73>.
- Jiang B., Iocozzia J., Zhao L., Zhang H., Harn Y.W., Chen Y., Lin Z., 2019. Barium titanate at the nanoscale: controlled synthesis and dielectric and ferroelectric properties. *Chem. Soc. Rev.* 48: 1194-1228. <https://doi.org/10.1039/C8CS00583D>.

- Jianqing F., Huipin Y., Xingdong Z., 1997 Promotion of osteogenesis by a piezoelectric biological ceramic. *Biomaterials* 18: 1531-1534. [https://doi.org/10.1016/S0142-9612\(97\)80004-X](https://doi.org/10.1016/S0142-9612(97)80004-X).
- Jones M.G., Blonder R., Gardner G.E., Albe V., Falvo M., Chevrier J., 2013. Nanotechnology and nanoscale science: educational challenges. *Int. J. Sci. Educ.* 35: 1490-1512. <https://doi.org/10.1080/09500693.2013.771828>.
- Juhn S.K., 1988. Barrier systems in the inner ear. *Acta Otolaryngol.* 105: 79-83. <https://doi.org/10.3109/00016488809125107>.
- Jun I., Han H.S., Edwards J.R., Jeon H., 2018. Electrospun fibrous scaffolds for tissue engineering: viewpoints on architecture and fabrication. *Int. J. Mol. Sci.* 19: 745. <https://doi.org/10.3390/ijms19030745>.
- Kalinec F., Kalinec G., Boukhvalova M., Kachar B., 1999. Establishment and characterization of conditionally immortalized organ of Corti cell lines. *Cell Biol. Int.* 23: 175-84. <https://doi.org/10.1006/cbir.1998.0339>.
- Kamali A.R. and Fray D.J., 2014. Preparation of lithium niobate particles via reactive molten salt synthesis method. *Ceram.* 40: 1835-1841. <https://doi.org/10.1016/j.ceramint.2013.07.085>.
- Kapat K., Shubhra Q., Zhou M., Leeuwenburgh S., 2020. Piezoelectric nano-biomaterials for biomedicine and tissue regeneration. *Adv. Funct. Mater.* 30: 1909045. <https://doi.org/10.1002/adfm.201909045>.
- Katzir S., 2003. The discovery of the piezoelectric effect. *Arch. Hist. Exact Sci.* 57: 61-91. <https://doi.org/10.1007/s00407-002-0059-5>
- Kejlová K., Labský J., Jírová D., Bendová H., 2005. Hydrophilic polymers—biocompatibility testing in vitro. *Toxicology in Vitro.* 19: 957-962. <https://doi.org/10.1016/j.tiv.2005.06.032>.

- Kelsay D.M. and Tyler R.S., 1996. Advantages and disadvantages expected and realized by pediatric cochlear implant recipients as reported by their parents. *Am. J. Otol.* 17: 866-873. PMID:8915415
- Keong L.C. and Halim A.S., 2009. In Vitro Models in Biocompatibility Assessment for Biomedical-Grade Chitosan Derivatives in Wound Management. *Int. J. Mol. Sci.* 10: 1300-1313. <https://doi.org/10.3390/ijms10031300>.
- Khorshidi S., Karkhaneh A., 2018. On-demand release of ciprofloxacin from a smart nanofiber depot with acoustic stimulus. *J. Biosci.* 43: 959-967. <https://doi.org/10.1007/s12038-018-9808-8>.
- Kim J.A., Lee N., Kim B.H., Rhee W.J., Yoon S., Hyeon T., Park T.H., 2011. Enhancement of neurite outgrowth in PC12 cells by iron oxide nanoparticles. *Biomaterials.* 32: 2871-2877. <http://doi.org/10.1016/j.biomaterials.2011.01.019>.
- Knipper M., van Dijk P., Schulze H., Mazurek B., Krauss P., Scheper V., Warnecke A., Schlee W., Schwabe K., Singer W., Braun C., Delano P.H., Fallgatter A.J., Ehlis A.C., Searchfield G.D., Munk M.H.J., Baguley D.M., Rüttiger L., 2020. The neural bases of tinnitus: lessons from deafness and cochlear implants. *J. Neurosci.* 40: 7190-7202. <https://doi.org/10.1523/JNEUROSCI.1314-19.2020>.
- Kollmeier B., 2008. Anatomy, physiology and function of the auditory system. In: Havelock D., Kuwano S., Vorländer M. (eds) *Handbook of Signal Processing in Acoustics*. Springer, New York, NY. 147-158. https://doi.org/10.1007/978-0-387-30441-0_10.
- Kuete V., Karaosmanoğlu O., Sivas H., 2017. Anticancer Activities of African Medicinal Spices and Vegetables. In book: *Medicinal Spices and Vegetables from Africa*, Academic Press. 271-297. <https://doi.org/10.1016/B978-0-12-809286-6.00010-8>.
- Kumari A., Yadav S.K., Yadav S.C., 2010. Biodegradable polymeric nanoparticles based drug delivery systems. *Colloids Surf. B. Biointerfaces.* 75: 1-18. <https://doi.org/10.1016/j.colsurfb.2009.09.001>.

- Langer R. and Folkman J., 1976. Polymers for the sustained release of proteins and other macromolecules. *Nature* 263: 797-800. <https://doi.org/10.1038/263797a0>.
- Latchoumane C.F.V., Jackson L., Sendi M.S.E., Tehrani K.F., Mortensen L.J., Stice S.L., Ghovanloo M., Karumbaiah L., 2018. Chronic electrical stimulation promotes the excitability and plasticity of ESC-derived neurons following glutamate-induced inhibition in vitro. *Sci. Rep.* 8: 10957. <https://doi.org/10.1038/s41598-018-29069-3>.
- Lee Y.S., Collins G., Arinzeh T.L., 2011. Neurite extension of primary neurons on electrospun piezoelectric scaffolds. *Acta Biomater.* 7: 3877-3886. <https://doi.org/10.1016/j.actbio.2011.07.013>.
- Lenarz T. (2018). Cochlear implant - state of the art. *GMS Curr. Top. Otorhinolaryngol. Head Neck Surg.* 16: Doc04. <https://doi.org/10.3205/cto000143>.
- Li J., Mou X., Qiu J., Wang S., Wang D., Sun D., Guo W., Li D., Kumar A., Yang X., Li A., Liu H., 2015. Surface charge regulation of osteogenic differentiation of mesenchymal stem cell on polarized ferroelectric crystal substrate. *Adv. Healthcare Mater.* 4: 998-1003. <https://doi.org/10.1002/adhm.201500032>.
- Li Y., Liao C., Tjong S.C., 2019. Electrospun polyvinylidene fluoride-based fibrous scaffolds with piezoelectric characteristics for bone and neural tissue engineering. *Nanomaterials.* 9: 952. <https://doi.org/10.3390/nano9070952>.
- Maeda Y., Jayakumar R., Nagahama H., Furuike T., Tamura H., 2008. Synthesis, characterization and bioactivity studies of novel beta-chitin scaffolds for tissue-engineering applications. *Int. J. Biol. Macromol.* 42: 463-467. <https://doi.org/10.1016/j.ijbiomac.2008.03.002>.
- Mahmoudi E, Zazove P, Pleasant T, Meeks L, McKee MM., 2021. Hearing loss and healthcare access among adults. *Semin Hear.* 42: 47-58. <https://doi.org/10.1055/s-0041-1726000>.

- Mamo S.K., Reed N.S., Price C., Occhipinti D., Pletnikova A., Lin F.R., Oh E.S., 2018. Hearing loss treatment in older adults with cognitive impairment: a systematic review. *J. Speech Lang. Hear.* 61: 2589-2603. https://doi.org/10.1044/2018_JSLHR-H-18-0077.
- Mandracchia B., Gennari O., Bramanti A., Grilli S., Ferraro P., 2018. Label-free quantification of the effects of lithium niobate polarization on cell adhesion via holographic microscopy. *J. Biophotonics.* 11: e201700332. <https://doi.org/10.1002/jbio.201700332>.
- Marchesano V., Gennari O., Mecozzi L., Grilli S., Ferraro P., 2015. Effects of lithium niobate polarization on cell adhesion and morphology. *ACS Appl. Mater. Interfaces.* 7: 18113-18119. <https://doi.org/10.1021/acsami.5b05340>.
- Marino A., Arai S., Hou Y., Sinibaldi E., Pellegrino M., Chang Y.T., Mazzolai B., Mattoli V., Suzuki M., Ciofani G., 2015. Piezoelectric nanoparticle-assisted wireless neuronal stimulation. *ACS Nano.* 9: 7678-7689. <https://doi.org/10.1021/acsnano.5b03162>.
- Marlow E.S., Hunt L.P., Marlow N., 2000. Sensorineural hearing loss and prematurity. *Arch. Dis. Child Fetal Neonatal.* Ed. 82: F141-F144. <https://doi.org/10.1136/fn.82.2.f141>.
- Martini A., Prosser S., Aimoni C., Bovo R., Ciorba A., Trevisi P., 2011. *Audiologia e Foniatria. Psicoacustica audiologia clinica otologia vestibologia foniatria.* Omega Edizioni. ISBN: 9788872415597
- Massa H.M., Spann K.M., Cripps AW., 2021. Innate immunity in the middle ear mucosa. *Front. Cell Infect. Microbiol.* 11: 764772. <https://doi.org/10.3389/fcimb.2021.764772>.
- Meinan L., Dongfeng X., Chao L., 2006. Wet chemical synthesis of pure LiNbO₃ powders from simple niobium oxide Nb₂O₅. *J. Alloys Compd.* 426: 118-122. <https://doi.org/10.1016/j.jallcom.2006.02.019>.
- Mendonça L.M., da Silva Machado C., Teixeira C.C., de Freitas L.A., Bianchi Mde L., Antunes L.M., 2013. Curcumin reduces cisplatin-induced neurotoxicity in NGF-differentiated PC12 cells. *NeuroToxicology* 34: 205-211. <https://doi.org/10.1016/j.neuro.2012.09.011>.

- Mills E.M., Gunasekar P.G., Pavlakovic G., Isom G.E., 1996. Cyanide-induced apoptosis and oxidative stress in differentiated PC12 cells. *J. Neurochem.* 67: 1039-1046. <https://doi.org/10.1046/j.1471-4159.1996.67031039.x>.
- Moczko E., Poma A., Guerreir, A., Pérez de Vargas Sansalvador I.M., Caygill S., Canfarotta F., Whitcombe M.J., Piletsky S.A., 2013. Surface-modified multifunctional MIP nanoparticles. *Nanoscale* 5: 3733-41. <https://doi.org/10.1039/C3NR00354J>.
- Morganti P., Febo P., Cardillo M., Donnarumma G., Baroni A., 2017. Chitin nanofibril and nanolignin: natural polymers of biomedical interest. *J. Clin. Cosmet. Dermatol.* 1. <http://dx.doi.org/10.16966/2576-2826.113>.
- Mota C., Danti S., D'Alessandro D., Trombi L., Ricci C., Puppi D., Dinucci D., Milazzo M., Stefanini C., Chiellini F., Moroni L., Berrettini S., 2015. Multiscale fabrication of biomimetic scaffolds for tympanic membrane tissue engineering. *Biofabrication* 7: 025005. <https://doi.org/10.1088/1758-5090/7/2/025005>.
- Mota C., Labardi M., Trombi L., Astolfi L., D'Acunto M., Puppi D., Gallone G., Chiellini F., Berrettini S., Bruschini L., Danti S., 2017. Design, fabrication and characterization of composite piezoelectric ultrafine fibers for cochlear stimulation. *Mater. Des.* 122: 206-219. <https://doi.org/10.1016/j.matdes.2017.03.013>.
- Mukherjee N., Roseman R.D., Willging J.P., 2000. The piezoelectric cochlear implant: concept, feasibility, challenges, and issues. *J. Biomed. Mater. Res.* 53: 181-187. [https://doi.org/10.1002/\(sici\)1097-4636\(2000\)53:2<181::aid-jbm8>3.0.co;2-t](https://doi.org/10.1002/(sici)1097-4636(2000)53:2<181::aid-jbm8>3.0.co;2-t).
- Müller U., 2008. In vitro biocompatibility testing of biomaterials and medical devices. *Med Device Technol.* 30: 32-4.
- Muzzarelli R.A., 2009. Chitins and chitosans for the repair of wounded skin, nerve, cartilage and bone. *Carbohydrate Polymers* 76: 167-182. <https://doi.org/10.1016/j.carbpol.2008.11.002>.

- Muzzarelli R.A., Morganti P., Morganti G., Palombo P., Palombo M., Biagini G., Mattioli Belmonte M., Giantomassi F., Orlandi F., Muzzarelli C., 2007. Chitin nanofibrils/chitosan glycolate composites as wound medicaments. *Carbohydr. Polym.* 70: 274-284. <https://doi.org/10.1016/j.carbpol.2007.04.008>.
- Naghdi T., Yousefi H., Sharifi A.R., Golmohammadi H., 2020. Nanopaper-based sensors (Chapter 9). In: *Comprehensive Analytical Chemistry*, Elsevier. 89: 257-312. <https://doi.org/10.1016/bs.coac.2020.02.003>.
- Niazi S.A., Khattak S.F., Atif K., Rafique A., Gohar M.S., 2021. Why myringoplasties fail? Impact of relevant clinical factors on the surgical outcome; a study from Pakistan. *J. Ayub. Med. Coll. Abbottabad.* 33: 412-415. PMID: 34487648.
- NIDCD, National Institute on Deafness and Other Communication Disorders, 2021. (Accessed May, 2021) <https://www.nidcd.nih.gov/health/cochlear-implants>.
- Norell M.C., Andersson H.S., Nicholls I.A., 1998. Theophylline molecularly imprinted polymer dissociation kinetics: a novel sustained release drug dosage mechanism. *J. Mol. Recognit.* 11: 98-102. [https://doi.org/10.1002/\(SICI\)1099-1352\(199812\)11:1/6<98::AID-JMR399>3.0.CO;2-Y](https://doi.org/10.1002/(SICI)1099-1352(199812)11:1/6<98::AID-JMR399>3.0.CO;2-Y).
- Panda P.K., 2009. Review: environmental friendly lead-free piezoelectric materials. *J. Mater. Sci.* 44: 5049-5062. <https://doi.org/10.1007/s10853-009-3643-0>.
- Pandey E., Srivastava K., Gupta S., Srivastava S., Mishra N., 2016. Some biocompatible materials used in medical practices - a review. *Int. J. Pharm. Sci. Res.* 7: 2748-2755. [https://doi.org/10.13040/IJPSR.0975-8232.7\(7\).2748-55](https://doi.org/10.13040/IJPSR.0975-8232.7(7).2748-55).
- Pärssinen J., Hammarén H., Rahikainen R., Sencadas V., Ribeiro C., Vanhatupa S., Miettinen S., Lanceros-Méndez S., Hytönen V.P., 2015. Enhancement of adhesion and promotion of osteogenic differentiation of human adipose stem cells by poled electroactive poly(vinylidene fluoride). *J. Biomed. Mater. Res. Part A.* 103A: 919-928. <https://doi.org/10.1002/jbm.a.35234>.

- Patil M., Mehta D.S., Guvva S., 2008. Future impact of nanotechnology on medicine and dentistry. *J. Indian Soc. Periodontol.* 12: 34-40. <https://doi.org/10.4103/0972-124X.44088>.
- Phaniendra A., Jestadi D.B., Periyasamy L., 2015. Free radicals: properties, sources, targets, and their implication in various diseases. *Indian J. Clin. Biochem.* 30: 11-26. <https://doi.org/10.1007/s12291-014-0446-0>.
- Poma A., Turner A.P., Piletsky S.A., 2010. Advances in the manufacture of MIP nanoparticles. *Trends Biotechnol.* 28: 629-637. <https://doi.org/10.1016/j.tibtech.2010.08.006>.
- Prabaharan M., 2008. Review paper: chitosan derivatives as promising materials for controlled drug delivery. *J. Biomater. Appl.* 23: 5-36. <https://doi.org/10.1177/0885328208091562>.
- Radio N.M., Mundy W.R., 2008. Developmental neurotoxicity testing in vitro: models for assessing chemical effects on neurite outgrowth. *Neurotoxicology.* 29: 361-76. <https://doi.org/10.1016/j.neuro.2008.02.011>.
- Rajabi A.H., Jaffe M., Arinzeh T.L., 2015. Piezoelectric materials for tissue regeneration: a review. *Acta Biomater.* 24: 12-23. <https://doi.org/10.1016/j.actbio.2015.07.010>.
- Ray P.C., Yu H., Fu P.P., 2009. Toxicity and environmental risks of nanomaterials: challenges and future needs. *J. Environ. Sci. Health C. Environ. Carcinog. Ecotoxicol. Rev.* 27: 1-35. <https://doi.org/10.1080/10590500802708267>.
- Refaat D., Aggour M.G., Farghali A.A., Mahajan R., Wiklander J.G., Nicholls I.A., Piletsky S.A., 2019. Strategies for molecular imprinting and the evolution of MIP nanoparticles as plastic antibodies - Synthesis and applications. *Int. J. Mol. Sci.* 20: 6304. <https://doi.org/10.3390/ijms20246304>.
- Russo M., Stella M., Sikora M., Pekić V., 2019. Robust cochlear-model-based speech recognition. *Computers* 8: 5. <https://doi.org/10.3390/computers8010005>.

- Sagiv D., Chin O.Y., Diaz R.C., Brodie H.A., 2020. State of the art regeneration of the tympanic membrane. *Curr. Opin. Otolaryngol. Head Neck Surg.* 28: 314-322. <https://doi.org/10.1097/MOO.0000000000000646>.
- Sakagami H, Hara Y, Shi H, Iwama S, Nakagawa M, Suzuki H, Tanaka K, Abe T, Tamura N, Takeshima H, Horie N, Kaneko T, Shiratsuchi H, Kaneko T., 2018. Change in anticancer drug sensitivity during neuronal differentiation of PC12 cells. *In Vivo.* 32: 765-770. <https://doi.org/10.21873/invivo.11306>.
- Saladin K.S., 2019. *Anatomia e fisiologia*. Piccin Nuova Libreria, ed. 2 a cura di Gaudio E. ISBN 978-88-299-2955-9
- Sánchez López de Nava A., Lasrado S., 2021. *Physiology, Ear*. [Updated 2021 Aug 30] In: StatPearls [Internet]. Treasure Island (FL): StatPearls Publishing; 2021 Jan-. <https://www.ncbi.nlm.nih.gov/books/NBK540992/>.
- Sánchez-Martín F.J., Valera E., Casimiro I., Merino J.M., 2010. Nerve growth factor increases the sensitivity to zinc toxicity and induces cell cycle arrest in PC12 cells. *Brain Res. Bull.* 81: 458-466. <https://doi.org/10.1016/j.brainresbull.2009.11.008>.
- Santos N.A.G.D., Ferreira R.S., Santos A.C.D., 2020. Overview of cisplatin-induced neurotoxicity and ototoxicity, and the protective agents. *Food Chem. Toxicol.* 136: 111079. <https://doi.org/10.1016/j.fct.2019.111079>.
- Sasaki N., Baba N., Matsuo M., 2001. Cytotoxicity of reactive oxygen species and related agents toward undifferentiated and differentiated rat pheochromocytoma PC12 cells. *Biol. Pharm. Bull.* 24: 515-519. <https://doi.org/10.1248/bpb.24.515>
- Schlaug G., Renga V., Nair D., 2008. Transcranial direct current stimulation in stroke recovery. *Arch. Neurol.* 65: 1571-1576. <https://doi.org/10.1001/archneur.65.12.1571>.
- Serra-Gómez R., Martínez-Tarifa J.M., González-Benito J., González-Gaitano G., 2016. Cyclodextrin-grafted barium titanate nanoparticles for improved dispersion and

stabilization in water-based systems. *J. Nanopart. Res.* 18: 24.
<https://doi.org/10.1007/s11051-015-3321-x>.

Sezer N., and Koç M., 2020. A comprehensive review on the state-of-the-art of piezoelectric energy harvesting. *Nano Energy* 80: 1-25.
<https://doi.org/10.1016/j.nanoen.2020.105567>.

Simoni E., Gentilin E., Candito M., Borile G., Romanato F., Chicca M., Nordio S., Aspidistria M., Martini A., Cazzador D., Astolfi L., 2020. Immune response after cochlear implantation. *Front. Neurol.* 11: 341. <https://doi.org/10.3389/fneur.2020.00341>.

Smyth P.G., Berman S.A., Bursztajn S., 2002. Markers of apoptosis: methods for elucidating the mechanism of apoptotic cell death from the nervous system. *Biotechniques* 32: 648-665. <https://doi.org/10.2144/02323dd02>.

Sōmiya S., 2003. Ceramics. *Encyclopedia of Physical Science and Technology* (Third edition), Academic Press. pp. 569–619. <https://doi.org/10.1016/B0-12-227410-5/00092-2>.

Sooriyamoorthy T., De Jesus O., 2021. Conductive Hearing Loss. [Updated 2021 Feb 7]. In: StatPearls [Internet]. Treasure Island (FL): StatPearls Publishing; 2021 Jan-. <https://www.ncbi.nlm.nih.gov/books/NBK563267/>.

Staecker H., Gochee P., Ferraro J., Storms R., 2008. Overview of treatment of hearing loss. In: *The Senses: A Comprehensive Reference*. Academic Press. 3: 447-467. <https://doi.org/10.1016/b978-012370880-9.00035-9>.

Sunar M., 2018. Piezoelectric materials (chapter 2.22). In: Dincer I., ed. *Comprehensive Energy Systems*, Elsevier. pp. 696-719. <https://doi.org/10.1016/B978-0-12-809597-3.00248-0>.

Sundar P.S., Chowdhury C., Kamarthi S., 2021. Evaluation of human ear anatomy and functionality by axiomatic design. *Biomimetics* 6: 31.
<https://doi.org/10.3390/biomimetics6020031>.

- Szymanski A., Toth J., Ogorevc M., Geiger Z., 2021. Anatomy, Head and Neck, Ear Tympanic Membrane. [Updated 2021 May 16]. In: StatPearls [Internet]. Treasure Island (FL): StatPearls Publishing; 2021 Jan-. <https://www.ncbi.nlm.nih.gov/books/NBK448117/>.
- Tabatabaei Mirakabad F.S., Nejati-Koshki K., Akbarzadeh A., Yamchi MR., Milani M., Zarghami N., Zeighamian V., Rahimzadeh A., Alimohammadi S., Hanifehpour Y., Joo S.W., 2014. PLGA-based nanoparticles as cancer drug delivery systems. *Asian Pac. J. Cancer Prev.* 15: 517-35. <https://doi.org/10.7314/apjcp.2014.15.2.517>.
- Tandon B., Blaker J.J., Cartmell S.H., 2018. Piezoelectric materials as stimulatory biomedical materials and scaffolds for bone repair. *Acta Biomater.* 73: 1-20. <https://doi.org/10.1016/j.actbio.2018.04.026>.
- Tanna R.J., Lin J.W., De Jesus O., 2021. Sensorineural Hearing Loss. [Updated 2021 Aug 30]. In: StatPearls [Internet]. Treasure Island (FL): StatPearls Publishing; 2021 Jan-. <https://www.ncbi.nlm.nih.gov/books/NBK565860/>.
- Turney J., 2008. Technology: Ethical debates about the application of science. Series: Dilemmas in Modern Science. Evans Publishing Group, United Kingdom, ISBN 9780237533700
- Uhl A.M., Andrew J.S., 2020. Sol-gel-based electrospray synthesis of barium titanate nanoparticles. *IEEE Trans. NanoBioscience* 19: 162-166. <https://doi.org/10.1109/TNB.2019.2963165>.
- Van de Heyning P., Atlas M., Baumgartner W.D., Caversaccio M., Gavilan J., Godey B., Gstöttner W., Hagen R., Yongxin L., Karltorp E., Kameswaran M., Kuzovkov V., Lassaletta L., Manoj M., Parnes L., Pillsbury H., Raine C., Rajan G., Schmutzhard J., Skarzynski H., Staecker H., Usami S.I., Zernotti M., 2020. The reliability of hearing implants: report on the type and incidence of cochlear implant failures. *Cochlear Implants Int.* 21: 228-237. <https://doi.org/10.1080/14670100.2020.1735678>.

- van Nostrum C.F., 2005. Molecular imprinting: A new tool for drug innovation. *Drug Discov. Today Technol.* 2: 119-124. <https://doi.org/10.1016/j.ddtec.2005.05.004>.
- Vannozzi L., Mariotti G., Ricotti L., 2019. Nanocomposite thin films based on polyethylene vinyl acetate and piezoelectric nanomaterials. 41st Annual International Conference of the IEEE Engineering in Medicine and Biology Society (EMBC). pp. 1050-1053. <https://doi.org/10.1109/EMBC.2019.8857556>.
- Vijatovic M.M., Bobic J.D., Stojanovic B.D., 2008. History and challenges of barium titanate: Part I. *Sci. Sinter.* 40: 155-165. <https://doi.org/10.2298/SOS0802155V>.
- Vilarinho P.M., Barroca N., Zlotnik S., Félix P., Fernandes M.H., 2014. Are lithium niobate (LiNbO₃) and lithium tantalate (LiTaO₃) ferroelectrics bioactive? *Mater. Sci. Eng. C. Mater. Biol. Appl.* 39: 395-402. <https://doi.org/10.1016/j.msec.2014.03.026>.
- Wall G.M., Stroman D.W., Roland P.S., Dohar J., 2009. Ciprofloxacin 0.3%/dexamethasone 0.1% sterile otic suspension for the topical treatment of ear infections: a review of the literature. *Pediatr. Infect. Dis. J.* 28: 141-144. <https://doi.org/10.1097/INF.0b013e31818b0c9c>.
- Ward T., Cummings J., Dean E, Greystoke A., Hou J.M., Backen A., Ranson M., Dive C., 2008. Biomarkers of apoptosis. *Br. J. Cancer.* 99: 841-846. <https://doi.org/10.1038/sj.bjc.6604519>.
- Weis R.S. and Gaylord T.K., 1985. Lithium niobate: summary of physical properties and crystal structure. *Appl. Phys. A.* 37: 191-203. <https://doi.org/10.1007/BF00614817>.
- WHO – World Health Organization. Accessed April, 2021. <https://www.who.int/news-room/fact-sheets/detail/deafness-and-hearing-loss>
- Wiatrak B., Kubis-Kubiak A., Piwowar A., Barg E., 2020. PC12 cell line: cell types, coating of culture vessels, differentiation and other culture conditions. *Cells.* 9: 958. <https://doi.org/10.3390/cells9040958>.

- Wilson J.S., 2005. Sensor technology handbook. Elsevier Science & Technology.
<https://doi.org/10.1016/B978-0-7506-7729-5.X5040-X>.
- Witt S., Scheper T., Walter J.G., 2019. Production of polycaprolactone nanoparticles with hydrodynamic diameters below 100 nm. *Eng. Life Sci.* 19: 658-665.
<https://doi.org/10.1002/elsc.201800214>.
- Wroblewska-Seniuk K., Dabrowski P., Greczka G., Szabatowska K., Glowacka A., Szyfter W., Mazela J., 2018. Sensorineural and conductive hearing loss in infants diagnosed in the program of universal newborn hearing screening. *Int. J. Pediatr. Otorhinolaryngol.* 105: 181-186. <https://doi.org/10.1016/j.ijporl.2017.12.007>
- Wul B., 1946. Barium Titanate: a New Ferro-Electric. *Nature* 157: 808.
<https://doi.org/10.1038/157808a0>.
- Xiao Y.L., Riesle J., Blitterswijk C.A.V., 1991. Static and dynamic fibroblast seeding and cultivation in porous PEO/PBT scaffolds. *J. Mater. Sci.: Mater. Med.* 10: 773-777.
<https://doi.org/10.1023/A:1008946832443>.
- Xu S., Sun X., Yang N., Yan A., 2021. Human-derived acellular dermal matrix may be an alternative to autologous grafts in tympanic membrane reconstruction: systematic review and meta-analysis. *J. Otolaryngol - Head Neck Surg.* 50: 43.
<https://doi.org/10.1186/s40463-021-00518-w>.
- Xue Z., Xiang Y., Li Y., Yang Q., 2021. A systematic review and meta-analysis of levofloxacin and ciprofloxacin in the treatment of urinary tract infection. *Ann. Palliat. Med.* 10: 9765-9771. <https://doi.org/10.21037/apm-21-2042>.
- Yang F., Liu C., Ji J., Cao W., Ding B., Xu X., 2021. Molecular characteristics, antimicrobial resistance, and biofilm formation of *Pseudomonas aeruginosa* isolated from patients with aural infections in Shanghai, China. *Infect. Drug Resist.* 14: 3637-3645.
<http://doi.org/10.2147/IDR.S314441>.

- Yang X., Liu X., Zhang X, Lu H., Zhang J., Zhang Y., 2011. Investigation of morphological and functional changes during neuronal differentiation of PC12 cells by combined hopping probe ion conductance microscopy and patch-clamp technique. *Ultramicroscopy* 111: 1417-1422. <https://doi.org/10.1016/j.ultramic.2011.05.008>.
- Yu Y., Sun H., Orbay H., Chen F., England C.G., Cai W., Wang X., 2016. Biocompatibility and in vivo operation of implantable mesoporous PVDF-based nanogenerators. *Nano Energy* 27: 275-281. <https://doi.org/10.1016/j.nanoen.2016.07.015>.
- Zeng F., Rebscher S., Harrison W., Sun X., Feng H., 2008. Cochlear implants: system design, integration, and evaluation. *IEEE Reviews in Biomedical Engineering*. 1: 115-142. <https://doi.org/10.1109/RBME.2008.2008250>.
- Zhang H., 2020. Molecularly imprinted nanoparticles for biomedical applications. *Adv. Mater.* 32: 1806328. <https://doi.org/10.1002/adma.201806328>.
- Zhang Q. & Duan M., 2009. Anatomy and physiology of peripheral auditory system and common causes of hearing loss. *J. Otol.* 4: 7-14. [https://doi.org/10.1016/S1672-2930\(09\)50002-5](https://doi.org/10.1016/S1672-2930(09)50002-5).
- Zou J., Pyykkö I., Hyttinen J., 2016. Inner ear barriers to nanomedicine-augmented drug delivery and imaging. *J. Otol.* 11: 165-177. <https://doi.org/10.1016/j.joto.2016.11.002>.